OFFICE OF NAVAL RESEARCH

CONTRACT N5 ORI-76 PROJECT ORDER X

NR-384-903

TECHNICAL MEMORANDUM
NO. 27

CORRELATORS FOR SIGNAL RECEPTION

BY

JAMES J. FARAN, JR.

ROBERT HILLS, JR.

SEPTEMBER 15, 1952

ACOUSTICS RESEARCH LABORATORY

DIVISION OF APPLIED SCIEN

HARVARD UNIVERSITY - CAMBRIDGE MASSAC

Technical Memorandum No. 27

Correlators for Signal Reception

by

James J. Faran, Jr. and Robert Hills, Jr.

September 15, 1952

Summary

Correlators (multiplier-averagers) are analyzed and compared with detectors (rectifier-averagers) of various power laws from the point of view of their possible use in signal reception systems. Comparison is made in terms of signal-to-noise ratio for the limiting case of small input signal-to-noise ratio and long averaging time. Of the detectors, the square-law is found to be slightly superior for determining the presence of a small signal in a noise background, while, if two samples of the signal in incoherent background noises are available, although the correlator cannot improve the signal-to-noise ratio, it does have the advantage that no constant terms independent of the signal appear at its output. The design of electronic correlators is discussed, and several practical circuits are given. Two other types of circuits, similar in operation to correlators, but much simpler to construct, are also analyzed. Both of these are very slightly inferior to true correlators in output signal-to-noise ratio.

PREFACE

An investigation of the possible application of correlation techniques to acoustic receiving systems is under way at this Laboratory. In this first technical memorandum on the subject are presented findings which pertain especially to electronic correlators, including theoretical analysis and practical circuit design. Consideration of applications to specific acoustic systems will be reserved for a subsequent memorandum.

This study of correlation techniques was suggested by Professor F. V. Hunt, and the authors are greatly indebted to him for his helpful and stimulating guidance of the project. The authors also gratefully acknowledge the assistance of Professor Harvey Brooks, who demonstrated to them many of the methods of analysis used herein, and of Professor David Middleton, who contributed his time in many helpful discussions.

TABLE OF CONTENTS

Correlators for Signal Reception

by

James J. Faran, Jr. and Robert Hills, Jr.

Acoustics Research Laboratory, Harvard University

I

INTRODUCTION

There are many possible criteria for comparing the efficacy of various systems for the reception of acoustic signals. Many of these depend upon the particular type of system being considered. However, we have attempted to keep our consideration general rather than specific, and have chosen as a criterion of system performance the output signal-to-noise ratio, and in most cases have concentrated attention on the important case of very small input signal-to-noise ratio. In order to evaluate signal-to-noise ratios theoretically, we must make use of certain statistical methods for dealing with the random functions we encounter. While these methods are by now relatively well known, the following sections will serve as a review of some of the basic ideas, as well as a definition of our notation.

Mathematical Treatment of Random Functions[1]

A particular example of a random noise voltage is, of course, an explicit function of time and could, in principle, be so represented. However, such a representation would be of no physical interest, since each example of random noise is different and could never be exactly repeated. We must instead make use of certain average properties of all noises belonging to the same class. For example, if we are concerned with the output of an electronic noise generator, we focus

-1-

attention on what would be the average properties of all the
outputs of a large number of identical noise generators. The
outputs of all these noise generators comprise an **ensemble** of
random functions; the complete ensemble is called a random
process (as soon as certain mathematical properties of the
ensemble are specified -- finite mean-square amplitude, for
example). The description of the random process is then
formulated statistically, and we can speak, for example, of
the probability that at some time one of the noise voltages v
will lie between v and v+dv. A more complex probability func-
tion will give the probability that at some time one of the
noise voltages will lie between v_1 and v_1+dv_1 and that at a
definite time later the same noise voltage will lie between
v_2 and v_2+dv_2. The random process can be completely described
by a sufficiently complex set of such probability densities.
From these usually complicated functions, however, may be
derived certain average properties which are much more use-
ful in describing and measuring the noise, these include the
mean value, mean-square value, power spectrum, and correlation
function. For example, if P(v)dv is the probability that the
noise voltage v(t) lies between v and v+dv, then the mean value
of the noise is

$$\langle v(t) \rangle = \int_{-\infty}^{\infty} vP(v)dv,$$

and its mean-square value is

$$\langle v^2(t) \rangle = \int_{-\infty}^{\infty} v^2 P(v)dv.$$

Of course $\int_{-\infty}^{\infty} P(v)dv = 1$, since P(v) is a proper probability den-
sity. In the above examples, the average values are denoted
by angular brackets, $\langle \rangle$, to indicate that they are statistical
averages, computed from the probability densities which describe
the ensemble. In most experimental measurements of random func-
tions, on the other hand, as when a d c voltmeter is used to measure

the mean value of a noise voltage, what is measured is a time average of one member of the ensemble. Time averages, which we shall indicate by overlines, can be represented mathematically as

$$\overline{v(t)} = \lim_{T \to \infty} \frac{1}{2T} \int_{-T}^{T} v(t)dt$$

and

$$\overline{v^2(t)} = \lim_{T \to \infty} \frac{1}{2T} \int_{-T}^{T} v^2(t)dt.$$

If none of the probability distributions which describe a random process changes with time, the process is said to be __stationary__ If each member of a stationary ensemble of random functions is typical of the ensemble as a whole, that is, if each member function can be expected, as time progresses, to go through, with the proper frequency, all the convolutions of any of the member functions, the ensemble is said to be __ergodic__.[2] An important theorem, the ergodic theorem, states that for an ergodic ensemble, time and statistical averages are equal, i e , if $v(t)$ is a member of an ergodic ensemble,

$$\overline{v(t)} = <v(t)>$$

It is not usually possible to prove that a given physical system is ergodic; the above description of the ergodic property may serve as a guide in deciding whether or not it is possible to make such an assumption. The ergodic theorem allows us to replace measurements which in our mathematical model represent averages over many members of an (ergodic) ensemble with long-time-average measurements of one member of the ensemble. All the stationary ensembles with which we shall be concerned in this memorandum are assumed to be ergodic.

The Gaussian Distribution

It can be shown that all the probability distributions of thermal and shot noise, the types most often encountered in

electronic circuits, are normal or gaussian distributions.[3]
(These types of noise are said to belong to a gaussian random
process.) Other fairly common types of noise are also more or
less accurately described by the gaussian distributions.* The
gaussian probability density (for the amplitude of the voltage
v) is

$$P(v) = \frac{1}{\sqrt{2\pi\sigma^2}} \, e^{-v^2/2\sigma^2} \, , \qquad (1.1)$$

where σ^2 is the mean-square amplitude of the voltage. It will
be useful later to determine the average of the fourth power
of a gaussian-distributed variable:

$$<v^4> = \frac{1}{\sqrt{2\pi\sigma^2}} \int_{-\infty}^{\infty} v^4 \, e^{-v^2/2\sigma^2} \, dv$$

$$= \frac{1}{\sqrt{\pi}} (2\sigma^2)^2 \int_{-\infty}^{\infty} u^4 \, e^{-u^2} \, du$$

$$= \frac{1}{\sqrt{\pi}} (2\sigma^2)^2 \cdot \frac{3}{4}\sqrt{\pi}$$

$$= 3\sigma^4 . \qquad (1.2)$$

In general it may be shown that

$$<v^{2m}> = \frac{(2m)!}{2^m (m)!} \, \sigma^{2m} \qquad (1.3)$$

and, because the distribution is here symmetrical

- - - - - -

*Note, however, that if gaussian noise is passed through a non-
linear device, the output is no longer gaussian. In Fig. 1 are
shown the probability distributions for gaussian noise, for the
output of a multiplier when the inputs are incoherent gaussian
noises, and for the output of a "squarer" when the input is gaus-
sian noise. The latter two are very definitely non-gaussian
For further examples, see Rice's papers and Middleton's paper,
cited in footnote 1.
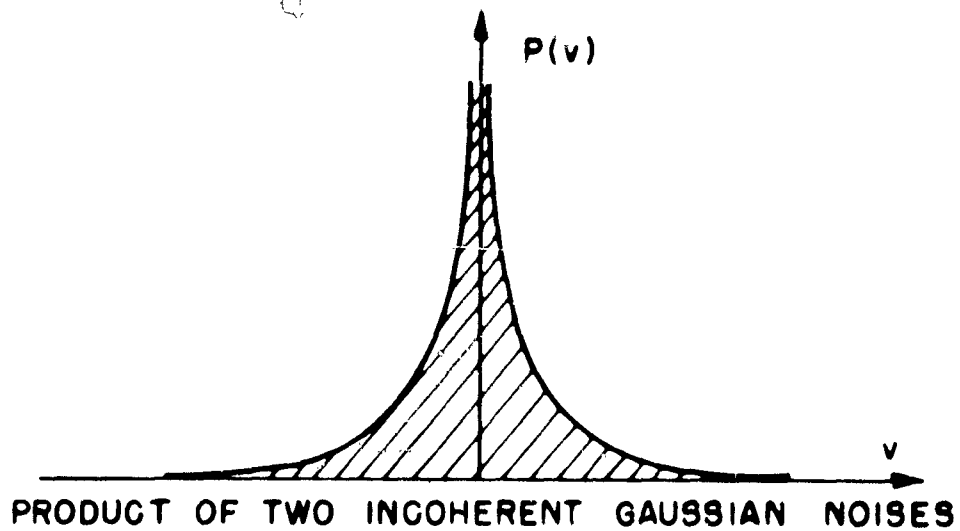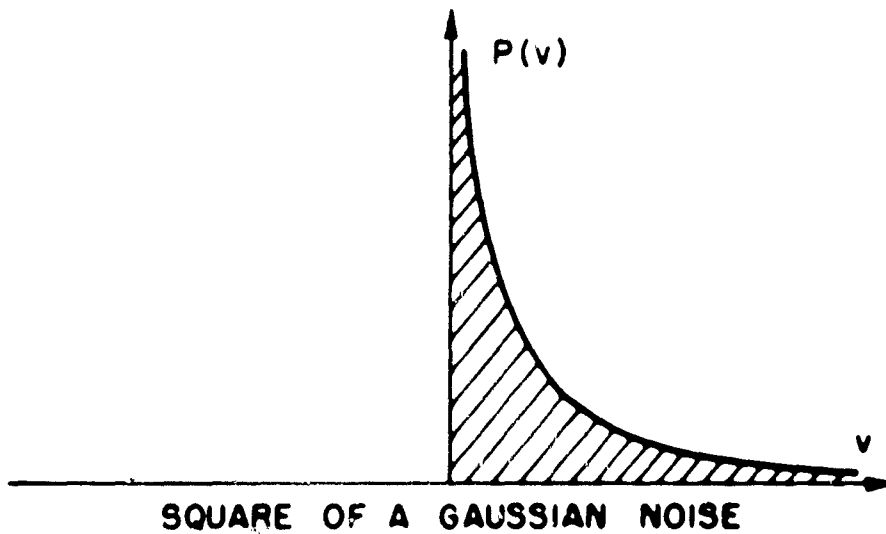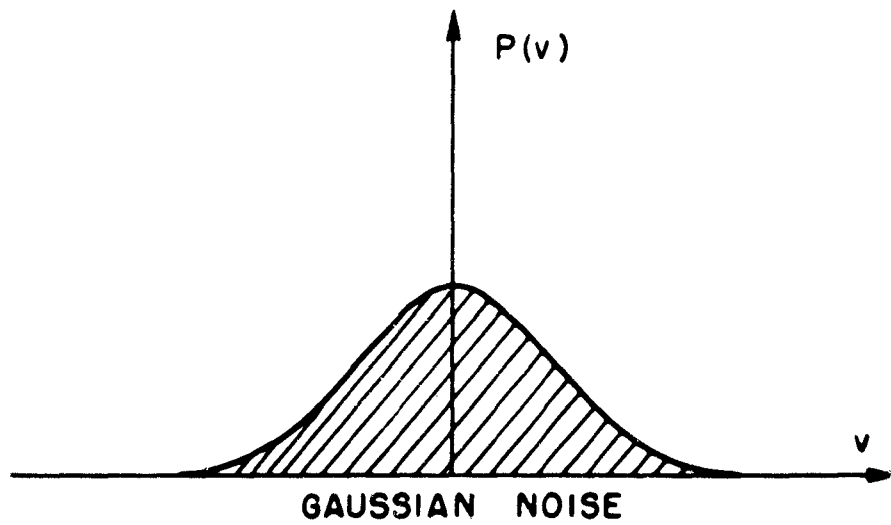
Fig. 1.1 Probability densities for the amplitude v of a gaussian noise, of its square, and of the product of two incoherent gaussian noises of the same amplitude.

$$\langle v^{2m+1} \rangle = 0. \tag{1.4}$$

Representations of Noise Voltages

There are several ways in which mathematical representations of noise voltages may be written, each of these being especially useful in different cases. As we have noted, a particular example of noise might be represented by an explicit function $v(t)$; however, a complete ensemble must be represented by a parametric function of the form

$$v(\alpha_1, \alpha_2, \ldots \alpha_R, t).$$

A particular example is thus characterized by a particular numerical choice of the parameters $\alpha_1, \alpha_2 \ldots \alpha_R$ (which may be infinite in number). The statistical character of the noise is completely specified if we know the probability density of the parameters α, in general given by a function

$$P(\alpha_1 \alpha_2 \quad \alpha_R).$$

The α's are called random variables and constitute the statistical parameters of the ensemble.

These ideas will become clearer in the light of several examples. We consider first noise which is made up by the superposition of a number of individual events, each of which has the explicit time-functional form $f(t)$ but with different starting times t_k, all of which fall inside some long time interval T. Then the noise voltage is given by[1,3]

$$v(t) = \sum_{k=1}^{R} f(t-t_k). \tag{1.5}$$

A particular choice of a family of R particular values of t_k gives a particular example of noise. The t_k's correspond to the α's and are the statistical parameters of the ensemble. The complete ensemble consists of an infinity of examples like Eq. (1.5), in

which each of the parameters t_k takes on all possible values within the time interval T, within which the noise is specified by Eq. (1.5). In the most usual case the probability density

$$P(t_1, \cdot t_k, \cdot t_R) dt_1 \circ \circ dt_k \circ \circ dt_R = \frac{dt_1 \circ \circ dt_k \circ \circ dt_R}{T^R} \, .$$

Another representation which will be used frequently is the Fourier series representation. Consider an example of noise in the time interval T. It may always be expanded in a Fourier series:

$$v(t) = \sum_{n=0}^{\infty} [a_n \cos \omega_n t + b_n \sin \omega_n t], \qquad (1.6)$$

where $\omega_n = \frac{2\pi n}{T}$. If we omit the term for $n = 0$, the average noise voltage vanishes, which is the case of usual interest. The a_n's and b_n's, infinite in number, are the statistical parameters corresponding to the α's. In order to specify the statistical character of the noise, we must know the probability distributions of the coefficients a_n, b_n. In the case of gaussian noise it is customarily **assumed** that the a_n, b_n obey the gaussian distribution law (Eq. (1.1)) and are statistically independent, so that the probability density function may be expressed as a product:

$$P(a_1 \circ \circ \circ a_\infty, b_1 \circ \circ \circ b_\infty) = \prod_{n=1}^{\infty} \frac{1}{\sqrt{2\pi\sigma_n^2}} e^{-\left(\frac{a_n^2}{2\sigma_n^2}\right)} \frac{1}{\sqrt{2\pi\sigma_n^2}} e^{-\left(\frac{b_n^2}{2\sigma_n^2}\right)}$$

Applying the properties of the gaussian distribution (Eqs. 1.3 and 1.4)), we find

$$\langle a_n^2 \rangle = \langle b_n^2 \rangle = \sigma_n^2 \; ; \; \langle a_n b_n \rangle = 0 \; ; \; \langle a_n a_m \rangle = \langle b_n b_m \rangle = 0, n \neq m.$$

$$(1.7)$$

Another method of representing a random function is to assume that the function vanishes outside the long interval $-T/2 \leq |t \leq T/2$. It can then be written in Fourier integral form as

$$v(t) = \int_{-\infty}^{\infty} A(f) \, e^{j2\pi f t} \, df, \qquad\qquad (1.8)$$

where the complex function $A(f)$ is the voltage spectrum. Now by the Parseval theorem,[4]

$$\int_{-\infty}^{\infty} v^2(t) \, dt = \int_{-T/2}^{T/2} v^2(t) \, dt = \int_{-\infty}^{\infty} |A(f)|^2 \, df.$$

This leads immediately to a definition of the _intensity spectrum_[*] of the random process, for, dividing by T and going to the limit $T \longrightarrow \infty$, and using the fact that $|A(f)|^2$ is an even function of f (because $v(t)$ is real), we have

$$\lim_{T \to \infty} \frac{1}{T} \int_{-T/2}^{T/2} v^2(t) \, dt = \overline{v^2(t)} = \int_{0}^{\infty} W(f) \, df,$$

where the intensity spectrum is defined as

$$W(f) = \lim_{T \to \infty} \frac{2|A(f)|^2}{T}.$$

In this representation the functions $A(f)$, which are different for each member of the ensemble, take the place of the statistical parameters.

Correlation Functions

A very useful method of expressing the properties of random processes is in terms of correlation functions. The _auto-correlation function_ of $v(t)$ is defined as

$$R(\tau) = \overline{v(t)v(t-\tau)} = \langle v(t)v(t-\tau) \rangle.$$

In terms of the representation of Eq. (1.6), this is

- - - - - - -

[*]Intensity has the dimensions of voltage squared. We use the term "intensity spectrum" rather than "power spectrum" to avoid the necessity of defining the resistance in which the power is dissipated.

$$R(\tau) = \left\langle \sum_{m=1}^{\infty} \sum_{n=1}^{\infty} [a_m \cos \omega_m t + b_m \sin \omega_m t] \right.$$

$$\left. \circ [a_n \cos \omega_n(t-\tau) + b_n \sin \omega_n(t-\tau)] \right\rangle \circ$$

Using the relations of Eq. (1.7), we have

$$R(\tau) = \sum_{n=1}^{\infty} [\langle a_n^2 \rangle \cos \omega_n t \cos \omega_n(t-\tau)$$

$$+ \langle b_n^2 \rangle \sin \omega_n t \sin \omega_n(t-\tau)].$$

$$= \sum_{n=1}^{\infty} \langle a_n^2 \rangle \cos \omega_n \tau \circ \qquad (1-9)$$

The autocorrelation function thus consists of terms equally spaced in frequency. If we pass to the limit as the interval of definition of $v(t)$ is made infinite in length, the spacing $2\pi/T$ becomes smaller and $\langle a_n^2 \rangle \rightarrow W(f)df$, where $W(f)$ is the power spectrum. In the limit, the sum can be replaced by an integral, and we have

$$R(\tau) = \int_0^{\infty} W(f) \cos 2\pi f \tau \, df \circ \qquad (1-10)$$

The above is a demonstration of the Wiener-Khintchine theorem,[5] which states that, with complete generality, the autocorrelation function is the cosine Fourier transform of the intensity spectrum. The inverse transformation is

$$W(f) = 4 \int_0^{\infty} R(\tau) \cos 2\pi f \tau \, d\tau \circ \qquad (1-11)$$

The value of the autocorrelation function for $\tau = 0$ is obviously the mean-square value of $v(t)$, while the value of the autocorrelation function of a random process for $\tau \rightarrow \infty$ is the square of the mean value. Autocorrelation functions also have the properties

$$R(\tau) = R(-\tau),$$

and $\quad |R(\tau)| \leq R(0).$

The normalized autocorrelation function is often useful. It can be written

$$\rho(\tau) = \frac{R(\tau)}{R(0)},$$

and has the property that $\rho(0) = 1.$

Cross-correlation functions are defined in an analogous way:

$$R_{12}(\tau) = \overline{v_1(t)v_2(t-\tau)} = \langle v_1(t)v_2(t-\tau) \rangle.$$

They have the properties that

$$R_{12}(\tau) = R_{21}(-\tau)$$

and

$$\left| R_{12}(\tau) \right| \leq \sqrt{R_{11}(0)R_{22}(0)},$$

where $R_{11}(\tau)$ and $R_{22}(\tau)$ are the autocorrelation functions of $v_1(t)$ and $v_2(t)$, respectively

References

1. For an excellent general introduction to the mathematical description of noise, see Lawson, J. L., and G. E. Uhlenbeck, Threshold Signals, McGraw-Hill, New York, 1950, Chap. III. A more comprehensive and detailed treatment is contained in S. O. Rice's two papers, "The Mathematical Analysis of Random Noise," Bell Syst. Tech. J. 23, 282-332 (1944), and 24, 46-158 (1945), while for a general account of noise and signals in nonlinear systems, see Middleton, D., "Some General Results in the Theory of Noise through Nonlinear Devices," Quart. Appl. Math. 5, 445-498 (1948). A fairly detailed bibliography, including these and other references listed here, is given at the end of this memorandum.

2. In more mathematical language, an ensemble is ergodic if it is stationary, and there is no subset of the functions in the ensemble with a probability different from 0 and 1 which is stationary. For more complete discussions of the ergodic property, see Shannon, C. E., and W. Weaver, The Mathematical

Theory of Communication, The University of Illinois Press, Urbana, Illinois (1949)., p. 51, and James, H. M., N. B. Nichols, and R. S. Phillips, *Theory of Servomechanisms*, McGraw-Hill, New York, 1947, Chap. VI.

3. Middleton, D., "On the Theory of Random Noise: Phenomenonological Models. I," *J. Appl. Phys.* 22, 1143-1152 (1951).

4. Wiener, N , *The Fourier Integral*, Dover, New York, p. 70.

5. Wiener, N., "Generalized Harmonic Analysis," *Acta Math.* 55, 117-258 (1930); Khintchine, A., "Korrelationstheorie stationärer stochastischen Prozesse," *Math. Ann.* 109, 604-615 (1934).

II

SIGNAL-TO-NOISE RATIO AT THE OUTPUT OF A CORRELATOR

In a practical application it is not possible to perform the infinite time averaging which, as indicated in the previous section, is an essential part of the computation of a correlation function. The best we can do electronically is to use some sort of low-pass filter as an averaging network. Because the averaging cannot be extended over an infinitely long time, there appears at the output of the averager, in addition to the correlation function we desire to measure, a fluctuating voltage which we can call the output noise. It is of great interest then to estimate the amplitude of this output noise, and especially what might be called the output signal-to-noise ratio.[1]

Correlator Output Signal-to-Noise Ratio

The mean-square noise (or error) in the output of a practical correlator can be found as the difference of the mean-square of the actual output and the square of the correlation function being measured. For example, if $R_g(\tau,t)$ is the actual output of the correlator, which is, of course, a function of time, and if $R(\tau) = \overline{R_g(\tau,t)}$ is the desired (signal) portion of the output, the mean-square noise is

$$\overline{[R_g(\tau,t) - R(\tau)]^2} = \overline{R_g^2(\tau,t)} - \overline{2R(\tau)R_g(\tau,t)} + R^2(\tau)$$

$$= \overline{R_g^2(\tau,t)} - 2R^2(\tau) + R^2(\tau)$$

$$= \overline{R_g^2(\tau,t)} - R^2(\tau)$$

This procedure will be used below to compute the output noise.

If $f(t)$ is the input to a filter, the output is given by

$$\int_{\infty}^{t} f(t'')g(t-t'')dt'' \ ,$$

which can be written, after a change of variable,

$$\int_0^\infty f(t-t')g(t')dt' \ , \tag{2.1}$$

where $g(t)$ is the **weighting function**[2] of the filter, and has the properties, for a stable filter,

$$g(t) = 0, \text{ for } t < 0, \text{ and } \int_{0-}^\infty g(t)dt = 1 \tag{2.2}$$

When a correlator is used to measure an autocorrelation function, the input to the filter is the product function

$$v(t)v(t-\tau) \ .$$

We can then write the output of the correlator as

$$R_g(t,\tau) = \int_0^\infty g(t')v(t-t')v(t-t'-\tau) \ dt'$$

Its mean-square value is

$$\overline{R_g^2(\tau,t)} = \int_0^\infty g(t')v(t-t')v(t-t'-\tau)dt' \int_0^\infty g(t')v(t-t')v(t-t'-\tau) \ dt'.$$

If we change t in the second integral to t'' to distinguish between the variables of integration, we can write the above as a double integral.

$$\overline{R_g^2(t,\tau)} = \int_0^\infty \int_0^\infty \overline{g(t')g(t'')v(t-t')v(t-t'-\tau)v(t-t'')v(t-t''-\tau)}dt' \ dt''$$

Interchanging the order of summing (integrating) and averaging, we have

$$\overline{R_g^2(t,\tau)} = \int_0^\infty \int_0^\infty g(t')g(t'') \ \overline{[v(t-t'')v(t-t'-\tau)v(t-t'')v(t-t''-\tau)]}dt' \ dt''$$

The brackets enclose what might be called a third-order autocorrelation function. In Appendix I, an expression is derived for the third-order autocorrelation function of a gaussian random process,* in terms of the ordinary autocorrelation function. By comparing the above expression with the first form of Eq. (A1.3) we see that we can write

$$\overline{v(t-t')v(t-t'-\tau)v(t-t'')v(t-t''-\tau)} = R^2(\tau) + R^2(t''-t')$$
$$+ R(t''-t'+\tau)R(t''-t'-\tau),$$

where $R(\tau) = \overline{v(t)v(t-\tau)}$, the (ordinary) autocorrelation function of $v(t)$. Then

$$\overline{R_g^2(t,\tau)} = \int_0^\infty \int_0^\infty g(t')g(t'') [R^2(\tau) + R^2(t''-t')$$
$$+ R(t'' - t'+\tau)R(t''-t'-\tau)]dt'\, dt''.$$

To simplify this expression, we note that the variables of integration appear in the correlation functions only as $t''-t'$, and we therefore make the change of variables

$$t''-t' = \xi \qquad\qquad t''+t' = \eta$$

whence

$$t'' = \frac{\eta+\xi}{2} \qquad\qquad t' = \frac{\eta-\xi}{2}.$$

The Jacobian of this transformation is

$$J\left(\frac{t' t''}{\xi \eta}\right) = \begin{vmatrix} \dfrac{\partial t'}{\partial \xi} & \dfrac{\partial t''}{\partial \xi} \\ \dfrac{\partial t'}{\partial \eta} & \dfrac{\partial t''}{\partial \eta} \end{vmatrix} = -1/2,$$

*At this point we must restrict our consideration to gaussianly-distributed random signals as well as to a gaussianly-distributed background noise. For sinusoidal signals, for example, where $v(t-t')$, $v(t-t'-\tau)$, etc., might consist of a random noise plus a sinusoid, the reduction derived in Appendix I is not valid. Our results below for the limiting case of small input signal-to-noise ratio will not be greatly in error, however, regardless of the character of the signal, since the distribution of the gaussian noise plus small signal will still be very closely gaussian.

so $dt'dt'' = (1/2)d\xi\,d\eta$.

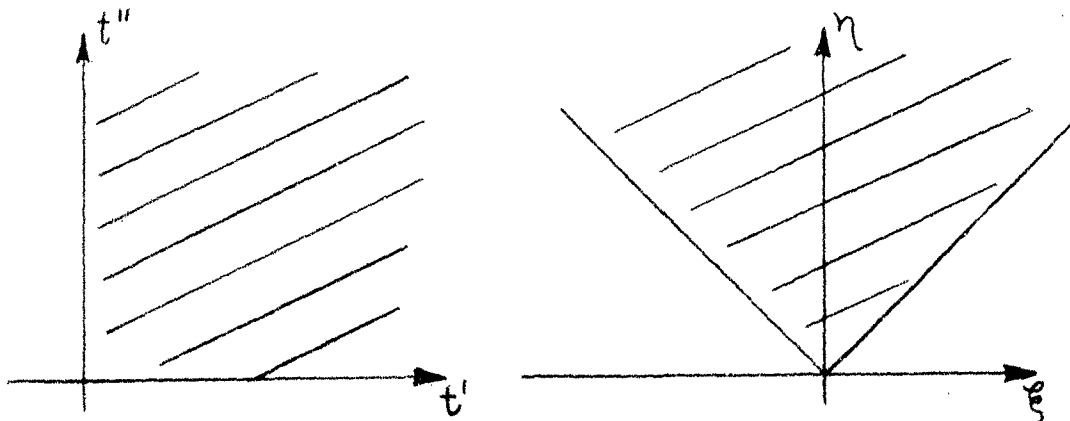The regions of integration are indicated in Fig. 2.1. We see

Fig. 2.1   Regions of integration in the t',t", and in
the ξ- ,η-planes.

that η must be integrated from $|\xi|$ to $+\infty$ and ξ, from $-\infty$ to $+\infty$.
We then have

$$\overline{R_g^2(t,\tau)} = (1/2) \int_{|\xi|}^{\infty} d\eta \int_{-\infty}^{\infty} g(\tfrac{\eta-\xi}{2})g(\tfrac{\eta+\xi}{2})[R^2(\tau)$$

$$+ R(\xi)R(\xi) + R(\xi+\tau)R(\xi-\tau)]d\xi, \qquad (2.3)$$

The η-integration can be performed directly, since η appears only
in the g-functions. We define the <u>transformed weighting function</u>

$$w(\xi) = (1/2) \int_{|\xi|}^{\infty} g(\tfrac{\eta-\xi}{2})g(\tfrac{\eta+\xi}{2})d\eta ,$$

which, after substituting $t = \frac{\eta-\xi}{2}$, becomes

$$w(\xi) = \int_{\frac{|\xi|-\xi}{2}}^{\infty} g(t)g(t+\xi)dt .$$

The lower limit, which might just as well have been taken as $-\infty$,
simply serves to remind us that the weighting functions g(t) vanish

for negative arguments. With that in mind we can write

$$w(\xi) = \int_{-\infty}^{\infty} g(t)g(t+\xi)dt \ .$$

It is readily seen, however, that when $\xi > 0$,

$$w(\xi) = \int_{0}^{\infty} g(t)g(t+\xi)dt$$

and, furthermore, that

$$w(-\xi) = w(\xi) \ . \qquad\qquad (2.4)$$

Equations (2.4) are the most useful form for evaluating the transformed weighting function. It is readily demonstrated that

$$\int_{-\infty}^{\infty} w(\xi)d\xi = 1. \qquad\qquad (2.5)$$

In terms of $w(\xi)$, as defined above, we can write Eq. (2.3)

$$\overline{R_g^2(t,\tau)} = R^2(\tau) + \int_{-\infty}^{\infty} w(\xi)\,[R^2(\xi) + R(\xi+\tau)R(\xi-\tau)]d\xi.$$

The mean square of the correlator output noise is then

$$\overline{R_g^2(t,\tau)} - R^2(\tau) = \int_{-\infty}^{\infty} w(\xi)[R^2(\xi) + R(\xi+\tau)R(\xi-\tau)]d\xi \ , \qquad (2.6)$$

and, taking as the signal the average output of the correlator, the mean-square output signal-to-noise ratio is

$$(S/N)_{out} = \frac{R^2(\tau)}{\displaystyle\int_{-\infty}^{\infty} w(\xi)[R^2(\xi) + R(\xi+\tau)R(\xi-\tau)]d\xi} \ . \qquad (2.7)$$

When the correlator is used to measure a cross-correlation

function, the input to the averager is the product function

$$v_A(t)v_B(t-\tau)$$

and, using the first form of Eq. (A1.4), we can show by the same method as above that the mean-square output signal-to-noise ratio is

$$(S/N)_{out} = \frac{R_{AB}^2(\tau)}{\int_{-\infty}^{\infty} w(\xi) \ [R_{AA}(\xi)R_{BB}(\xi) + R_{AB}(\xi+\tau)R_{BA}(\xi-\tau)]d\xi} \ . \tag{2.8}$$

Weighting Functions

The evaluation of a correlator's output signal-to-noise ratio depends upon the weighting function of the averager which is used, and more specifically, in the above formulation, on the transformed weighting function. The weighting functions and transformed weighting functions for three simple averagers will be given below.

The weighting function of a filter network is its impulse response, or output for a delta-function input, initiated at time $t = 0$, and may conveniently be found, for stable filters, as the Fourier transform of the voltage response spectrum of the filter, which is simply the complex ratio of the open-circuit output voltage to the input voltage. For the low-pass averager of Fig. 2.2, the voltage response spectrum is

$$\frac{e_o}{e_i} = \frac{1/j\omega C}{R + 1/j\omega C},$$

and the weighting function is readily determined to be

$$g(t) = \frac{1}{RC} e^{-t/RC}, \quad t > 0;$$
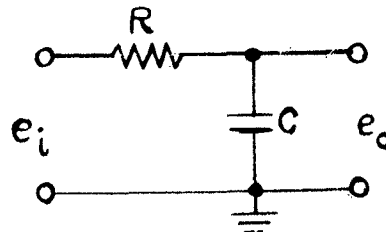
$$= 0, \quad t < 0.$$

Fig. 2.2. RC Averaging Network.

Then from Eqs. (2.4), we find the transformed weighting function to be

$$w(\xi) = \frac{1}{2RC} e^{-|\xi|/RC}, \quad \text{for all } \xi. \tag{2.9}$$

A simple and quick comparison of different averagers may be made on the basis of their responses to a unit step input. Just as the unit step is the integral of the unit impulse, the response of a network to a unit step is the integral with respect to t of the impulse response. Calling the unit step response $U(t)$, we have, for the RC network,

$$U(t) = 1 - e^{-t/RC}, \quad t \geq 0.$$

In the same way, these three functions may be determined for the critically damped RLC circuit of Fig. 2.3. The voltage response spectrum is

$$\frac{e_o}{e_i} = \frac{1}{1 + j\frac{L'}{R'}\omega - L'C'\omega^2},$$

and critical damping occurs when $R' = \frac{1}{2}\sqrt{L'/C'}$, making the voltage spectrum for this case

$$\frac{1}{(1 + j\frac{1}{2}\sqrt{\frac{L'}{C'}}\omega)^2}.$$

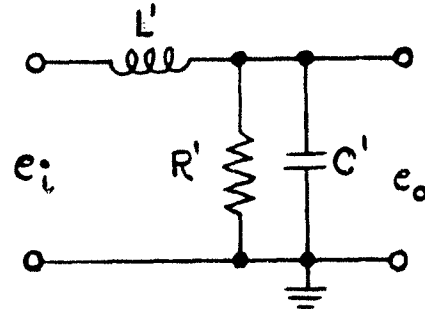Fig. 2.3. Critically damped RLC averager. $(R=\frac{1}{2}\sqrt{L'/C'})$.

The weighting function is then

$$g(t) = \frac{1}{4(R'C')^2} t\, e^{-t/R'C'}, \quad t \geq 0,$$

and the transformed weighting function is

$$w(\xi) = \frac{1}{16(R'C')^2} [2R'C' + |\xi|] e^{-|\xi|/2R'C'}.$$

The unit step response is

$$U(t) = 1 - (1 + t/2R'C')e^{-t/2R'C'}, \qquad t \geq 0.$$

The response of a finite-time "perfect averager" to an input function $f(t)$ is

$$\frac{1}{T_1} \int_0^{T_1} f(t-t')dt',$$

where T_1 is the length of the interval over which the average is computed. By comparison with Eq. (2.1) we see that the weighting function is

$$g(t) = 1/T_1, \qquad\qquad 0 < t < T_1;$$

$$= 0, \qquad\qquad t < 0 \text{ and } t > T_1.$$

No realizable network has this weighting function; it is, however, mathematically convenient for comparison purposes, and, if necessary, its operation could be approximated by various arrangements, one of which is shown schematically in Fig. 2.4.
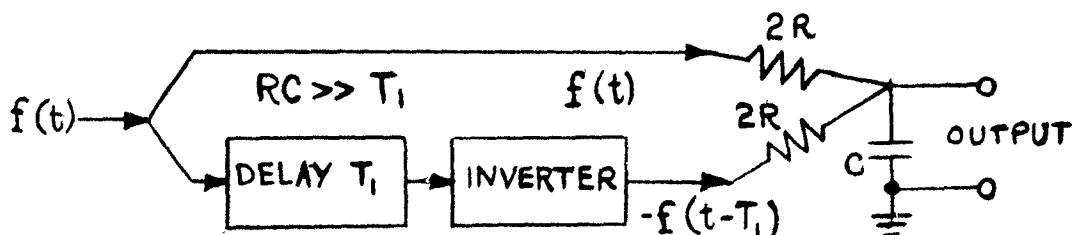

Fig. 2.4. Circuit for Approximating Operation of a Finite-time Perfect Averager.

The transformed weighting function is

$$w(\xi) = \frac{1}{T_1} (1 - |\xi|/T_1), \qquad |\xi| \leq T_1;$$

$$= 0, \qquad\qquad |\xi| > T_1,$$

and the unit step response is

$$U(t) = t/T_1, \qquad\qquad 0 < t \leq T_1;$$

$$= 1, \qquad\qquad t > T_1.$$

These three averaging systems may be compared by examining their step responses after adjusting their time constants so that their noise-reducing properties for wide-band input noise are the same. Equation (2.6) gives the mean-square value of the noise at the output of the averager. Now the range of τ over which a correlation function $R(\tau)$ is appreciably different from zero is roughly equal to the reciprocal of the signal bandwidth. Similarly, the extent of the transformed weighting function $w(\zeta)$ is inversely proportional to the width of the pass-band of the averaging network. For good smoothing the pass-band of the averager must be small compared to the bandwidth of the signal. Usually, therefore, the principal contribution to the integral of Eq. (2.6) comes in the region where $w(\zeta)$ is not substantially different from $w(0)$. In this case, then, Eq. (2.6) may be replaced by the approximate form

$$\overline{R_g^2(t,\tau)}-R^2(\tau) = w(0) \int_{-\infty}^{\infty} [R^2(\zeta)+R(\zeta+\tau)R(\zeta-\tau)]d\zeta.$$

The mean-square noise output for a given (wide) input spectrum is therefore proportional to $w(0)$. Numerical values of the time constants of the three averaging networks discussed above were chosen so that $w(0)$ was the same in all three cases, and the resulting weighting functions, transformed weighting functions, and responses to a unit step are plotted, to the same scale, in Figs. 2.5, 2.6, and 2.7, respectively. It is to be noted that the rise times are roughly equal when the noise-reducing properties are equal. There does exist an advantage in using the optimum filter for a given input function; this will be discussed in a following section.

Correlator Output Signal-to-Noise Ratio; Specific Examples

The correlator output signal-to-noise ratio was shown in Eq. (2.8) to depend on the transformed weighting function of the averager and on the auto- and cross-correlation functions

of the inputs. Using the transformed weighting function given
in the preceding section for the RC averager, and the autocorre-
lation functions derived in Appendix II, we can reduce Eq. (2.8)
to a much simpler expression, subject to a few restrictive condi-
tions which often pertain. We assume first that the two inputs
to the correlator are made up of various combinations of two
random noises $n_1(t)$ and $n_2(t)$, of equal amplitude, and a noise
signal $s(t)$, all three being statistically independent and
having the same rectangular spectrum of half-width Δf and center
frequency f_o. These signals then have the autocorrelation func-
tions

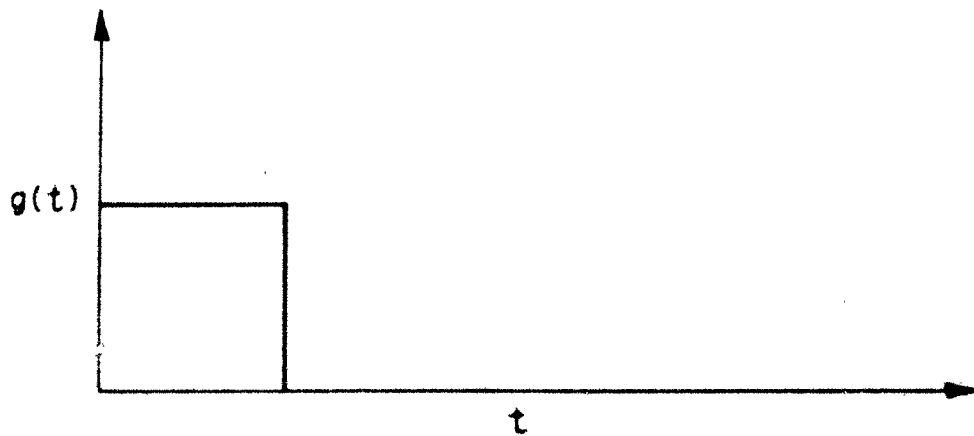$$R_1(\tau) = N\left(\frac{\sin 2\pi\Delta f \tau}{2\pi\Delta f \tau}\right) \cos 2\pi f_o \tau$$

$$R_2(\tau) = N\left(\frac{\sin 2\pi\Delta f \tau}{2\pi\Delta f \tau}\right) \cos 2\pi f_o \tau$$

$$R_s(\tau) = S\left(\frac{\sin 2\pi\Delta f \tau}{2\pi\Delta f \tau}\right) \cos 2\pi f_o \tau$$

where N and S are the mean-square values of the noise and the
signal, respectively. We assume that the correlator uses an
RC averager, and we use the transformed weighting function
given in Eq. (2.9). Now, as we noted above, if the pass-band
of the averaging network is small compared to the bandwidth
of the signal, we may assume that the principal contribution to
the integral in Eq. (2.8) comes in the region where $w(\xi)$ is not
substantially different from $w(0)$. Subject to this assumption
that $1/RC \ll \Delta f$, Eq. (2.8) becomes (with τ set equal to zero, to
give the maximum signal output, the signal $s(t)$ being assumed
present in both channels without relative delay), ·

$$(S/N)_{out} = \frac{R_{AB}^2(0)}{\frac{1}{2RC}\int_{-\infty}^{\infty} [R_{AA}(\xi) R_{BB}(\xi) + R_{AB}(\xi)R_{BA}(\xi)]d\xi}.$$

We consider four different modes of operation:

g(t)

t

FINITE-TIME PERFECT AVERAGER

g(t)

t

RC LOW-PASS NETWORK

g(t)

t
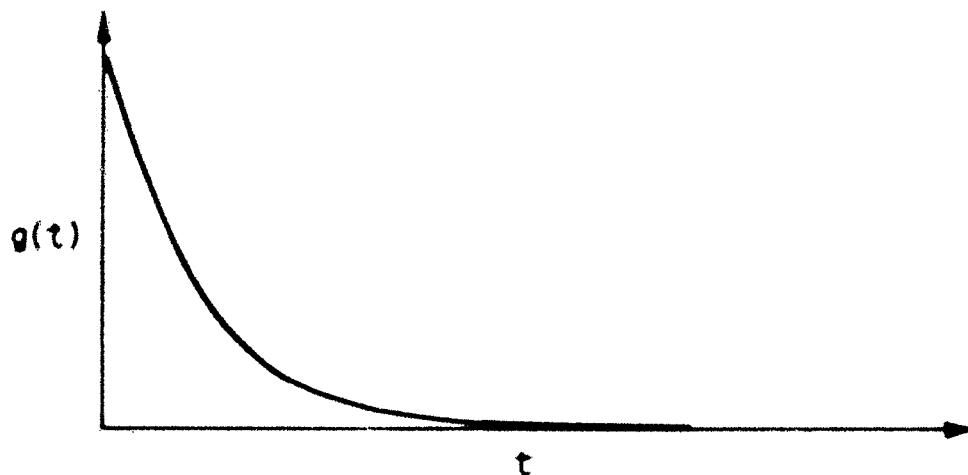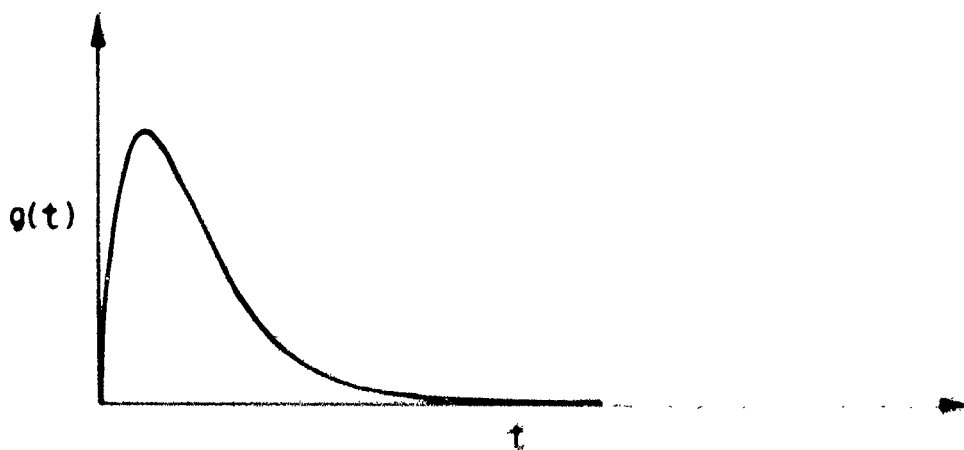
CRITICALLY-DAMPED RLC NETWORK

Fig. 2.5. Weighting functions for three averagers.

W(ξ)

FINITE-TIME PERFECT AVERAGER

W(ξ)

RC LOW-PASS NETWORK

W(ξ)

CRITICALLY-DAMPED RLC NETWORK
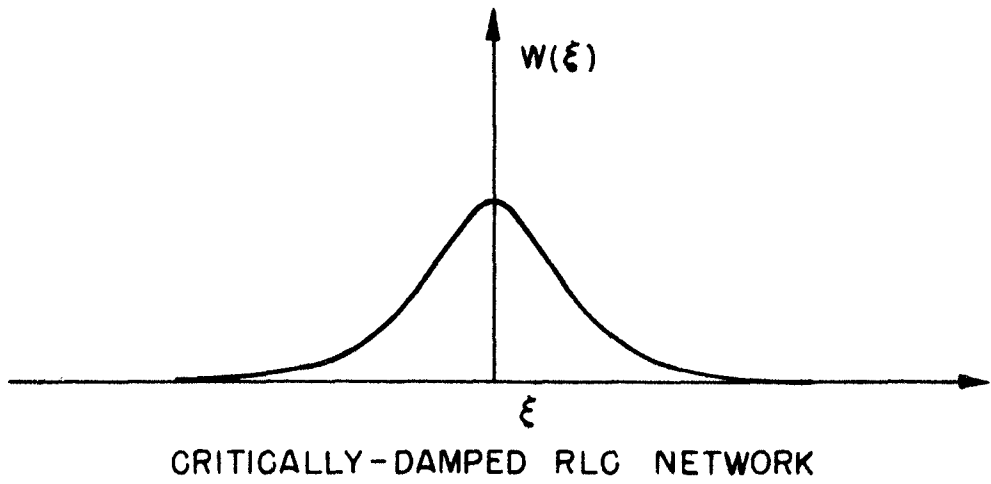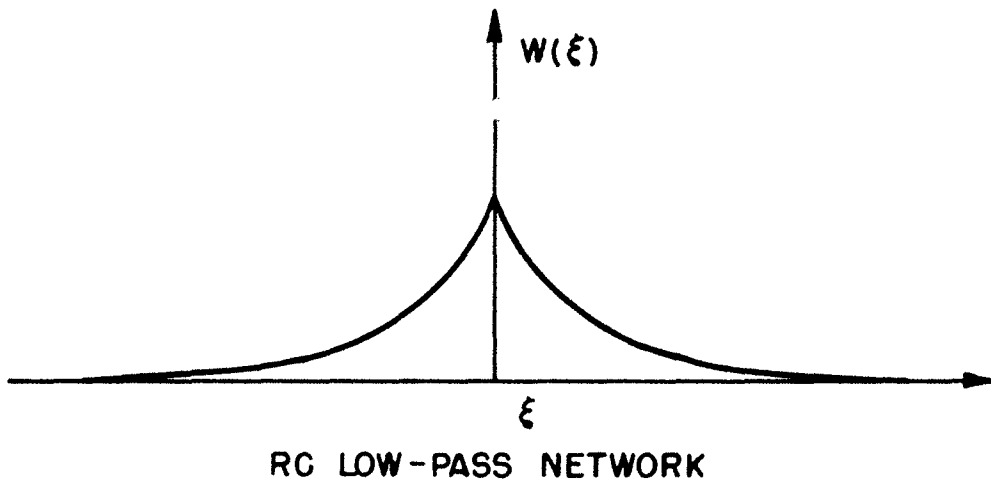
Fig. 2.6. Transformed weighting functions for three averagers.
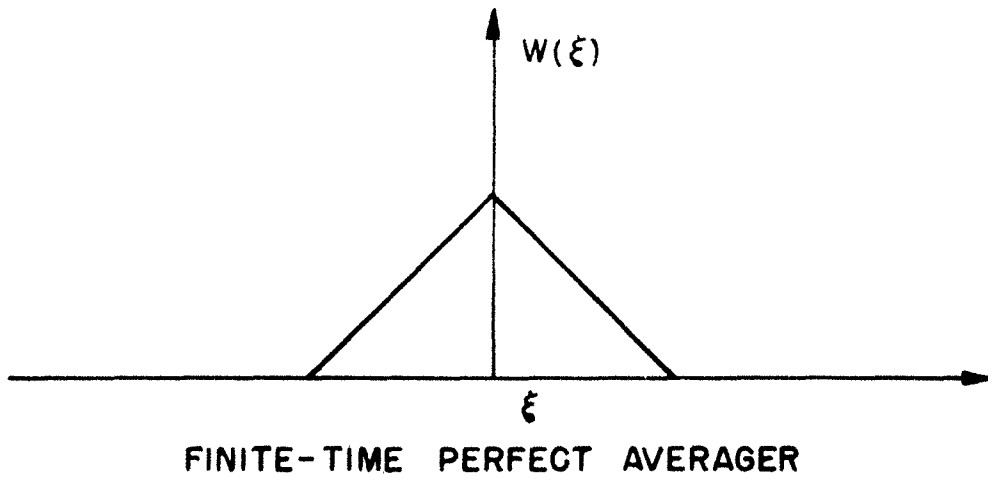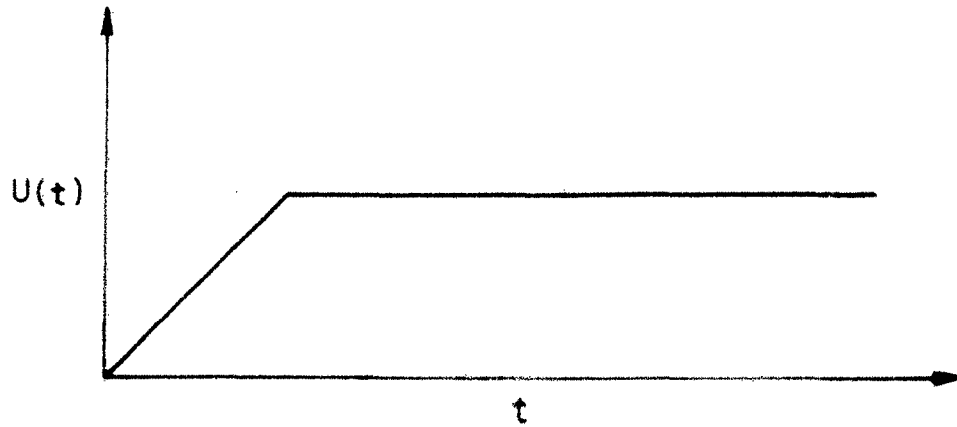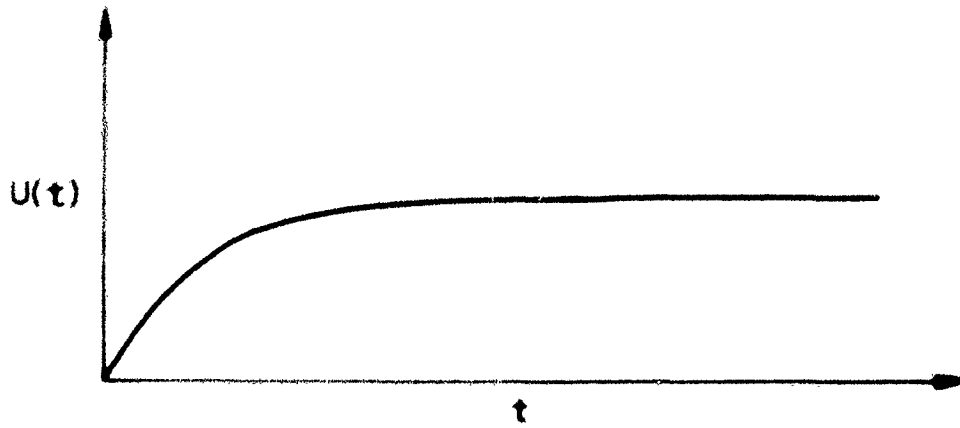
U(t)

t

FINITE-TIME PERFECT AVERAGER

U(t)

t

RC LOW-PASS NETWORK

U(t)

t
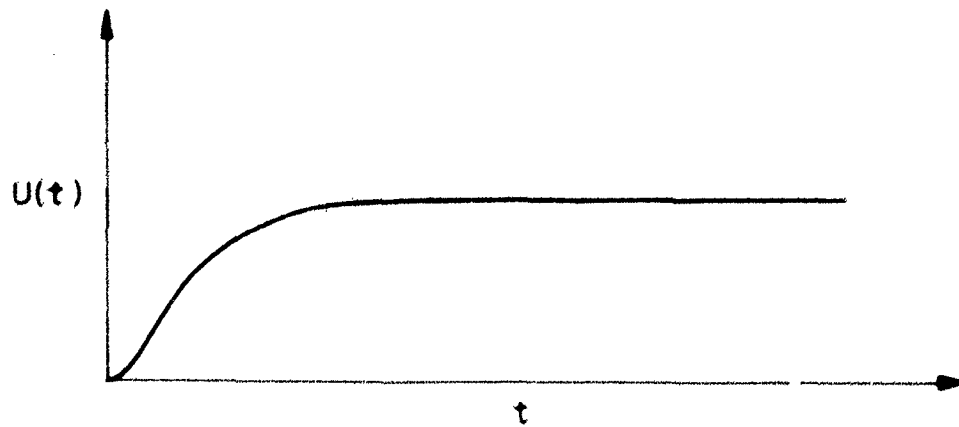
CRITICALLY-DAMPED RLC NETWORK

Fig. 2.7. Unit step responses for three averagers.

I. **Both inputs s(t):** In this case we have the maximum output signal-to-noise ratio which occurs in the measurement of an autocorrelation function or the "signal-to-noise ratio" for the measurement of the mean-square of s(t). We have

$$R_{AA}(\xi) = R_{BB}(\xi) = R_{AB}(\xi) = R_{BA}(\xi) = S(\frac{\sin 2\pi\Delta f \xi}{2\pi\Delta f \xi})\cos 2\pi f_0 \xi,$$

so

$$(S/N)_{out} = \frac{S^2}{\frac{S^2}{RC} \int_{-\infty}^{\infty} (\frac{\sin 2\pi\Delta f \xi}{2\pi\Delta f \xi})^2 \cos^2 2\pi f_0 \xi \, d\xi}$$

$$= \frac{2RC\Delta\omega}{\pi},$$

where $\Delta\omega = 2\pi\Delta f$. We see for the first time here the very general and well-known result that the output mean-square signal-to-noise ratio is proportional to the product of the input bandwidth and the output time constant.

II. **Both inputs $[n_1(t)+s(t)]$:** Here the correlator is simply used as a square-law detector to determine the presence of a signal in noise. We have

$$R_{AA}(\xi) = R_{BB}(\xi) = R_{AB}(\xi) = R_{BA}(\xi) = (N+S) \frac{\sin 2\pi\Delta f \xi}{2\pi\Delta f \xi} \cos 2\pi f_0 \xi.$$

The d-c output in this case is $R_{AB}(0) = N + S$. We take as the output signal simply S, assuming that the d-c voltage N can be biased out, or ignored. The output signal-to-noise ratio is then

$$(S/N)_{out} = \frac{S^2}{\frac{(N+S)^2}{RC} \int_{-\infty}^{\infty} (\frac{\sin 2\pi\Delta f \xi}{2\pi\Delta f \xi})^2 \cos^2 2\pi f_0 \xi \, d\xi}$$

$$= \frac{2S^2 RC}{\pi(N+S)^2} \Delta\omega$$

and, if $S \ll N$,

$$(S/N)_{out} = \frac{2RC\Delta\omega}{\pi} (S/N)^2_{in} \quad .$$

III. <u>One Input $[n_1(t)+s(t)]$, other input $[n_2(t)+s(t)]$</u>:

The correlator is used here to determine the presence of a common signal in two different samples of signal in noise.

$$R_{AA}(\xi) = R_{BB}(\xi) = (N+S) \frac{\sin 2\pi\Delta f \xi}{2\pi\Delta f \xi} \cos 2\pi f_o \xi$$

$$R_{AB}(\xi) = R_{BA}(\xi) = S \frac{\sin 2\pi\Delta f \xi}{2\pi\Delta f \xi} \cos 2\pi f_o \xi$$

and

$$(S/N)_{out} = \frac{4S^2 RC \Delta\omega}{[(N+S)^2 + S^2] \pi} \quad .$$

In the limiting case where $S \ll N$,

$$(S/N)_{out} = \frac{4RC \Delta\omega}{\pi} (S/N)^2_{in} \quad .$$

IV. <u>One Input $[n_1(t) + s(t)]$, other input $\sqrt{N/S} \, s(t)$</u>:

Here a standard sample of the signal of constant mean-square amplitude N is cross-correlated with the signal and noise. We have

$$R_{AA}(\xi) = (N+S) \left(\frac{\sin 2\pi\Delta f \xi}{2\pi\Delta f \xi}\right) \cos 2\pi f_o \xi$$

$$R_{BB}(\xi) = N \left(\frac{\sin 2\pi\Delta f \xi}{2\pi\Delta f \xi}\right) \cos 2\pi f_o \xi$$

$$R_{AB}(\xi) = R_{BA}(\xi) = \sqrt{SN} \left(\frac{\sin 2\pi\Delta f \xi}{2\pi\Delta f \xi}\right) \cos 2\pi f_o \xi$$

and

$$(S/N)_{out} = \frac{4NS \, RC \, \Delta\omega}{[N(N+S) + NS] \pi} \quad ,$$

which becomes, if $S \ll N$,

$$(S/N)_{out} = \frac{4RC\Delta\omega}{\pi} (S/N)_{in} .$$

In this mode of operation the output signal-to-noise ratio is pro-
portional to the _first_ power of the input signal-to-noise ratio,
resulting in an advantage of a _factor 2 in decibels_ over the other
arrangements above, for small input signal-to-noise ratios. The
process from which this saving results is known as "predetector
integration," and always involves knowing the instantaneous wave-
form (phase) of the signal being sought. This is the principle
behind so-called phase or coherent detectors. In cases II and III,
where the small-signal output signal-to-noise ratio is proportional
to the square of the input signal-to-noise ratio, we have the phe-
nomenon of "signal suppression."[4]

Comparison of cases II and III for the square-law detector
and the correlator must be made very carefully The results
above show that if two samples of the same signal in incoherent
background noises are available, the correlator can produce a sig-
nal-to-noise ratio 3 db better than that of the square-law detec-
tor (operating on one sample of the signal in noise). Obviously,
if two samples of the signal in incoherent noises are available,
they can be added and applied to the square-law detector, where,
with the input signal-to-noise ratio increased by 3 db, the out-
put signal-to-noise ratio will be increased by 6 db, a result
3 db better than for the correlator The correlator, on the
other hand, produces no d-c output independent of the signal, a
practical advantage that should not be overlooked

For the case of noise whose spectrum is that of a single-
tuned resonant circuit of at least moderately high Q, we use the
autocorrelation function derived in Appendix II,

$$R(\tau) = e^{-\omega_P|\tau|} \cos\omega_0\tau,$$

where $\omega_P/2\pi$ is the half-bandwidth to the half-power point, and
$\omega_0/2\pi$ is the center frequency Assuming, as before, that
$1/RC \ll \omega_P$, and also that $\omega_P \ll \omega_0$, so that with little error
we may replace the $\cos^2\omega_0\tau$ by its average value $(1/2)$ we

have*

$$\int_{-\infty}^{\infty} w(\xi)R^2(\xi)d\xi$$

$$= \frac{1}{2RC}\int_0^{\infty} e^{-2\omega_F\xi}\, d\xi$$

$$= \frac{1}{2RC} \cdot \frac{1}{2\omega_F} = \frac{1}{4RC\omega_F} \, .$$

The formulas derived above for the rectangular spectrum may then be specialized to the case of the tuned-circuit spectrum of moderately high Q by replacing the factor $\frac{\pi}{4RC\triangle\omega}$ by $\frac{1}{4RC\omega_F}$. These output signal-to-noise ratios are summarized for the two cases in Table 2.1.

Averager Efficiency and Optimum Filters

Unfortunately, the signal-to-noise ratios derived theoretically in the preceding section are never achieved in practice. It was assumed in the derivation that the d-c signal in the output of the averager had built up to its ultimate value, while with the exception of the finite-time perfect averager, this requires an infinitely long time. In practice, either because the receiver is scanned in one or more angular dimensions, or because of the transitory nature of the signals themselves, an infinitely long observation time is not available. If one used an averager with such a short time constant that the d-c signal in the output does very nearly attain its ultimate value during the epoch of the

- - - - - - -

*Although the integration could be carried out easily without replacing the $\cos^2$ by its average, it would not be exactly correct to do so, since the more exact form of the autocorrelation function for low-Q circuits (see Appendix II) should be used in the wide-band case.

TABLE ...: PEAK SIGNAL-TO-NOISE RATIO AT THE OUTPUT OF A CORRELATOR FOR TWO DIFFERENT INPUT SPECTRA AND AN RC AVERAGER, ASSUMING LONG AVERAGING TIME.

INPUTS	OUTPUT SIGNAL-TO-NOISE RATIO	
	Rectangular Spectrum	Tuned-Circuit Spectrum (Moderately High-Q)
BOTH INPUTS S(t) Maximum output signal-to-noise ratio which occurs (at $\tau = 0$) in the measurement of an autocorrelation function = "signal-to-noise ratio" in measurement of mean-square of s(t).	$\dfrac{2RC\Delta\omega}{\pi}$	$2RC\omega_F$
BOTH INPUTS $[N_1(t)+S(t)]$ DC output due to noise ignored. Correlator used here as a square-law detector.	Formulae below valid for small input signal-to-noise ratio only: $\dfrac{2RC\Delta\omega}{\pi}\,(S/N)^2_{IN}$	$2RC\omega_F\,(S/N)^2_{IN}$
$\left[N_1(t)+S(t)\right]$ and $\left[N_2(t)+S(t)\right]$	$\dfrac{4RC\Delta\omega}{\pi}\,(S/N)^2_{IN}$	$4RC\omega_F\,(S/N)^2_{IN}$
$\left[N_1(t)+S(t)\right]$ and $\sqrt{\dfrac{N}{S}}\,S(t)$ Second input is pure signal of ... amplitude N.	$\dfrac{4RC\Delta\omega}{\pi}\,(S/N)_{IN}$	$4RC\omega_F\,(S/N)_{IN}$

signal, then one is not obtaining the greatest possible output
signal-to-noise ratio because increasing the time constant will,
for a while, cause the noise to decrease faster than the signal.
It is therefore important to consider the time-functional form
of the signal as it appears at the input to the averager, and
the general problem of specifying the optimum type of averager
for detecting the presence of that signal in noise. We here
define the optimum averager (for a signal of finite duration)
as that one which produces the greatest peak-signal-to-rms-
noise ratio at its output. It is not necessarily true that
such an averager produces at the same time the most easily
discernible signal (in the presence of noise) to the eye. It
is reasonable to assume that this is a fairly satisfactory
criterion of detectability, however, and it is mathematically
convenient. Woodward,[5] by applying the theory of inverse proba-
bility, has specified much the same criterion for extracting the
greatest possible amount of information from a radar signal.
Other optimum filter criteria have been used; for example:
(1) minimization of the mean-square error[6] (best possible re-
covery of the shape of the input signal) and a closely related
method of minimizing an arbitrarily defined "distortion,"[7] and
(2) minimization of the mean-square error in determining the
average value of a noise wave (or of measuring a steady d-c
voltage in the presence of noise) when there is only a finite
time available for the measurement.[8]

It has been shown by Van Vleck and Middleton[9] that the
filter which gives the best output peak-signal-to-rms-noise
ratio when the input noise bandwidth is much larger than that
of the signal pulse is simply that filter whose weighting func-
tion is proportional to the time-functional form of the signal
backwards.* (The result was expressed originally in spectral
language.) This optimum filter is called the "matched" filter.
- - - - - - -
*The weighting function of a physically realizable passive net-
work must vanish for negative arguments. This makes difficult
the problem of constructing a passive filter to match a pulse
whose time-functional form extends a considerable distance

Their mathematical proof will not be repeated here; it was
applied by them specifically to the case of a pre-detection
filter on the basis of maximizing the post-detector signal-to-
noise ratio, but exactly the same arguments may be applied in
this case. Van Vleck and Middleton state further that if the
optimum pre-detection filter is used, no post-detection filter
can improve the signal-to-noise ratio further.[10] In a correla-
tion system, on the other hand, pre-multiplication filters are
used (with broad-band signals) mainly to determine the shape of
the correlation function being measured, by establishing the
signal spectrum, the signal at the output of the correlator
being determined in many cases by the relative delay of the
two input signals rather than by modulation of a carrier.
The greatest part of the signal-to-noise ratio improvement by
filtering must then be obtained in a post-multiplication filter.

We here define the "efficiency" of an averager for a signal
of finite duration to be the output peak-signal-squared-to-mean-
square-noise ratio divided by that same quantity for the matched
filter. Efficiency thus is a numeric which runs from 0 to 1.
Our averager efficiency differs from that defined by Eckart[11]
in that we assume that the background noise has always been
present at the input to the filter, while he assumed that the
noise and signal were applied simultaneously.[12] We feel that
our definition is more realistic for the case where the receiver
is "on" continuously and signals arrive at the input from time
to time. The efficiencies have been computed by very straight-
forward methods, by finding the peak value of the transient
response of the filter, squaring that value, and dividing by
the transformed weighting function of zero argument, which, as

- - - - - - -
either side of its peak or center. However, one method has been
suggested for constructing an active filter which can have weight-
ing functions that do not necessarily vanish for negative argu-
ments (see Ref. 7 above). If the pulse is symmetrical, there
is an advantage of 3 db in using the symmetrical weighting
function over using (the physically realizable) half of it.

we showed above, is proportional to the mean-square noise output, when the averager band-pass is narrow compared to the input bandwidth, and normalizing. The illustrations below are thus valid only for relatively wide-band input background noise. Averager efficiencies for detection of a rectangular pulse of length T_0 are plotted in Fig. 2.8. for the three averagers whose weighting functions were given above. The abcissa, x, is, for the finite-time perfect averager, T_1/T_0; for the RC averager, $2RC/T_0$; and for the critically damped LRC circuit, $8R'C'/T_0$. It can be seen that the time constant of the averager must be adjusted carefully to the pulse to achieve the best signal-to-noise ratio, and particularly so in the case of the finite-time perfect averager.

Averager efficiencies for detection of a "backwards" exponential pulse having the time-functional form

$$f(t) = e^{t/T_0}, \qquad t \leq 0,$$

$$= 0, \qquad t > 0,$$

are plotted for the same three averagers in Fig. 2.9. In this graph, x is RC/T_0 for the RC averager; T_1/T_0 for the finite-time perfect averager; and $8R'C'/T_0$ for the critically damped LRC circuit. The backwards exponential pulse was chosen to match the RC averager, and the advantage of this filter over the others is clearly apparent. As here defined, averager efficiency is proportional to relative peak-signal-squared-to-mean-square-noise ratio, so that a decibel scale can be used to compare the different averagers. A decibel scale has therefore been added to the right-hand side of Figs. 2.8 and 2.9. The differences between these three filters in the region near x = 1 are thus seen to be rather small in decibel measure.

By reference to Figs. 2.8 and 2.9 it may be seen that the degree to which a filter is optimum is closely related to the extent to which its weighting function matches the pulse being detected. One would therefore expect that an RC averager, for

example, would be a relatively poor averager for the detection
of the presence of a signal pulse having the form of a correla-
tion function such as that shown in Fig. 2.10. This is the
autocorrelation function of random noise having a spectrum
equal to the intensity response of a tuned circuit with $Q = 8$.
Approximate calculations have been made comparing the RC
averager with the best time constant for the purpose with the
matched symmetrical (physically unrealizable) filter. For
fairly high Q's it was found that there is an improvement in
the peak-signal-squared-to-mean-square-noise ratio of approxi-
mately a factor Q. This improvement factor diminishes to unity
as $Q \longrightarrow 0$. It is noteworthy that the optimum filter for such a
correlation function is not an averager but a band-pass filter!
This is the best filter for detecting the presence of correlation
but not the best filter for an accurate measurement of the corre-
lation function, which requires a d-c measurement.

Incidental to the above calculations, the relative efficiency
of an RC averager for the detection of a sinusoid of frequency
$\omega_0/2\pi$ in wide-band noise has been computed and is displayed in
Fig. 2.11 as a function of the product $RC\omega_0$. The maximum
efficiency occurs at $RC = 1/\omega_0$; this may be taken as an approxi-
mate best value of the time constant RC for the detection of a
correlation function of the form of Fig. 2.10, where $\omega_0/2\pi$ is
the frequency of the modulated cosine wave of the correlation
function as it appears at the output of the multiplier

It is possible that the filtering process might be re-
placed by a correlation method, especially for the purpose of
achieving nonphysically realizable weighting functions. If an
electrical function generator could be constructed to generate
the desired weighting function, the operations of multiplication
and integration indicated in Eq. (2.1) could be performed elec-
tronically. (This would require at least an approximation to a
finite-time perfect averager to perform the indicated integra-
tion.) This method would be somewhat complicated by the fact
that each different possible time of arrival of a signal would

"EFFICIENCY" OF AVERAGER

RELATIVE PEAK-SIGNAL-SQUARED-TO-MEAN-SQUARE-NOISE RATIO – DECIBELS

X →
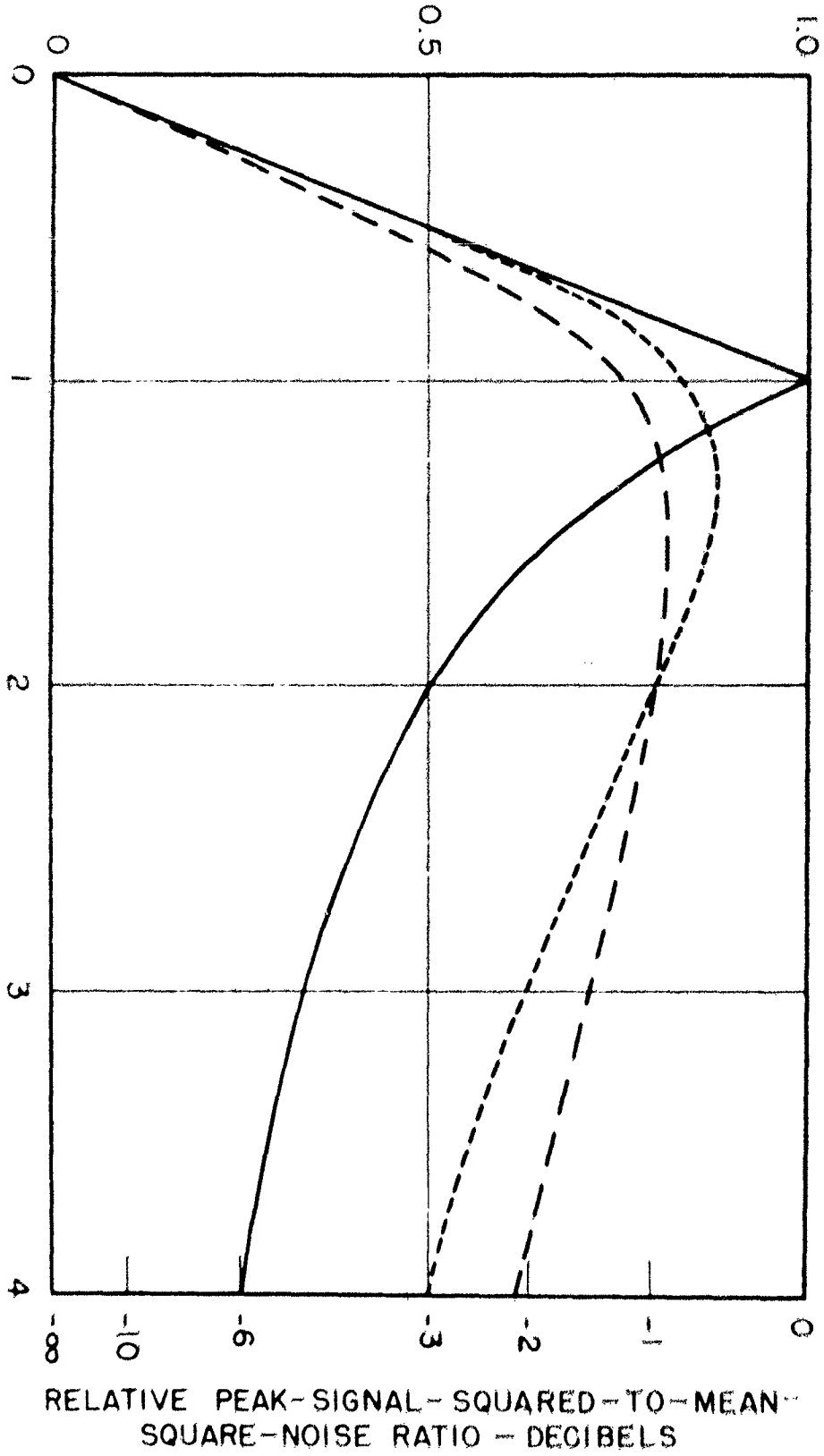
Fig. 2.2. "Efficiency" of averagers for detection of rectangular pulse of length T_0 in wide-band noise. Solid curve: Finite-time perfect averager over interval T_1, $x = T_1/T_0$; Long-dash curve: RC averager, $x = 2RC/T_0$; Short-dash curve: Critically-damped LC circuit, $x = RC/T_0$.

"EFFICIENCY" OF AVERAGER

RELATIVE PEAK-SIGNAL-SQUARED-TO-MEAN-SQUARE-NOISE RATIO — DECIBELS

X →

Fig. 2.9. "Efficiency" of averagers for detection of backwards exponential pulse, e^{t/T_o}, $-\infty < t \le 0$, in wide-band noise. Solid curve: Finite-time perfect averager over interval T_1, $x = T_1/T_o$; Long-dash curve: RC averager, $x = RC/T_o$; Short-dash curve: Critically-damped LRC circuit, $x = 8R'C'/T_o$.

Fig. 2.15. Autocorrelation function of tuned-circuit noise; Q = 8.

Fig. 2.11. Relative "efficiency" of an RC averager for the detection of a sinusoid of frequency $\omega_o/2\pi$ in wide-band noise.

have to be investigated separately, while, with a passive filter
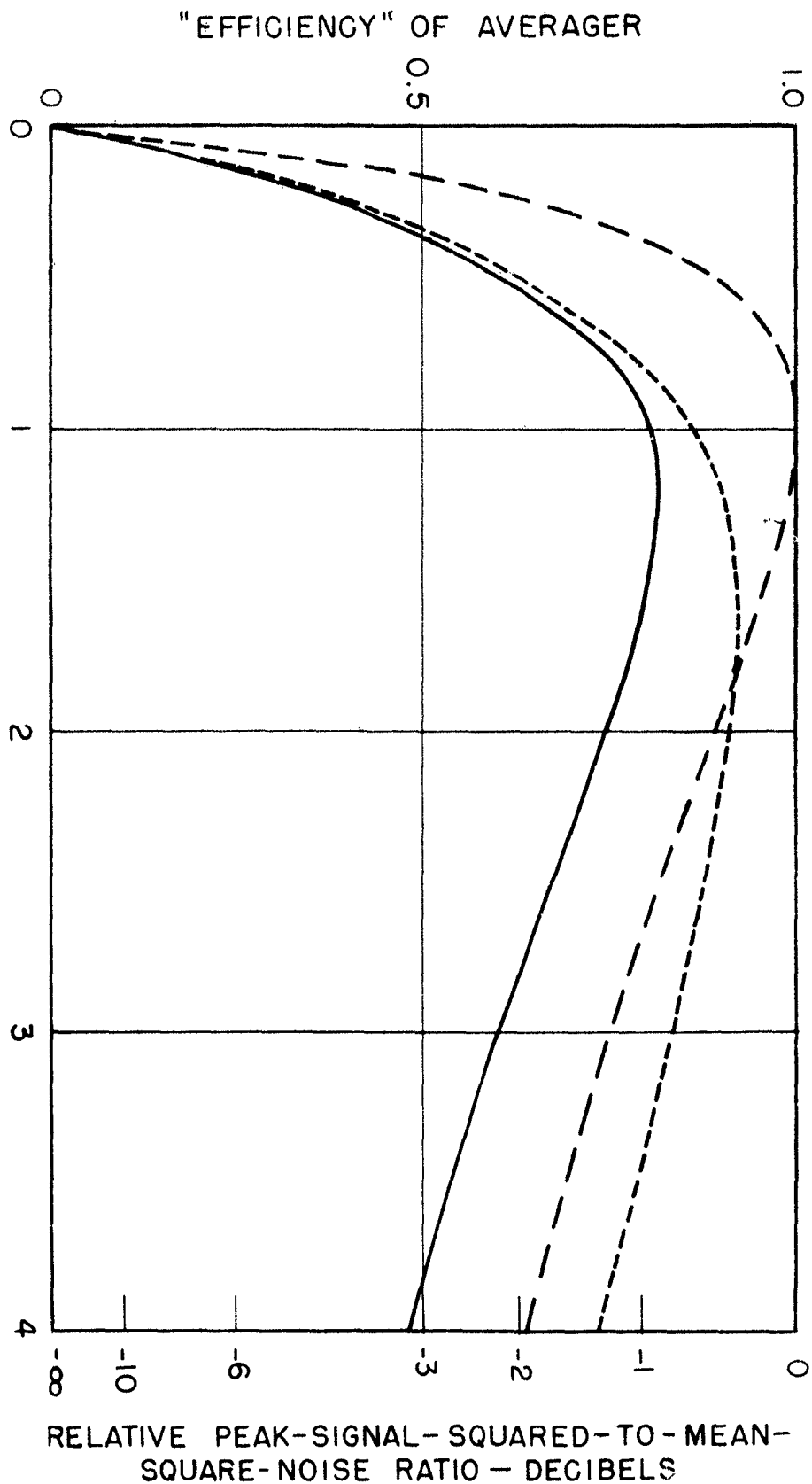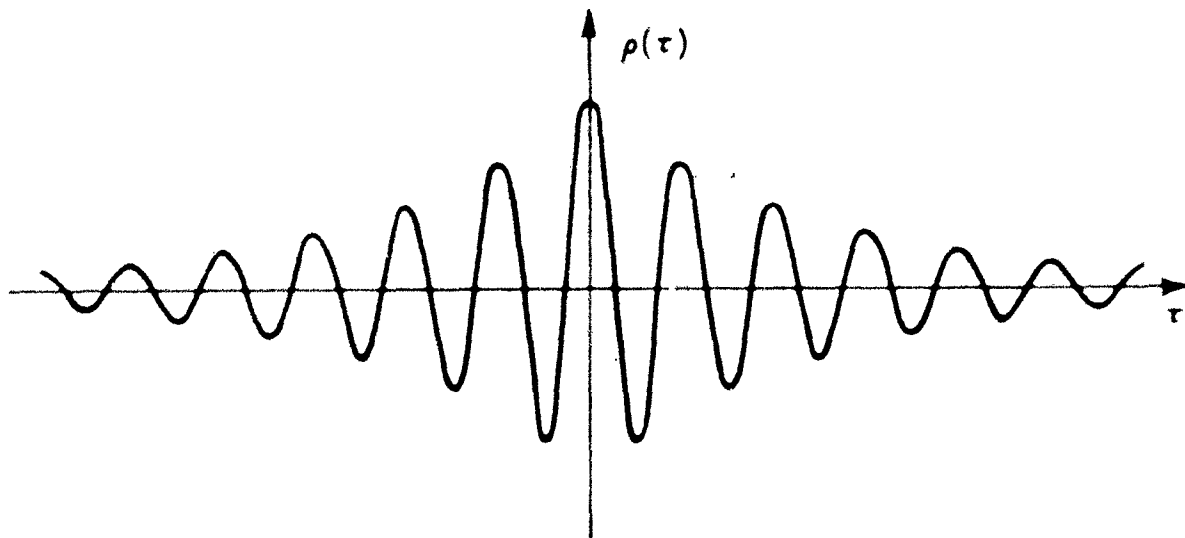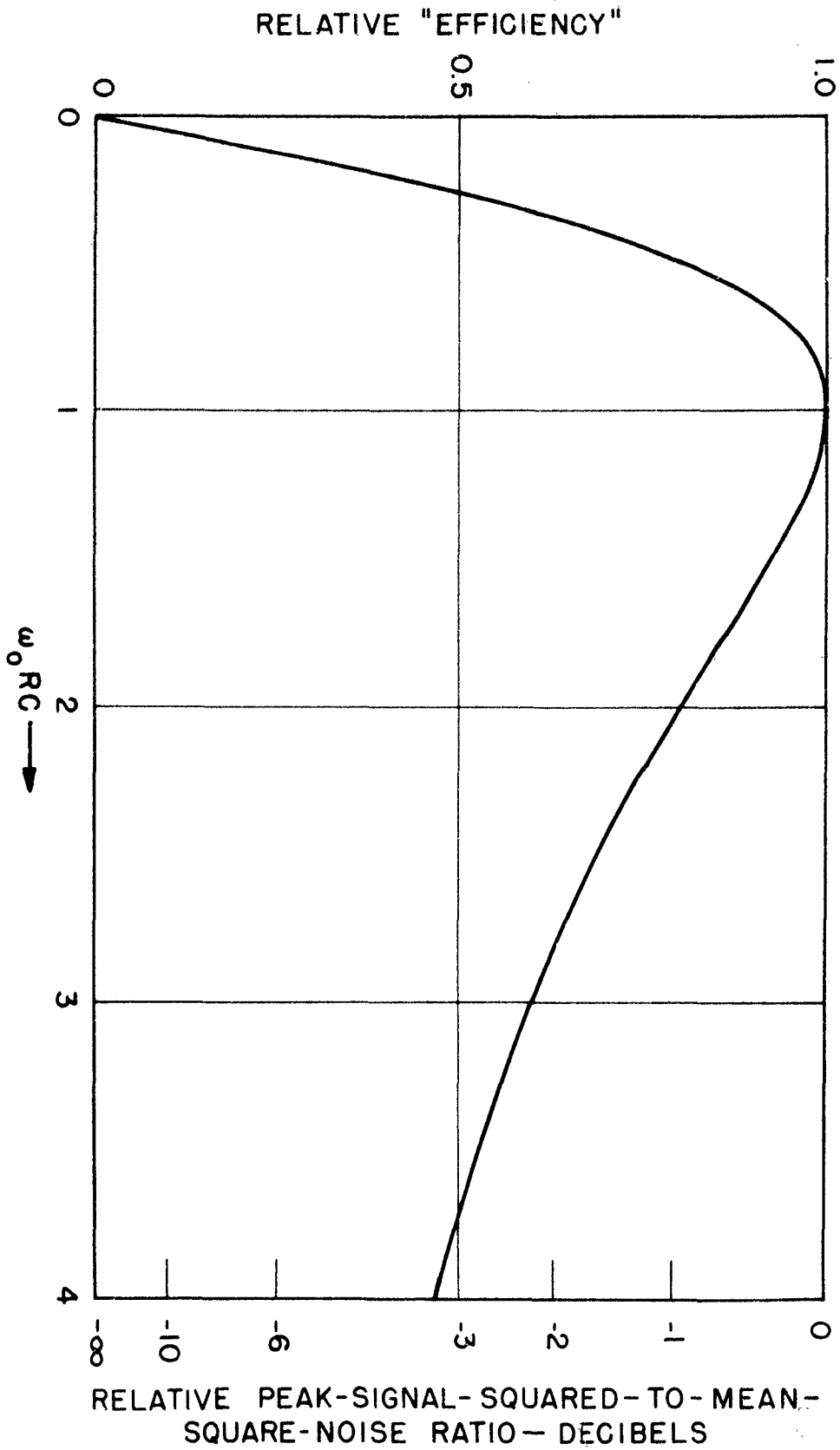we have simply to observe the output as a function of time and
note at what time a signal appears. Either a multichannel sig-
nal processer or a receiver which would record the received
signals for later high-speed playback and processing might make
such a system feasible.

References

1. For other analyses which use somewhat different methods,
   see Fano, R. M., Signal-to-Noise Ratio in Correlation
   Detectors, T. R. No. 186 (February 19, 1951). and
   Davenport, W. B., Jr., Correlator Errors due to Finite
   Observation Intervals, T. R. No. 191 (March 8, 1951),
   both from the Research Laboratory of Electronics, Massa-
   chusetts Institute of Technology, Cambridge, Massachusetts.

2. James, H. M., N. B. Nichols, and R. S. Phillips, Theory of
   Servomechanisms, McGraw-Hill, New York, 1947, Chap. II.

3. Because of the similarity of the first of Eqs. (2.4) to
   the definition of an autocorrelation function, $w(\xi)$ has
   sometimes been called the autocorrelation function of the
   filter. Cf. Davenport, W. B., Jr., R. A Johnson and
   D. Middleton, "Statistical Errors in Measurements on
   Random Time Functions," J. Appl. Phys. 23, 377-388
   (April 1952).

4. Middleton, D."Rectification of a Sinusoidally Modulated
   Carrier in the Presence of Noise," Proc. I.R.E. 36,
   1467-1477 (December 1948).

5. Woodward, P. M., "Information Theory and the Design of
   Radar Receivers," Proc. I.R.E. 39, 1521-1524 (December
   1951); Woodward, P. M., and I. L. Davies, "Information
   Theory and Inverse Probability in Telecommunication,"
   Proc. Inst. Elec. Engrs. (London) 99, Part III, 37-44
   (March 1952).

6. Wiener, N., Exptrapolation, Interpolation, and Smoothing
   of Stationary Time Series, John Wiley, New York, 1950.
   Esp. Appendixes B and C. Also, Bode, H. W., and C. E.
   Shannon, "A Simplified Derivation of Linear Least Square
   Smoothing and Prediction Theory," Proc. I.R.E. 38, 417-
   425 (April 1950).

7. Eckart, Carl, The Theory of Noise Suppression by Linear
   Filters, University of California Marine Physical

Laboratory of the Scripps Institution of Oceanography (October 8, 1951).

8. Davenport, W. B., Jr., R. A. Johnson, and D. Middleton, "Statistical Errors in Measurements on Random Time Functions," J. Appl. Phys. 23, 377-388 (April 1952), Appendix B.

9. Van Vleck, J. H., and D. Middleton, "A Theoretical Comparison of the Visual, Aural, and Meter Reception of Pulsed Signals in the Presence of Noise," J. Appl. Phys. 17, 940-971 (November 1946).

10. See also Middleton, D., "The Effect of a Video Filter on the Detection of Pulsed Signals in Noise," J. Appl. Phys. 21, 734-740 (August 1950).

11. Eckart, Carl, The Measurement and Detection of Steady A-C and D-C Signals in Noise, University of California Marine Physical Laboratory of the Scripps Institution of Oceanography (October 4, 1951).

12. Davenport, W. B., Jr., R. A. Johnson, and D. Middleton (footnote 8) also consider the error in a measurement of the average value of a quantity when there is only a finite observation time available; that is, when the average must be read a finite time after the function to be measured is applied to the averager.

III

ELECTRONIC CORRELATORS

A correlator is assumed to consist of a multiplier and an averaging network or output filter. We have discussed filters in the preceding chapter, and therefore the problem of the design of a practical correlator reduces to that of designing the multiplier. An electronic multiplier is an electronic circuit whose instantaneous output voltage is proportional to the product of the instantaneous values of its two input voltages. We have given consideration only to electronic multipliers although there are a good many other methods of performing the multiplication of the two input signals. It was desired to keep the apparatus simple and rugged, and to make it possible to use various electrical filters as averaging networks. For these reasons, we have not used dynamometer or wattmeter systems (where the average force between two coils carrying currents proportional to the input signals is proportional to the average product of those signals). Sampling correlators[1] or digital correlators,[2] although inherently capable of considerable accuracy, fall into the class of laboratory instruments or computing machinery, and are too complex for purposes of signal reception. One electronic multiplication scheme reported in the literature[3] has also been considered more complex than necessary for these purposes. In this arrangement, the frequency of a carrier is modulated in proportion to one of the multiplicands and its amplitude is modulated in proportion to the other. The resulting signal is fed to a phase discriminator whose average output is proportional to the required product. A good many other possible schemes of multiplying two voltages will come to mind.[4]

Two types of electronic multipliers have been considered

in some detail; these are multigrid-vacuum-tube multipliers, in
which signals applied to different control grids of a multigrid
tube are directly multiplied together in the plate current, and
multipliers based on the "quarter-difference-squares method" of
multiplication, which reduces the problem to one of addition and
squaring.

Multigrid Multipliers

This circuit makes use of the type 6AS6 pentode.* In this
tube, the total (cathode) current is controlled mainly by the
grid voltage, and the fraction of this current which reaches
the plate is controlled mainly by the suppressor voltage.
The plate current then depends, in a sense, upon the product
of the grid and suppressor voltages. A multiplier can be
built in the form shown in Fig. 3.1. To adjust this circuit
for accurate operation, it is necessary to balance the d-c grid
and suppressor voltages, and the a-c (signal) grid and suppressor
voltages, first for each pair of tubes, and then from pair to
pair. While this arrangement permits perfect balancing-out of
error terms up to the second order, the large number of adjust-
ments makes it unwieldy to use. Fortunately, some simplifica-
tions can be made in the multiplier when it is used as a signal
processing device. We need a multiplier whose average output is
proportional to the average product of the inputs, not necessarily
one which generates the instantaneous product. Furthermore, we
are concerned only with input signals which have zero average
value, and which are usually symmetrically distributed in ampli-
tude. For these reasons, it does not matter if the input signals
themselves appear at the output of the "multiplier," since they
will be averaged out and will contribute no error. Thus, if it
is recognized that the output is to be averaged, we may use the
circuit of Fig. 3.2., which uses only two tubes. A detailed

- - - - - - -

*The use of this type of circuit was first suggested to us by
Dr. Peter Elias of Harvard University. Dr. Elias has applied
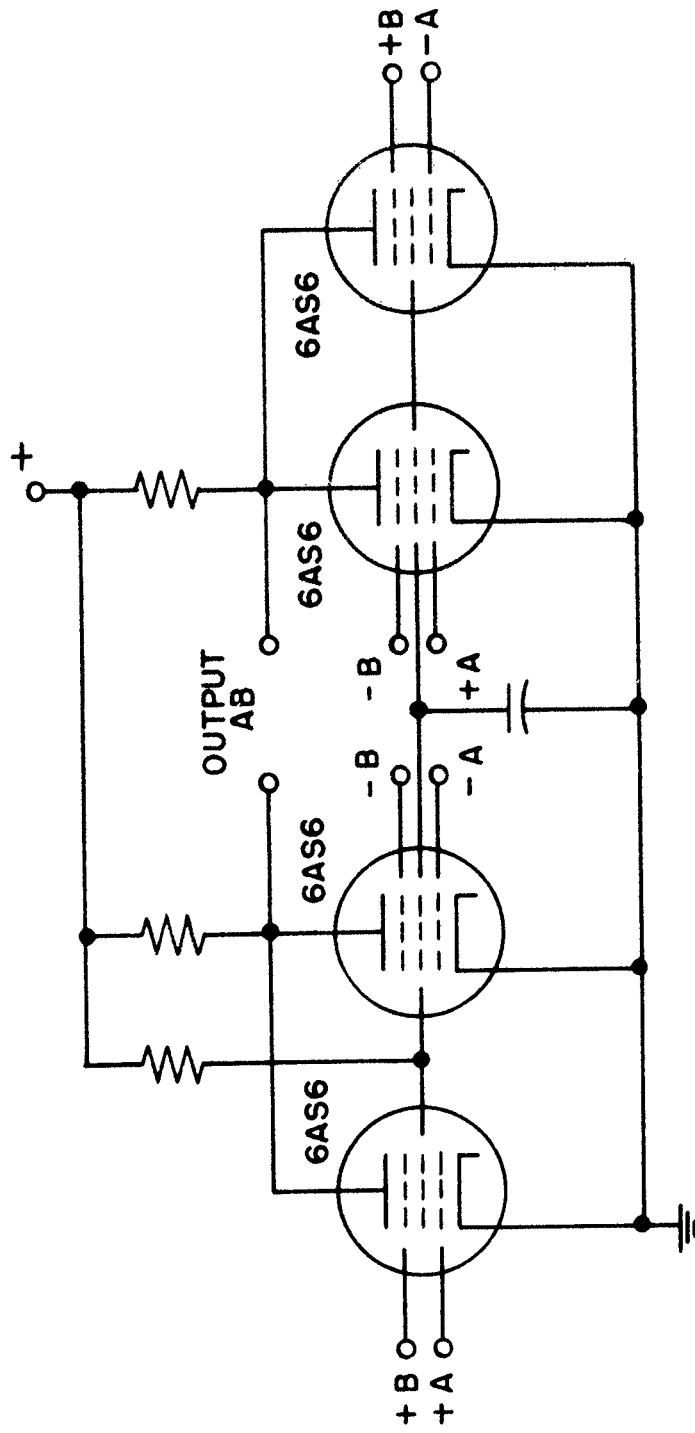for a patent covering multiplier circuits of this general type.

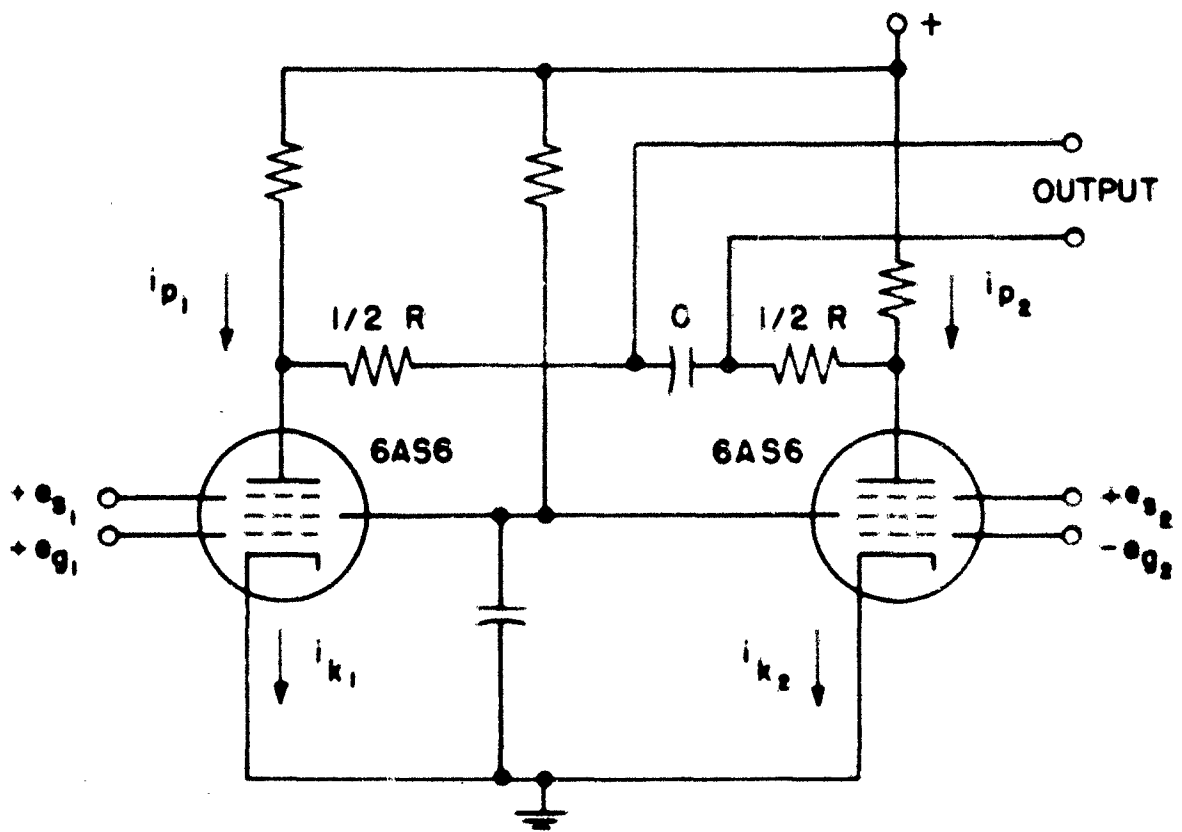Fig. 3.1. An electronic multiplier using the 6AS6 pentode.

Fig. 3.2. An electronic multiplier-averager using the 6AS6.

analysis of this circuit will best demonstrate how it works. A schematic diagram of a practical circuit of this type is shown in Fig. 3.3.

In tube No. 1, we assume that the total cathode current is

$$i_{k1} = a_{01} + a_{11}e_{g1} + a_{21}e_{g1}^2 + \ldots$$

and that the fraction of that current which reaches the plate is

$$\alpha_1 = i_{p1}/i_{k1} = b_{01} + b_{11}e_{s1} + b_{21}e_{s1} + \ldots ,$$

where e_{g1} is the signal voltage on the grid and e_{s1} is the signal voltage on the suppressor. Then the plate current is

$$i_{p1} = a_{01}b_{01} + a_{01}b_{11}e_{s1} + a_{11}b_{11}e_{g1}e_{s1} + a_{01}b_{21}e_{s1}^2$$

$$+ a_{21}b_{01}e_{g1}^2 \qquad + a_{11}b_{21}e_{g1}e_{s1}^2 + a_{21}b_{11}e_{g1}^2e_{s1}^2$$

$$+ a_{21}b_{21}e_{g1}^2e_{s1}^2 + \ldots .$$

In tube No. 2, with the sign of e_{g2} opposite that of e_{g1}

$$i_{k2} = a_{02} - a_{12}e_{g2} + a_{22}e_{g2}^2 + \ldots ,$$

$$\alpha_2 = b_{02} + b_{12}e_{s2} + b_{22}e_{s2}^2 + \ldots ,$$

and

$$i_{p2} = a_{02}b_{02} + a_{02}b_{12}e_{s2} - a_{12}b_{02}e_{g2} - a_{12}b_{12}e_{s2} + a_{02}b_{22}e_{s2}^2$$

$$+ a_{22}b_{02}e_{g2}^2 - a_{12}b_{22}e_{g2}e_{s2}^2 + a_{22}b_{12}e_{g2}^2e_{s2} + a_{22}b_{22}e_{g2}^2e_{s2}^2 + \ldots .$$

The difference of these plate currents is then

$$(a_{01}b_{01} - a_{02}b_{02}) + (a_{01}b_{11}e_{s1} - a_{02}b_{12}e_{s2} + a_{11}b_{01}e_{g1} + a_{12}b_{02}e_{g2})$$

$$+ (a_{11}b_{11}e_{g1}e_{s1} + a_{12}b_{12}e_{g2}e_{s2}) + (a_{01}b_{21}e_{s1}^2 - a_{02}b_{22}e_{s2}^2) + (a_{21}b_{01}e_{g1}^2$$

$$- a_{22}b_{02}e_{g2}^2) + (a_{11}b_{21}e_{g1}e_{s1}^2 + a_{12}b_{22}e_{g2}e_{s2}^2) + (a_{21}b_{11}e_{g1}^2e_{s1}$$

$$- a_{22}b_{12}e_{g2}^2e_{s2}) + (a_{21}b_{21}e_{g1}^2e_{s1}^2 - a_{22}b_{22}e_{g2}^2e_{s2}^2) + \ldots .$$

The circuit is balanced for operation as follows: We first set $a_{01} = a_{02}$ by adjusting the d-c grid voltages (Balance No. 1 in Fig. 3.3. With matched 120-ohm resistors in the cathode circuit the cathode currents in the two tubes will be equal when the cathodes are at the same voltage.) Then an adjustment of the d-c suppressor voltages (Balance No. 2) will make the sum of the terms in the first parentheses zero. (The 68,000-ohm plate resistors are also matched.) The terms in the second pair of parentheses all have zero average value provided that the signal inputs have zero average value, and therefore they contribute nothing to the d-c output. The third pair of parentheses enclose the wanted output terms. The fourth and fifth parentheses enclose error terms proportional to the squares of the input signals, and these can be made zero by adjusting the relative amplitudes of e_{g1} and e_{g2}, and e_{s1} and e_{s2}. In the circuit of Fig. 3.3, this is accomplished by first applying an a-c signal input to the grids only and adjusting the balance No. 3 control for zero d-c output, then by applying an a-c signal to the suppressors only, and adjusting the balance No. 4 control for zero d-c output. The sixth pair of parentheses enclose terms proportional to $e_g \cdot e_s^2$ which cannot be balanced out, but which for sinusoidal or symmetrically distributed noise signals have zero average value and contribute nothing to the d-c output. It is possible that a signal having zero average value but unequal moments either side of the axis could contribute a large error at this point; in using this circuit with such unsymmetrical waveforms care should be taken to determine whether such errors are negligible or not. The remaining terms in the last parentheses are small and nearly balanced out.

Measurements of the characteristics of 6AS6's indicate that the following are good operating conditions for multiplier use:

$$E_{screen} = E_{plate} = 120 \text{ v}$$

$$E_{grid} = -2.5 \text{ v}$$

$$E_{suppressor} = -4.5 \text{ v}$$
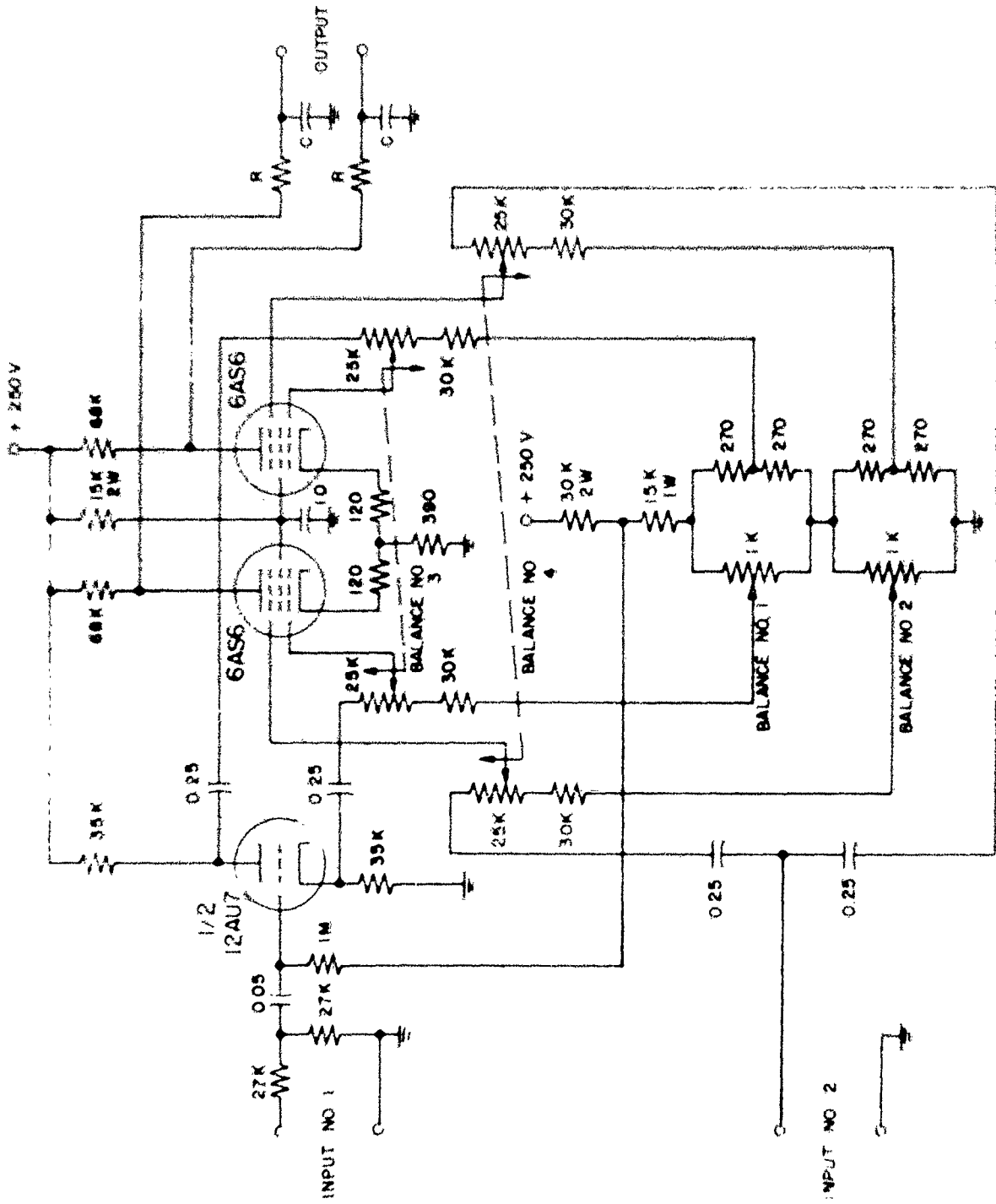
Fig. 3.3. Schematic diagram of a multiplier-averager using the 6AS6.

$$i_k \quad = \quad 6.0 \text{ ma}$$

$$i_p \quad = \quad 1.7 \text{ ma}$$

The characteristics are fairly linear for a peak grid swing of
1 v and a peak suppressor swing of 2 v. The performance of the
multiplier as a squarer was checked by applying the same sinu-
soidal voltage to both inputs and plotting the square root of
the d-c output voltage against the a-c input voltage. The
resulting curve was quite linear for input voltages up to the
limits given above.

As originally tried, the circuit of Fig. 3.3 suffered
from instability of the d-c balance and this instability was
traced in part to extreme sensitivity to fluctuations of the
heater voltage. An electronically regulated a-c supply and
some selection of tubes have improved the circuit greatly in
this respect. However, because of the large number of balance
adjustments, this circuit is somewhat unwieldy to use, and the
d-c fluctuations in the output set a definite limit to this
correlator's ability to detect small signals.

The assumptions of the preceding analysis are a little too
simple since i_k depends to a small extent on e_s and α depends
to a greater extent on e_g. Feedback systems for linearizing
the $i_k - e_g$ characteristic (and making it independent of e_s)
will come to mind. It must be remembered, however, that it is
impossible to feed back around the entire multiplier. It is
possible that α can be made more nearly independent of e_g by
feeding some of the e_g signal in on the suppressor grid.

"Quarter-Difference-Squares" Multipliers

Another method of multiplying two signals is the quarter-
difference-squares method, which is simply based on the fact
that the product $AB = 1/4(A+B)^2 - 1/4(A-B)^2$. The operation of
multiplication is thus reduced to that of forming the sum and
the difference of the multiplicands, and squaring. A block
diagram of a correlator based on this principle is shown in

Fig. 3.4.

Because of curvature of the plate current-grid voltage characteristic, many vacuum tubes operate very satisfactorily as squarers. For example, a twin-triode squarer can be built as shown in Fig. 3.5. We again assume that the plate currents in the individual tubes can be expressed in power series in the signal voltage at the grid. The current in the first tube may be written:

$$i_1 = a_{01} + a_{11}e_{g1} + a_{21}e_{g1}^2 + a_{31}e_{g1}^3 + a_{41}e_{g1}^4 + \ldots\ldots$$

and that in the second,

$$i = a_{02} + a_{12}e_{g2} + a_{22}e_{g2}^2 + a_{32}e_{g2}^3 + a_{42}e_{g2}^4 + \ldots\ldots$$

$$= a_{02} - a_{12}e_{g1} + a_{22}e_{g1}^2 - a_{32}e_{g1}^3 + a_{42}e_{g1}^4 - \ldots\ldots ,$$

where e_{g1} and e_{g2} are the signal voltages at the two grids. The output voltage is proportional to the sum of these two currents,

$$i_1 + i_2 = (a_{01} + a_{02}) + (a_{11}e_{g1} - a_{12}e_{g1}) + (a_{21}e_{g1}^2 + a_{22}e_{g1}^2)$$

$$+ (a_{31}e_{g1}^3 - a_{32}e_{g1}^3) + (a_{41}e_{g1}^4 + a_{42}e_{g1}^4) + \ldots\ldots .$$

The terms in the first parentheses represent simply the d-c plate current, while those in the second can be made zero by balancing the amplitudes of the signals applied to the grids. The terms in the third pair of parentheses represent the desired squared output. The terms in the fourth pair are small and nearly balanced out, and those in the fifth and higher are small until the grid signals become very large (or until the circuit becomes overloaded, so to speak). If, however, we apply the same argument given in the section above, we see that it is not necessary to have perfect (instantaneous) squarers, but simply a circuit whose average output is proportional to the square of the input. A single tube is thus adequate to perform the squaring operation, if the average output of the multiplier is all that is required. A circuit arrangement for a single-triode squarer is shown in
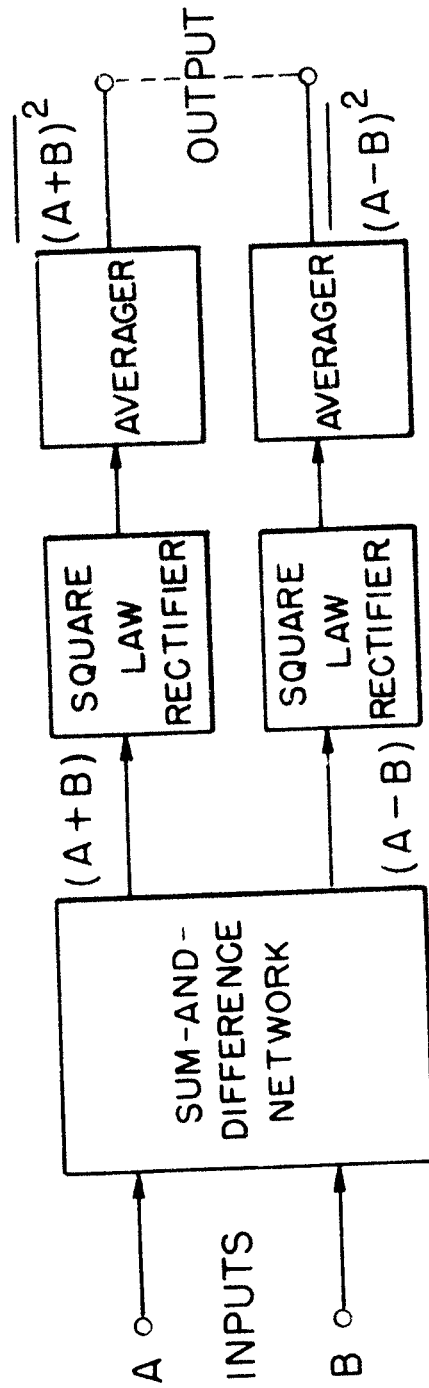
Fig. 3.4. Block diagram of a "quarter-difference-squares" multiplier-averager, based on the principle that $AB = 1/4(A+B)^2 - 1/4(A-B)^2$.
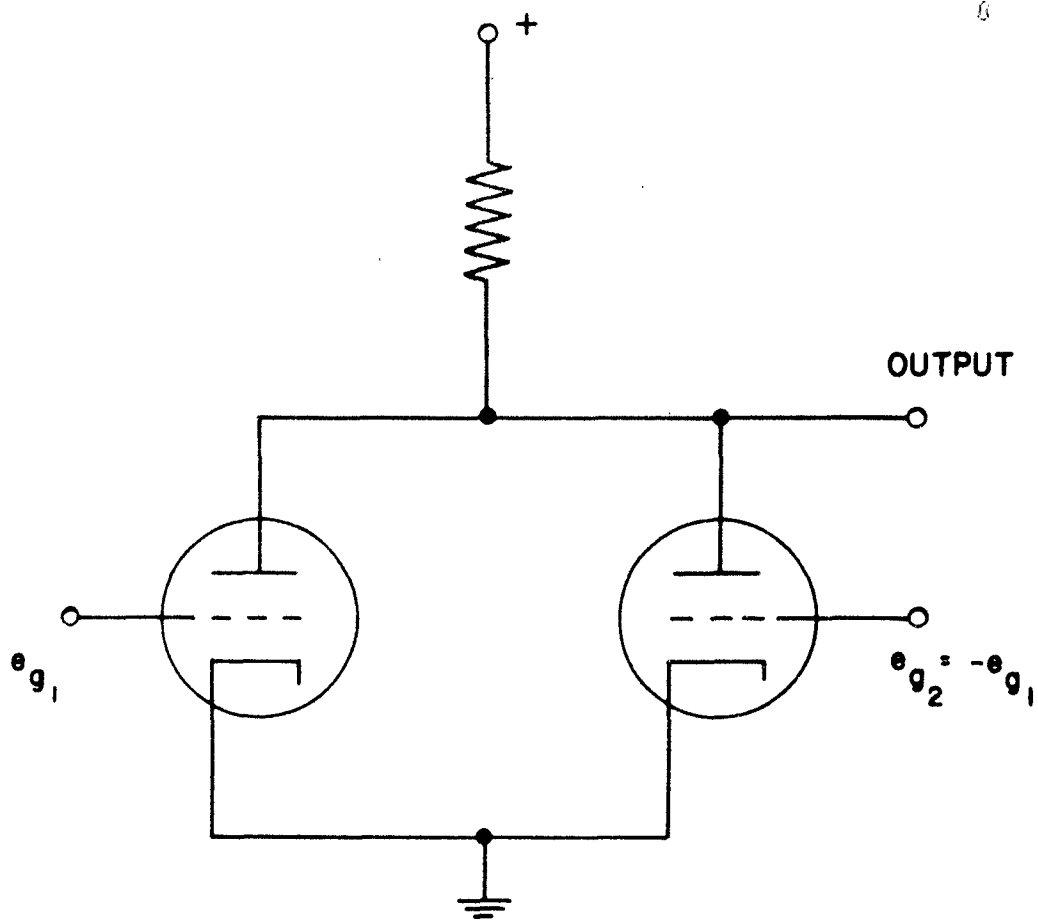
Fig. 3.5. A twin-triode squarer.

Fig. 3.6. It is necessary to use fixed bias with such a squarer, since with a cathode bias resistor, the degeneration linearizes the operation of the tube to such an extent that it loses much of its square-law sensitivity. A graph of the change in the average plate voltage as a function of the rms amplitude of random sinusoidal grid voltages for this circuit is given in Fig. 3.7. Pentodes may also be used in the same way, if well-stabilized voltages are applied to all the fixed-voltage electrodes. A schematic diagram of a pentode squarer using a 6SJ7 is shown in Fig. 3.8, and a graph of its average output voltage as a function of the rms input voltage is shown in Fig. 3.9.

A circuit diagram of a quarter-difference-squares multiplier using the two halves of a 6SN7 twin triode as the squarers is shown in Fig. 3.10. Self-bias is used, but the resistive bias network is by-passed by a large capacitor, so that cathode-circuit degeneration cannot linearize the tube characteristics. A d-c balance potentiometer in the cathode circuit allows one to set the no-signal output at zero. Two ganged potentiometers in the grid circuits allow adjustment of the signal amplitudes at the grids to compensate for possible inequality in the square-law sensitivities of the two halves of the tube. This control is adjusted so that the output remains zero when a signal is applied to only one of the inputs. The inputs should not exceed 3 v rms. An RC averaging network is shown at the output; in adjusting this network to a particular time-constant, account must be taken of the non-zero source impedance at the plate circuits of the squarers. We have found it easiest to measure this (resistive) impedance using a simple resistance voltage-divider. Circuits of this type, but using fixed bias derived from a battery, exhibit a considerably greater zero-drift stability than the 6AS6 multipliers discussed in the previous section, and the circuit described above, which uses a common cathode bias circuit, is even a little more stable in this respect. Because of charging of the capacitor in the cathode circuit,

the operating points of the squarer tubes change slightly
with the amplitude of the input signals. This change was
found to be very small, however, and apparently has negli-
gible effect on the operation of the correlator.

A solution to the problem of the drift in the output
was sought in the use of synchronous switches or choppers
which were used to interchange the two squaring tubes period-
ically. The choppers serve to convert any d-c unbalance which
may arise in the squarers to an a-c voltage whose average value
is zero. A block diagram illustrating the application of chop-
pers to the correlator of Fig. 3.10 is shown in Fig. 3.11. The
choppers used were double-pole double-throw, break-before-make
Type 258 AC-DC Choppers.* They are powered by the 6.3-v,
60-cps heater supply. The two switches in these choppers are
well synchronized, and are open for about 1 millisecond of
their 8 1/3-millisecond period. The alternate periods of
contact in the chopper are factory-adjusted to be equal within
5 per cent, but can be balanced more accurately by adjusting
the amplitude of the driving voltage. Measurements of the
output signal-to-noise ratio were made by the method to be
described below for a correlator of this type. They indicate
that for random inputs the output signal-to-noise ratio is not
more than 1 db less for a correlator with choppers than for
one without choppers. In addition, the output drift is very
substantially reduced. Unfortunately, if there is in the in-
put a sinusoidal wave of a frequency which is a near multiple
of 60 cps, there appear "beats" of fairly large amplitude in
the output, presumably due to the imperfect action of the syn-
chronous switches (the fact that they are open for about 1/8
of their period). If a switch could be built which would in-
staneously change from one position to the other this beat
phenomenon would disappear, and there would be no difference
between a correlator equipped with such perfect choppers and

- - - - - - -

*Manufactured by Stevens-Arnold, Inc., South Boston, Massachusetts.
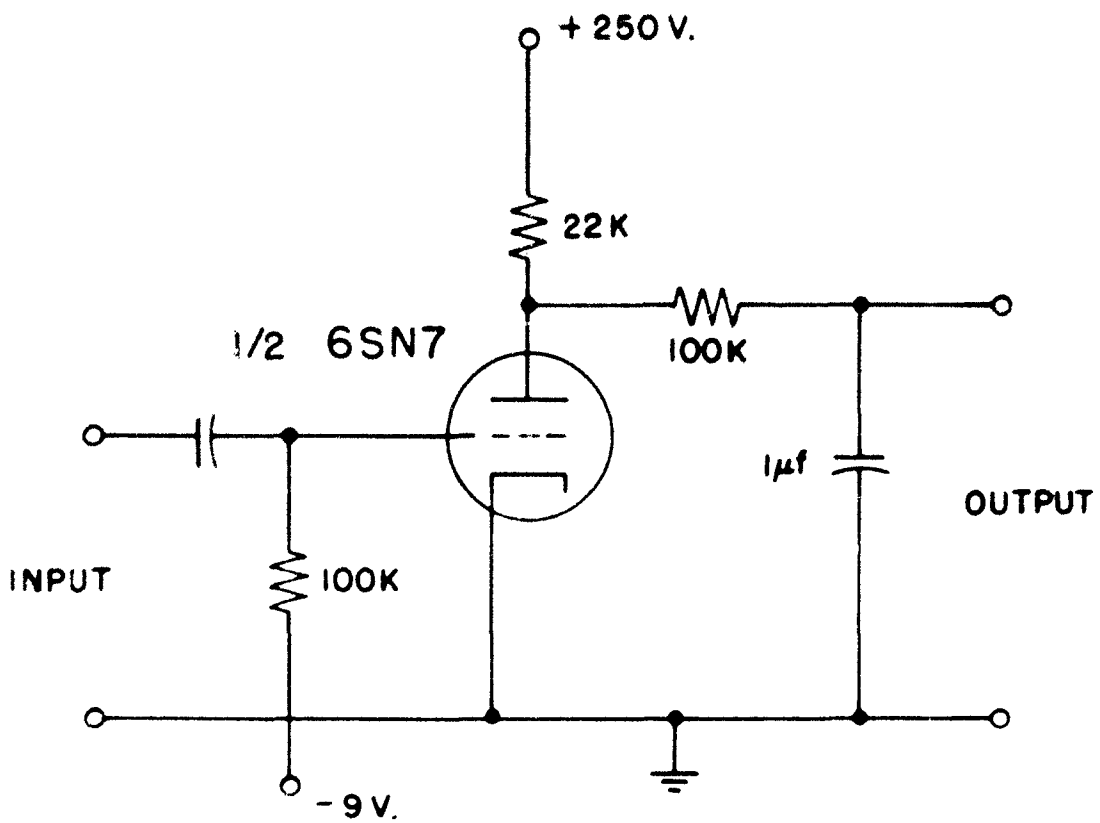
Fig. 3.6. Schematic diagram of a triode squarer-averager.
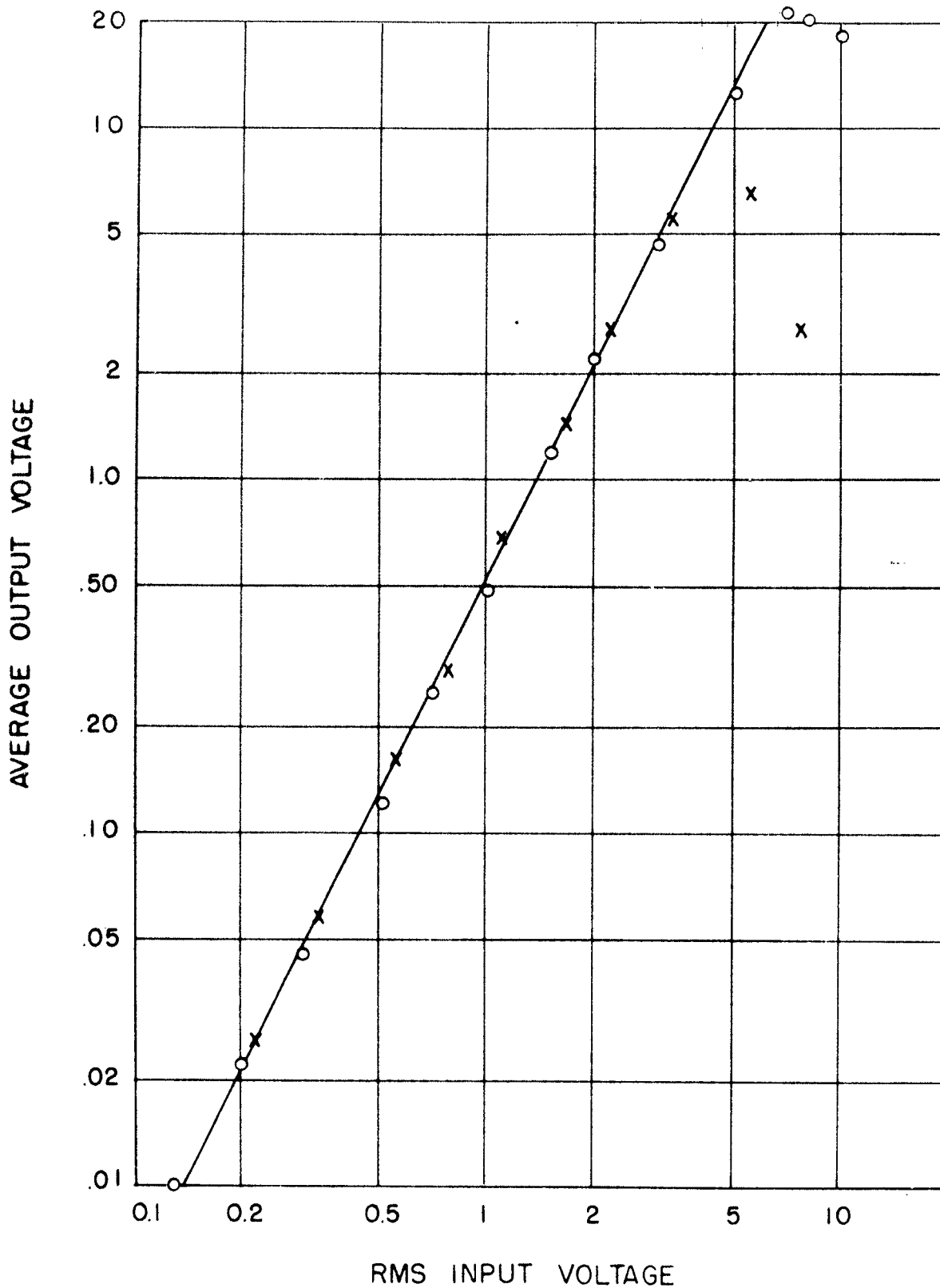
Fig. 3.7. Graph of the change in the output voltage as a function of the rms input amplitude for the squarer-averager of Fig. 3.6. Circles are measured points for a sinusoidal input, crosses are measured points for a normal random noise input. The straight line is the perfect square-law characteristic.
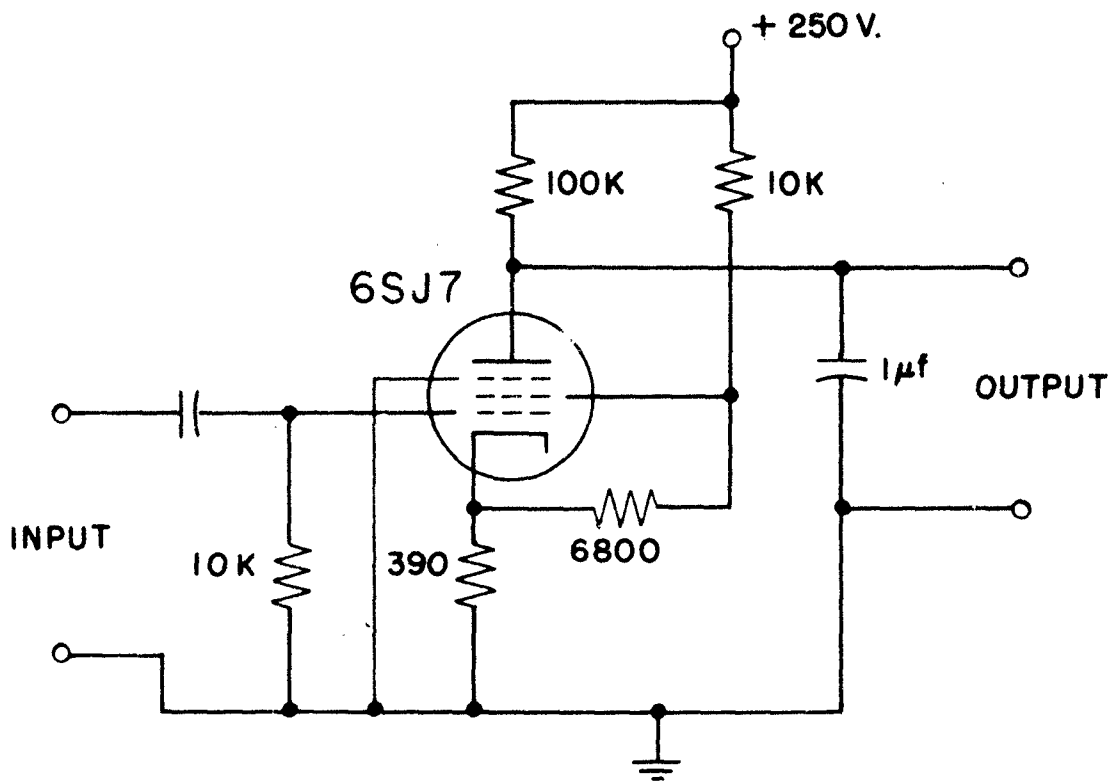
Fig. 3.8. Schematic diagram of a pentode squarer-averager.
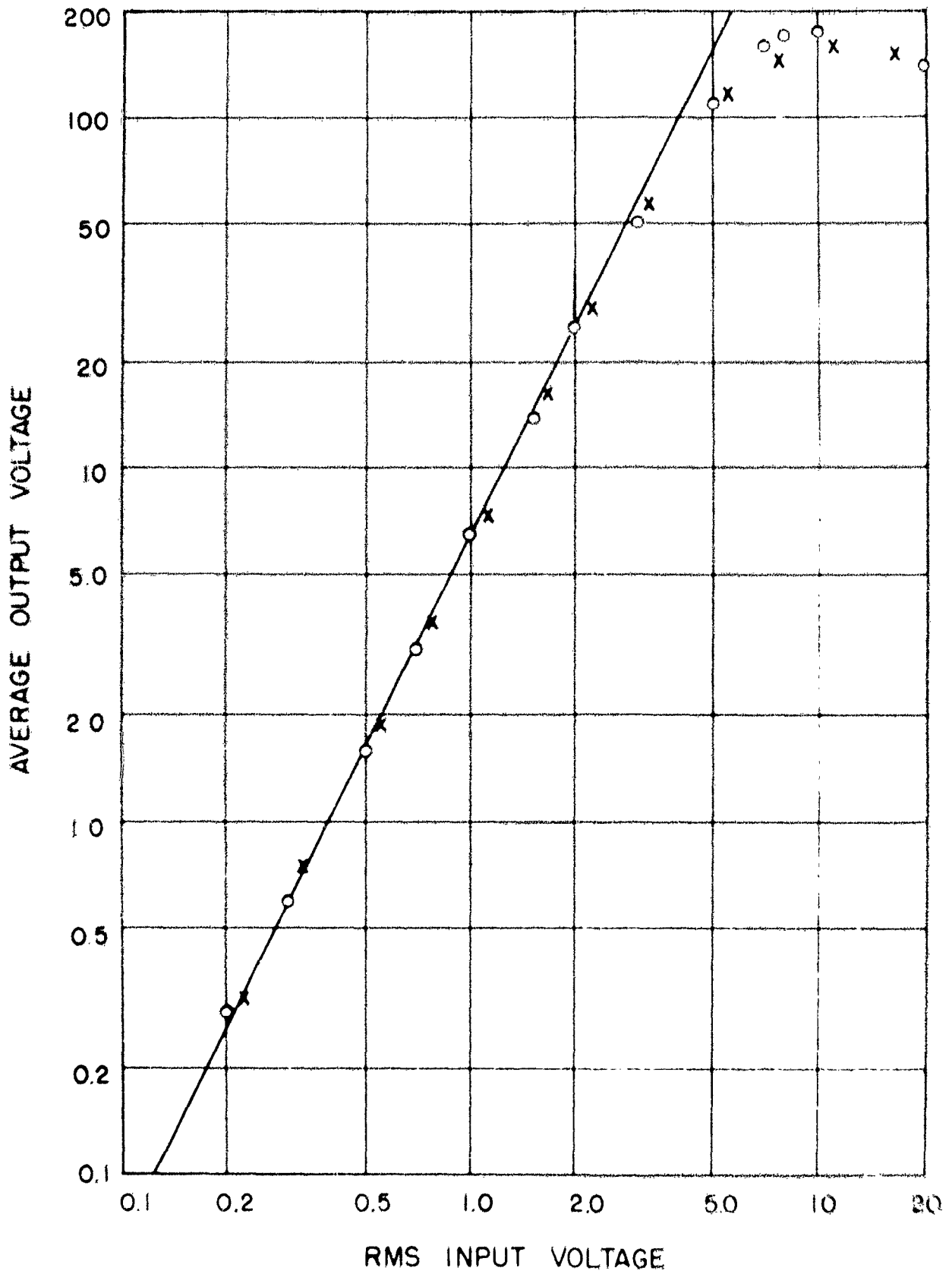
Fig. 3.9. Graph of the change in the output voltage as a function of the rms input amplitude for the squarer-averager of Fig. 3.8. Circles are measured points for a sinusoidal input, crosses are measured points for a normal random noise input. The straight line is the perfect square-law characteristic.

Fig. 2.10. Schematic diagram of a multiplier-averager using triode squarer-averagers.

Fig. 3.11. Block diagram showing the method of applying choppers to the multiplier-averager of Fig. 3.10.

one without, except that the drift noise would be removed. It
appears that the amplitude of the chopper driving voltage must
be well regulated in order to prevent zero drift due to changes
in the lengths of alternate periods of contact.

If one can tolerate imperfect choppers, that is, if one
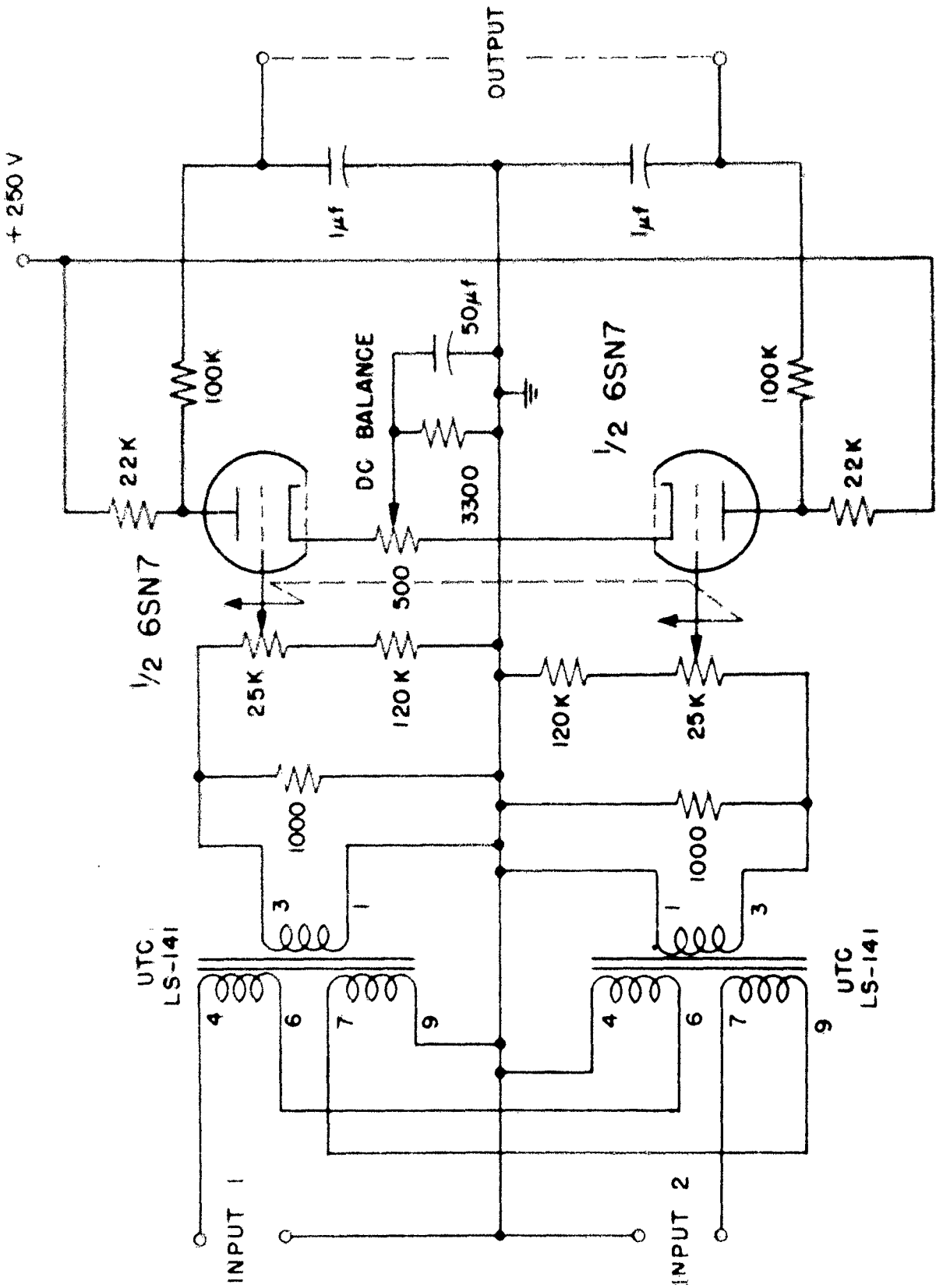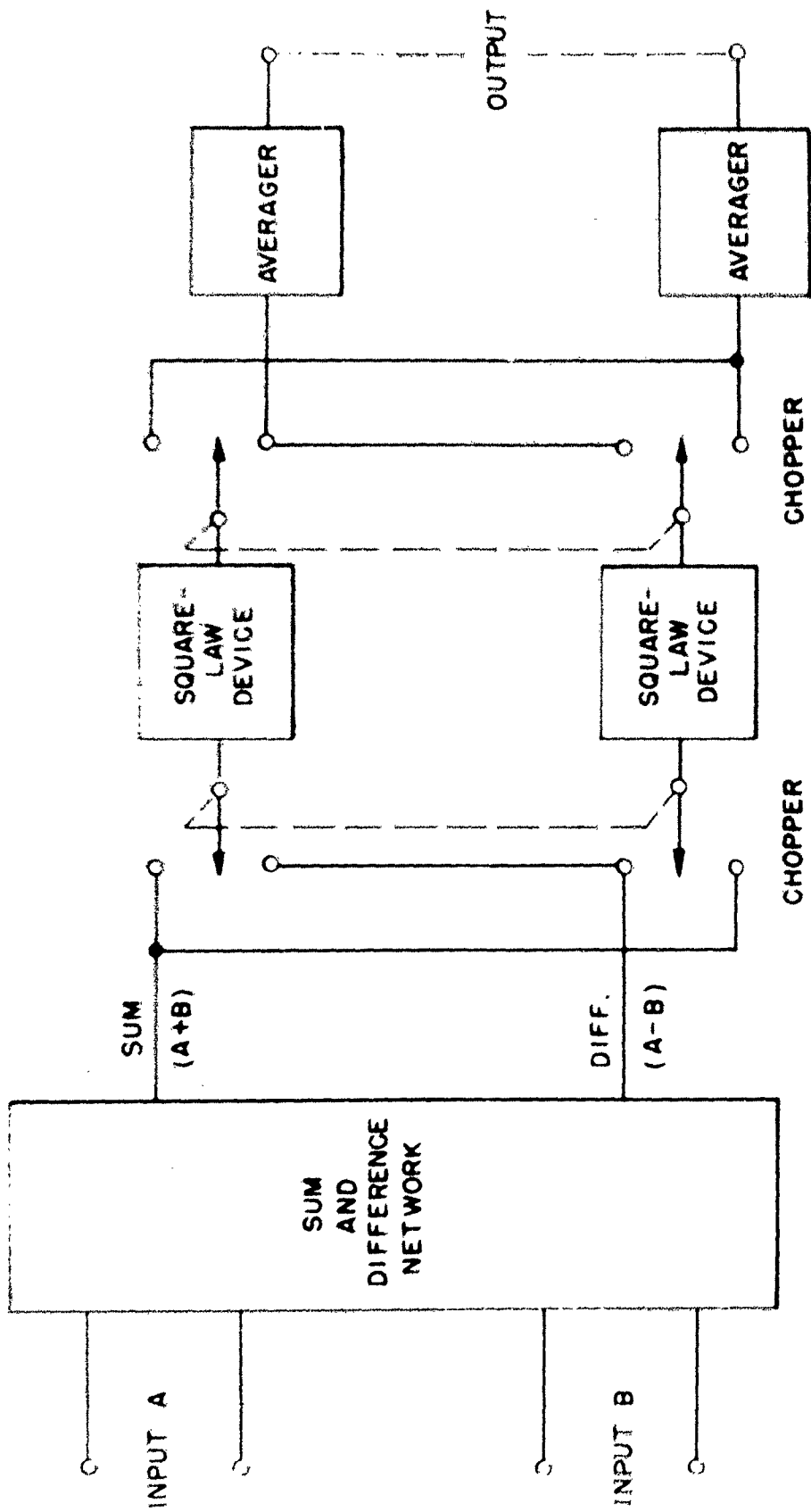is performing cross-correlations of purely random functions,
one can use a "single-channel" correlator in which only one square-
law device is used, being alternately switched back and
forth from the sum channel to the difference channel. A
schematic diagram of such a correlator is shown in Fig. 3.12,
where a 6SJ7 pentode squarer is used. A little greater sta-
bility of the output is expected here, since only one chopper
is used instead of two, and it is only necessary to maintain
the symmetry of operation of one chopper. An output d-c bal-
ance control is provided in this circuit, although it would
not be necessary with perfectly matched components in the
plate circuits, and a perfectly symmetrical chopper. Be-
cause of the much greater square-law sensitivity of the
6SJ7, this correlator has a much greater output voltage for
a given input amplitude than the correlator of Fig. 3.10.

Reasonably accurate square-law rectifiers can be con-
structed of contact rectifiers such as the 1N34 germanium
diode. One method is to use a large number of rectifiers,
each biased at a different voltage, so that each starts con-
ducting at a different input amplitude. By means of suitable
resistive combining networks any monotonic characteristic can
be approximated. Because of possible variations in the
characteristics of the individual rectifiers, it is necessary
to use fairly large bias voltages so that the rectifiers are
essentially nothing more than switches. This, in turn, re-
quires that the input voltage be of a fairly large amplitude,
which may require special amplifiers. However, good accuracy
is claimed for this method, eleven diodes being required to
match a square-law curve for inputs from 0 to 100 v with
1 per cent accuracy.[5] Another method is simply to make use

of the fact that the characteristic of the contact rectifier,
is, for small signals, a good approximation to a square law.
Because it is necessary to keep the voltages across the
individual diodes low, it is necessary to connect many diodes
in series, to obtain square-law operation at convenient input
voltage levels.[6] Figure 3.13 is a schematic diagram of a
squarer of this type. When it is connected for full-wave
operation, as shown, it is a perfect squarer, whose output
is proportional to the square of the input. If only the
average square is required, it is only necessary to provide
half-wave operation. In Fig. 3.14 are shown curves of average
output voltage as a function of the rms input voltage for the
squarer of Fig. 3.13. These curves show the effect of chang-
ing the load resistance R while keeping the number of recti-
fiers (11 in this case) constant. In Fig. 3.15 are shown
curves illustrating the effect of changing the number of
rectifiers while keeping the load resistance fixed. These
curves show that if the load resistor is too small, there is
a departure from the true square-law curve at the small input
voltage end, while if it is too large, the actual operation de-
parts from true square-law at the high input voltage end. The
diodes used in these tests were selected to have nearly equal
conductances at a forward voltage of 1.5 v. A schematic
diagram of a "many-rectifier" correlator is given in Fig. 3.16.
The maximum allowable input amplitude is about 1.4 v, and the
sensitivity of this unit is considerably less than that of the
6SN7 correlator of Fig. 3.10. Because of this lack of sensi-
tivity, this unit has been much less useful to us than other
correlators, but it does have the great advantages of having
no zero drift, and requiring no power of any kind. We are
hopeful that it may be possible to devise a network of these
contact rectifiers which will accurately reproduce a square-
law dynamic characteristic over a wider range

Measurements of Correlator Signal-to-Noise Ratio

Measurements of the signal to-noise ratio at the output of
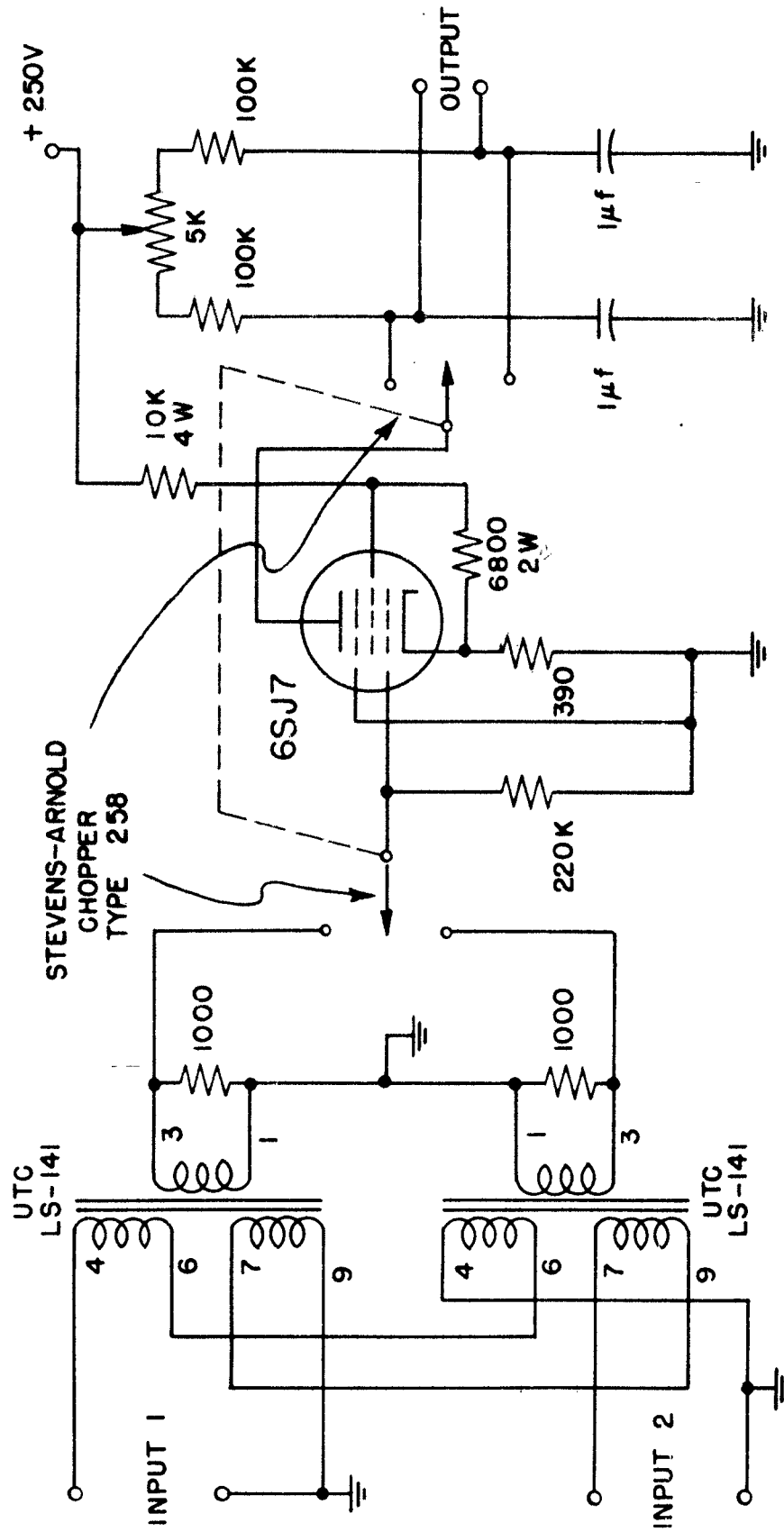
Fig. 3.12. Schematic diagram of a "single-channel" multiplier-averager using one chopper and the pentode squarer-averager of Fig. 3.8.
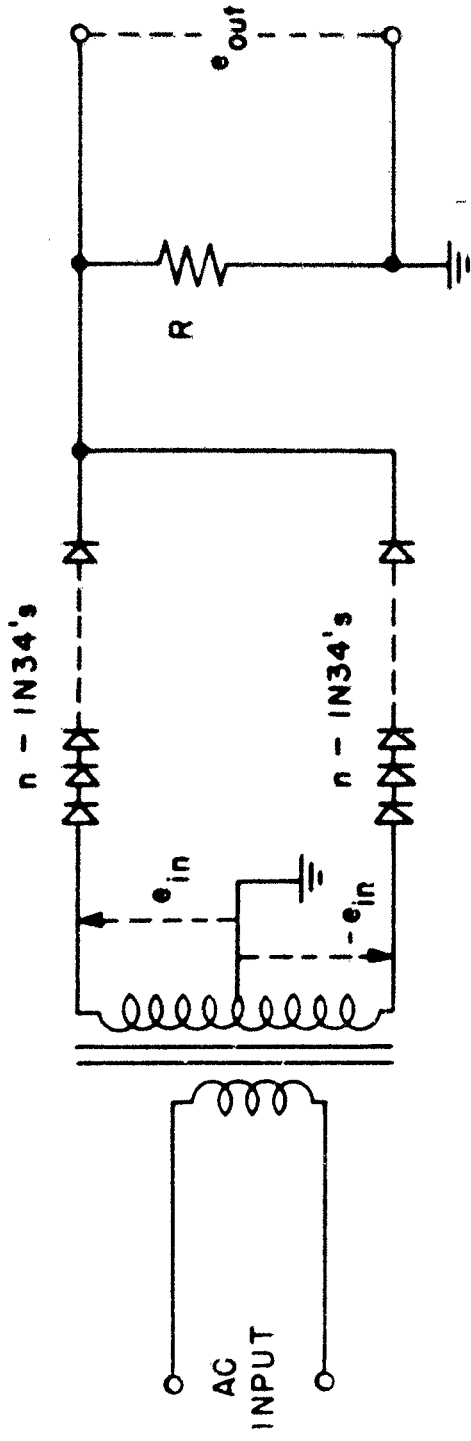
Fig. 3.13.   A squarer using several 1N34 germanium diodes.
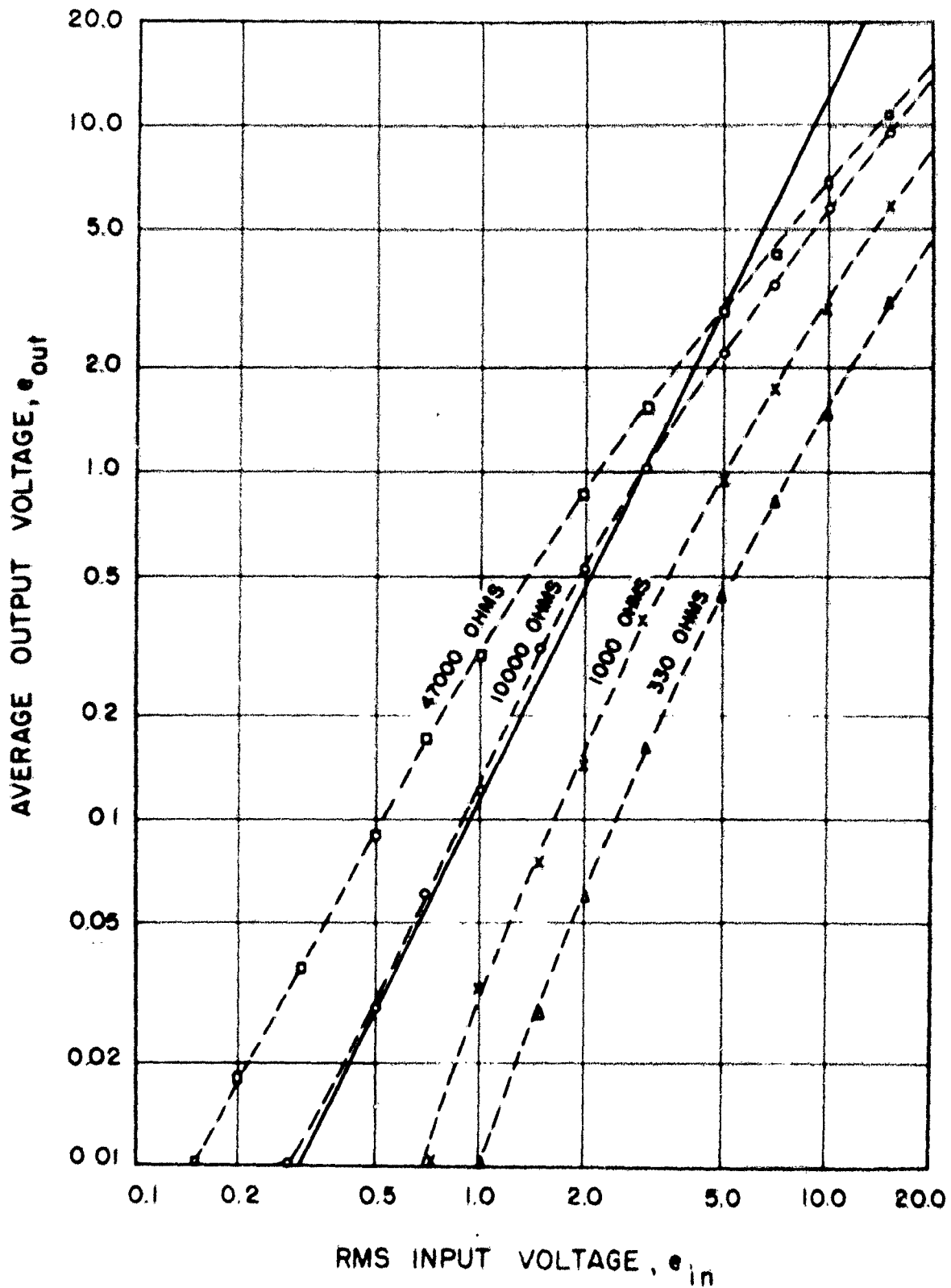
Fig. 3.14. Graph of the average output voltage of the circuit of Fig. 3.13 with 11 diodes in each chain for various values of the load resistor as a function of the rms value of a sinusoidal input voltage.
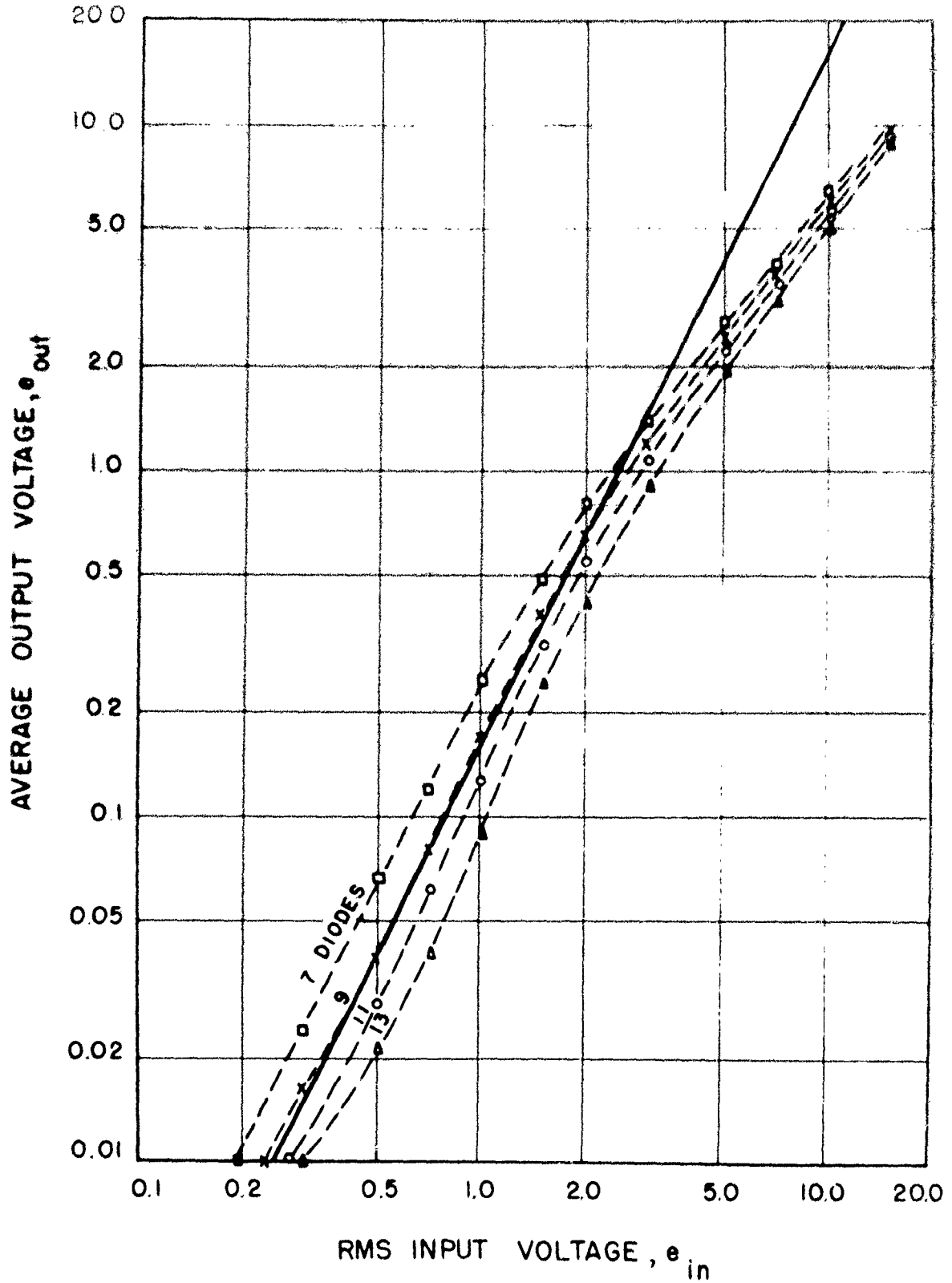
Fig. 3.15. Graph of the average output voltage of the circuit of Fig. 3.1 with a 10,000-ohm load resistor and various numbers of diodes in each chain as a function of the rms value of a sinusoidal input voltage.
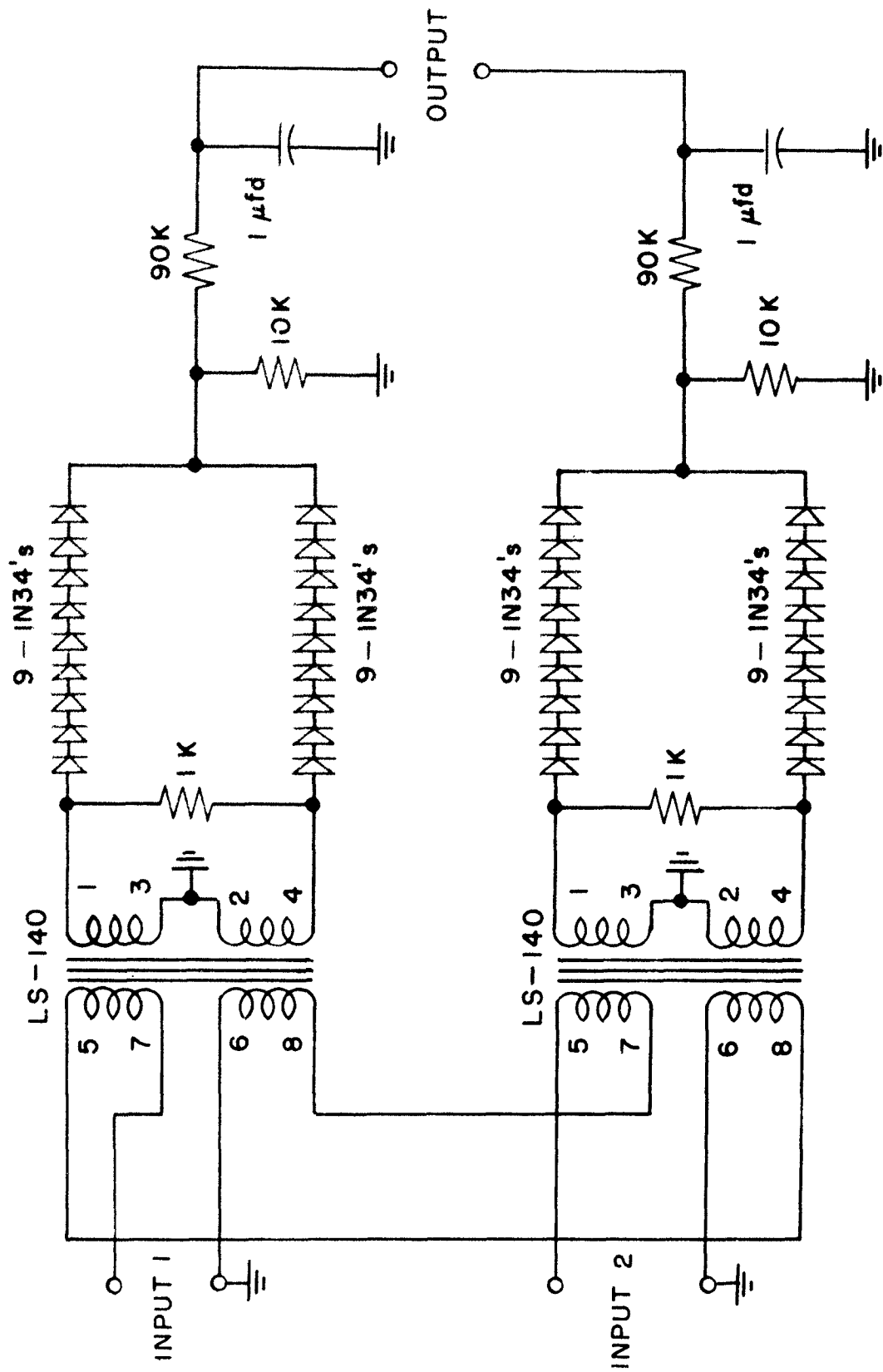
Fig. 3.16. Schematic diagram of a "many-rectifier" correlator.

a correlator are of interest not only in checking the theory,
but also in evaluating the performance of the multiplier.
Noise in the output can be divided into two categories:
the fluctuation noise which always appears when random volt-
ages are applied to the inputs, and other steady or fluctuat-
ing voltages which are present because of improper operation
of the multiplier. The latter may consist of

    (1) d-c balance instability or drift,
    (2) d-c voltages which may appear because of
         improper operation of the multiplier (de-
         parture from square-law characteristics,
         imperfect sum-and-difference network, etc.),
    (3) self-noise (thermal or shot noise),
and (4) periodic noise due to choppers.

The signals were measured and noises of the first two kinds
were evaluated by recording the output of the correlator on a
level recorder.[7] The fluctuation noise and chopper noise were
measured with the low-frequency square-law voltmeter described
below. Self-noise was proved negligible for the simple corre-
lators tested.

    It is reasonable to assume that drift noise in the output
of a correlator exists in a frequency band much smaller than
the band-pass of the RC averager. Neglecting this very-low-
frequency drift noise, it can be shown that the spectrum of the
input to the averager may be assumed uniform with little error
if the bandwidth of the correlator input signals is wide com-
pared to the band-pass of the averager. We therefore evaluate
the output noise by measuring that above 1 cps in frequency and
extrapolating to estimate the total noise output. Since drift
noise occurs at frequencies much lower than 1 cps, it does not
disturb this measurement.

    The circuit of the noise meter constructed for this
purpose is shown in Fig. 3.17. Because the output of most of
the correlators we have built is not push-pull, the first two

stages effectively take the difference of the voltages at the
two input terminals and convert this difference into a true
push-pull signal which is applied to the grids of a 12AU7
squarer of the form of that shown in Fig. 3.5. The meter thus
reads the true mean square of the input. All the correlators
which were tested were equipped with RC averagers each of
which consisted of a 100,000-ohm resistor and a 1-microfarad
capacitor. It can be shown that the input circuits of this
meter do not load these averaging networks enough to make a
significant change in the effective time constant of the
averager. Because of the extreme sensitivity of a voltmeter
circuit of this type to supply voltage changes (both plate
and heater), the unit is operated from an a-c line voltage
regulator. Long warm-up and frequent zero checks are neces-
sary for accurate operation. The meter is calibrated by
measurement of a 30-50 cps sinusoid of known amplitude. A
condenser across the grid circuits of the third pair of tubes
limits the response of the meter at high frequencies (3 db
down at 160 cps) to reduce the effects of self-noise in the
meter. The time constant of the meter averager is adjusta'le
from 0.1 second to 100 seconds so that it can be made appropri-
ate for the particular measurement being made.

This meter measures the noise above 1 cps in the output
of the correlator. The extrapolation to the total noise out-
put (not including drift noise, of course) can be carried out
in terms of the equivalent rectangular pass-bands of the aver-
ager and the noise meter. The intensity-frequency characteris-
tic of the RC averager is

$$\frac{\omega_0^2}{\omega^2 + \omega_0^2} \quad ,$$

where $\omega_0 = 1/RC$. The width of a rectangular band (with unity
response) which would pass the same power is then

$$\int_0^\infty \frac{\omega_0^2 \, d\omega}{\omega^2 + \omega_0^2} = \frac{\pi \omega_0}{2} \quad \text{cycles.}$$
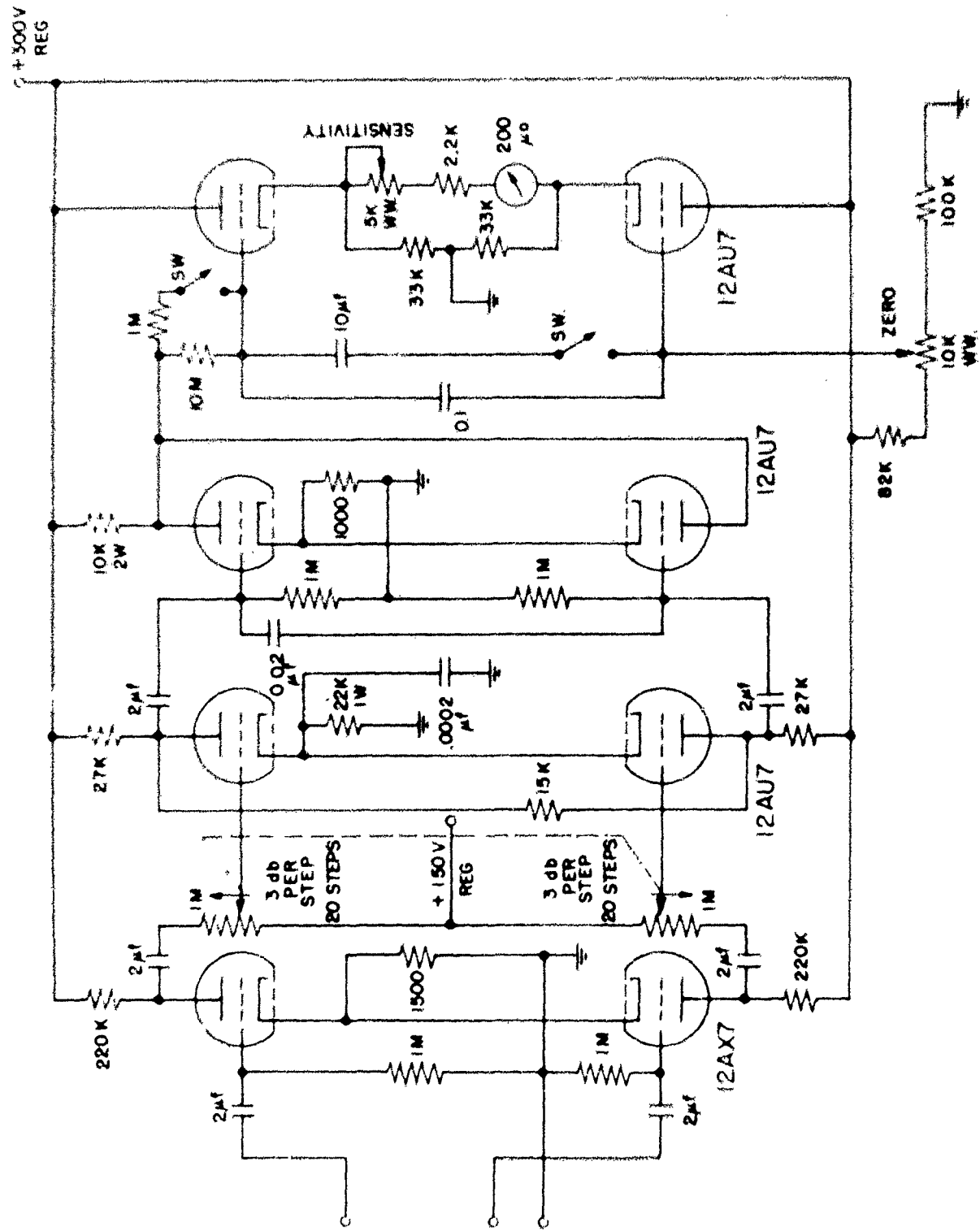
Fig. 4.17. Schematic diagram of the low-frequency square-law voltmeter.

The noise meter has three RC high-pass coupling networks which act independently on the frequency response. Its intensity-frequency characteristic is then

$$\left(\frac{\omega^2}{\omega^2 + \omega_1^2}\right)^3 \quad ,$$

where $\omega_1 = 1/R_1 C_1$, the cut-off frequency of one of the three coupling networks, so the cut-off frequency of the equivalent rectangular high-pass filter is

$$\int_0^\infty \left[1 - \left(\frac{\omega^2}{\omega^2 + \omega_1^2}\right)^3\right] d\omega = \frac{15\pi\omega_1}{16} .$$

The reading of the square-law meter must then be multiplied by

$$\frac{\frac{\pi\omega_0}{2}}{\frac{\pi\omega_0}{2} - \frac{15\pi\omega_1}{16}} = \frac{1}{1 - 1.87 \frac{\omega_1}{\omega_0}}$$

to obtain the mean-square value of the output noise.

Output signal-to-noise ratios have been measured for the correlators of Figs. 3.10, 3.11, and 3.12. Input background noises and a random (noise) signal were derived from gas-tube noise generators and combined in resistive adding networks. The input signal-to-noise ratios were measured with a Ballantine Model 300 Electronic Voltmeter.* The input signals were passed through an amplifier which had a single-tuned-circuit filter with a center frequency of 3800 cps and adjustable Q. The correlator time constants were always adjusted to be 0.1 second as accurately as possible. The theoretical output signal-to-noise ratios were computed from the formulas in Table 2.1 from the above data and

- - - - - - -

*It has been found that when the Ballantine voltmeter is used to measure the normal random noise used in these experiments, 1 db must be added to the meter reading to obtain the true rms value. This correction is constant over the entire scale.

the measured input signal-to-noise ratio. The correction factor for the low-frequency square-law voltmeter for the above averager time constant is 0.4 db. The results of these measurements are compared with the theoretically predicted values in Table 3.1.

Because of the inherent difficulties of noise measurements occasioned by the requirements of long averaging time, and because of zero drift in the low-frequency voltmeter, the accuracy of these measurements is probably not better than ±1.5 db. With this in mind, the data in Table 3.1 show good agreement between theory and experiment. The last entry in the table (for the correlator of Fig. 3.12) which indicates a very poor output signal-to-noise ratio, is included simply as a reminder that with that circuit there is a comparatively large 60-cps component in the output because of the chopper. The fundamental and several harmonics of this frequency are within the pass-band of the low-frequency voltmeter, so that, even with no input signals, the voltmeter indicates a large output "noise." Comparison of fluctuation amplitudes on graphs made by the recorder, whose pen-drive system cannot respond to the 60-cps voltage, indicates that there is, as one would expect, no difference in the output signal-to-noise ratio for this correlator and an "honest" one, if the chopper "noise" is neglected.

References

1. Cheatham, T. P., Jr., *An Electronic Correlator*, Technical Report No. 122, Research Laboratory of Electronics, Massachusetts Institute of Technology, Cambridge, Massachusetts (March 28, 1951).

2. Singleton, H. E., *A Digital Electronic Correlator*, Technical Report No. 152, Research Laboratory of Electronics, Massachusetts Institute of Technology, Cambridge, Massachusetts (February 21, 1950).

3. Somerville, M. J., "An Electronic Multiplier," *Electronic*

TABLE 3.1

Comparison of Measured and Predicted Output
Signal-to-Noise Ratios for Several Correlators

Correlator	Input Signal-to-Noise Ratio	Bandwidth	Output Signal-to-Noise Ratio	
			Predicted	Measured
Fig. 3.10	-10 db	Q=2 (ω_p=1930π)	+13.9 db	+12.3 db
"	-13	Q=2	7.9	6.3
"	-10	Q=4 (ω_p=950π)	10.8	10.5
"	-10	Q=8 (ω_p=430π)	7.4	8.3
Fig. 3.10 as square-law detector (inputs parallel)	-10	Q=2	10.9	8.5
Fig. 3.10 with choppers (Fig. 3.11) as correlator	-10	Q=2	13.9	11.0
Fig. 3.12	-10	Q=2	13.9	-3.4

Eng. 24, 78-80 (February 1952); Price, Robert,"An FM-AM Multiplier of High Accuracy and Wide Range, Tecnnical Report No. 213, Research Laboratory of Electronics, Massachusetts Institute of Technology, Cambridge, Massachusetts (October 4, 1951).

4. See, for example, Chance, B., V. Hughes, E. F. McNichol, D. Sayre, and F. C. Williams, Waveforms, McGraw-Hill, New York (1949), Chap. 19.

5. Marshall, B. O., Jr., "An Analogue Multiplier," Nature (London), 167, 29-30 (January 6, 1951).

6. Weinberg, L., and L. G. Kraft, Experimental Study of Nonlinear Devices by Correlation Methods, Technical Report No. 178, Research Laboratory of Electronics, Massachusetts Institute of Technology, Cambridge, Massachusetts (January 20, 1951).

7. Miller, F. G. Development of the Type 48-A Power-Level Recorder, Technical Memorandum No. 10, Acoustics Research Laboratory, Harvard University, Cambridge, Massachusetts (August 15, 1949). The recorder has since been provided with a d-c input circuit, giving recording sensitivities from .352 v/in. to .0262 v/in. The input impedance of the d-c amplifier is of the order of magnitude of one megohm, and causes negligible loading of the RC averagers, at the outputs of the correlators. While recording, the 1-microfarad capacitors in the averaging networks were shunted by 10-microfarad capacitors to reduce the noise output and thus give greater accuracy on the recorder traces. These condensers were removed for measurements with the low-frequency voltmeter.

IV

SIGNAL-TO-NOISE RATIO AT THE OUTPUT OF A DETECTOR

A detector is assumed to consist of a rectifier and an averaging network or filter. It is of interest to compute output signal-to-noise ratios from the detector both for comparison with those for correlators, and for estimating output signal-to-noise ratios for circuits which are similar in operation to correlators but somewhat easier to construct. These correlator-type circuits will be discussed in Chapter V.

Considerable attention has been given in the literature to the problem of the signal-to-noise ratio after a detector.[1] The problem solved here is one which can be handled by fairly straightforward mathematical techniques. We limit our consideration to the case of a noise signal in a noise background, where the signal and the noise have the same spectral distribution, to the case of the full-wave detector,* and to the case of relatively long averaging time and very small input signal-to-noise ratios. The problem of detection reduces to the question of whether the increment in the average output of the detector due to the signal can be seen in the presence of the output noise. As long as the input signal-to-noise ratio is very small, these results should be useful for any type of input signal, because the probability density for the sum of a gaussian noise and any small signal is approximately the same as that for a gaussian noise having a mean-square amplitude equal to the sum of the mean-square amplitudes of the noise and the signal.

Detector Output Signal-to-Noise Ratio

Let us suppose that the instantaneous voltage output of a rectifier circuit is f[v(t)], where v(t) is the instantaneous input voltage. We assume that v(t) is gaussianly distributed

----

* A more mathematically elegant solution of this problem by Middleton and Stone is included herewith as Appendix III.

and has the mean-square N. For a full-wave power law detec-
tor

$$f(v) = |v|^\nu$$

(4.1)

Then the average output of the detector is

$$\overline{F(t)} = \frac{1}{\sqrt{2\pi N}} \int_0^\infty |v|^\nu e^{-v^2/2N} \, dv$$

$$= \frac{\sqrt{2}}{\sqrt{\pi N}} \int_0^\infty v^\nu e^{-v^2/2N} \, dv$$

$$\left. \begin{array}{l} = N^{\nu/2} \left[\dfrac{\nu!}{2^{\nu/2} \left(\frac{\nu}{2}\right)!} \right] \quad \nu \text{ even;} \\[4mm] = \dfrac{(2N)^{\nu/2}}{\sqrt{\pi}} \left(\dfrac{\nu-1}{2}\right)!, \ \nu \text{ odd.} \end{array} \right\} \quad (4.2)$$

If the output is averaged by a network whose weighting func-
tion is $g(t)$, the output of the averaging network is (Eq. (2.1))

$$F(t) = \int_0^\infty g(t') \, f[v(t-t')] \, dt' \ ,$$

and its mean square is

$$\overline{F^2(t)} = \left\langle \left(\int_0^\infty g(t') \, f[v(t-t')] \, dt' \right) \left(\int_0^\infty g(t') \, f[v(t-t')] \, dt' \right) \right\rangle$$

$$= \left\langle \int_0^\infty \int_0^\infty g(t') \, g(t'') \, f[v(t-t')] f[v(t-t'')] \, dt' \, dt'' \right\rangle .$$

Let $v(t-t') = x$ and $v(t\ t'') = y$. Then

$$\overline{F^2(t)} = \left\langle \int_0^\infty \int_0^\infty g(t') \, g(t'') \, f(x) \, f(y) \, dt' \, dt'' \right\rangle .$$

We evaluate this by means of the joint probability density for

the gaussianly distributed variables x and y,

$$P(x,y,\xi) = \frac{1}{2\pi N} \frac{1}{\sqrt{1 - \rho^2(\xi)}} e^{-\frac{x^2 + y^2 - 2xy\,(\xi)}{2N[1-\rho^2(\xi)]}} \quad , \quad (4.3)$$

where $\rho(\xi)$ is the normalized autocorrelation function of x (or y). $P(x,y,\xi)\,dxdy$ is the probability that the voltage lies between x and $(x + dx)$ at some time t and between y and $(y + dy)$ at the time $t + \xi$. Thus

$$\overline{F^2(t)} = \int_0^\infty \int_0^\infty \int_{-\infty}^\infty \int_{-\infty}^\infty g(t') g(t'') f(x) f(y) P(x,y,t''-t')dxdydt'dt''.$$

We make the change of variables (cf. Chap. II),

$$t'' - t' = \xi \quad \text{and} \quad t'' + t' = \eta$$

perform the integration with respect to η, and find that

$$\overline{F^2(t)} = \int_{-\infty}^\infty \int_{-\infty}^\infty \int_{-\infty}^\infty w(\xi) f(x) f(y) P(x,y,\xi) \, dxdyd\xi, \qquad (4.4)$$

where $w(\xi)$ is the transformed weighting function of the averaging network. To evaluate the integral in Eq. (4.4), we note that Eq. (4.3) can be written

$$P(x,y,\xi) = \frac{1}{2\pi N\sqrt{1-\rho^2(\xi)}} e^{-\frac{(x-y)^2}{4N[1-\rho(\xi)]}} e^{-\frac{(x+y)^2}{4N[1+\rho(\xi)]}} \quad ,$$

and that, by Eq. (4.1),

$$f(x) f(y) = |xy|^\nu \quad ,$$

which can be written

$$|xy|^\nu = \left| \frac{(x+y)^2 - (x-y)^2}{4} \right|^\nu.$$

Then

$$\overline{F^2(t)} = \int_{-\infty}^\infty \int_{-\infty}^\infty \int_{-\infty}^\infty w(\xi) \left| \frac{(x+y)^2 - (x-y)^2}{4} \right|^\nu e^{-\frac{(x-y)^2}{4N[1-\rho(\xi)]}} \quad .$$

$$e^{-\frac{(x+y)^2}{4N[1+\rho(\xi)]}} \cdot \frac{dx\,dy\,d\xi}{2N\sqrt{1-\rho^2(\xi)}}$$

We now let

$$\frac{x-y}{\sqrt{4N[1-\rho(\xi)]}} = u \quad \text{and} \quad \frac{x+y}{\sqrt{4N[1+\rho(\xi)]}} = v ,$$

whence

$$\frac{dx\,dy}{2N\sqrt{1-\rho^2(\xi)}} = du\,dv,$$

and

$$\overline{F^2(t)} = \frac{N^\nu}{\pi} \int_\infty^\infty \int_\infty^\infty \int_\infty^\infty w(\xi) \left| u^2[1-\rho(\xi)] - v^2[1+\rho(\xi)] \right|^\nu \cdot$$

$$e^{-u^2} e^{-v^2}\,du\,dv\,d\xi. \qquad (4.5)$$

We now let

$$u^2 + v^2 = r^2, \quad u = r\cos\theta, \quad v = r\sin\theta,$$

and Eq. (4.5) becomes

$$\overline{F^2(t)} = \frac{N^\nu}{\pi} \int_\infty^\infty \int_0^{2\pi} \int_0^\infty w(\xi) \left| \cos 2\theta - \rho(\xi) \right|^\nu r^{2\nu+1} e^{-r^2}\,dr\,d\theta\,d\xi.$$

We perform the r-integration and set $2\theta = \phi$.

Then

$$\overline{F^2(t)} = N^\nu \nu! \int_{-\infty}^\infty w(\xi) \frac{1}{2\pi} \int_0^{2\pi} \left| \cos\phi - \rho(\xi) \right|^\nu d\phi\,d\xi. \qquad (4.6)$$

We have found it difficult to evaluate the integral

$$I = \frac{1}{2\pi} \int_0^{2\pi} \left| \cos\phi - \rho(\xi) \right|^\nu d\phi \qquad (4.7)$$

for arbitrary values of ν, although it must represent a continuous

function of v for $0 < v < \infty$. It is possible, however, to evaluate it for a few specific values of v:

When $v = 1$,

$$I = \frac{1}{\pi} \int_0^{\cos^{-1}\rho(\xi)} [\cos\phi - \rho(\xi)]\, d\phi + \frac{1}{\pi} \int_{\cos^{-1}\rho(\xi)}^{\pi} [\rho(\xi) - \cos\phi]\, d\phi$$

$$= \frac{2}{\pi}[\rho(\xi) \sin^{-1} \rho(\xi) + \sqrt{1 - \rho^2(\xi)}].$$

We substitute the following series expansions:

$$\rho(\xi) \sin^{-1} \rho(\xi) = \sum_{k=0}^{\infty} \frac{(2k)!}{2^{2k}(k!)^2} \frac{\rho^{2k+2}(\xi)}{2k+1},$$

$$\sqrt{1 - \rho^2(\xi)} = 1 - \sum_{k=0}^{\infty} \frac{(2k)!}{2^{2k}(k!)^2} \frac{\rho^{2k+2}(\xi)}{2k+2}.$$

Then, for $v = 1$,

$$I = \frac{2}{\pi} + \frac{2}{\pi} \sum_{k=0}^{\infty} \frac{(2k)!}{2^{2k}(k!)^2} \frac{1}{(2k+1)(2k+2)} \rho^{2k+2}(\xi),$$

and Eq. (4.6) is

$$\overline{r^2(t)} = \frac{2N}{\pi} + \frac{2N}{\pi} \sum_{k=0}^{\infty} \frac{(2k)!}{2^{2k}(k!)^2} \frac{1}{(2k+1)(2k+2)} \int_{-\infty}^{\infty} w(\xi) \rho^{2k+2}(\xi)\, d\xi.$$

$$(4.8)$$

If v in Eq. (4.7) is an even integer,

$$I = \frac{1}{2\pi} \int_0^{2\pi} [\cos\phi - \rho(\xi)]^v\, d\phi$$

$$= \frac{1}{2\pi} \int_0^{2\pi} \sum_{m=0}^{v} (-1)^m \frac{v!}{(v-m)!\, m!} \cos^{v-m}\phi\, \rho^m(\xi)\, d\phi.$$

This integral amounts simply to averaging over a period of ϕ. We can write

$$\overline{\cos^{\nu-m}\phi} = \overline{\left[\frac{e^{i\phi} + e^{-i\phi}}{2}\right]^{\nu-m}} \quad ,$$

and, after expanding by the binomial theorem, we see that the only term with nonvanishing average is the term independent of ϕ. That is,

$$\overline{\cos^{\nu-m}}\phi = \frac{(\nu-m)!}{2^{\nu-m}(\frac{\nu-m}{2})!^2} \quad , \quad (\nu-m) \text{ even,}$$

$$= 0, \quad (\nu-m) \text{ odd.}$$

$$\left.\right\} \quad (4.9)$$

Then, substituting 2ℓ for m, in order to retain only the terms for even values of m (and even values of $(\nu-m)$), we have

$$I = \sum_{\ell=1}^{\nu/2} \frac{\nu! \, \rho^{2\ell}(\xi)}{(2\ell)! \, 2^{\nu-2\ell}(\frac{\nu}{2}-\ell)!^2} + \frac{\nu!}{2^{\nu}(\frac{\nu}{2})!^2}$$

and, for ν even, Eq. (4.6) is

$$\overline{F^2(t)} = \frac{N^{\nu}\nu!^2}{2^{\nu}(\frac{\nu}{2})!^2} + \frac{N^{\nu}\nu!^2}{2^{\nu}} \sum_{\ell=1}^{\nu/2} \frac{2^{2\ell}}{(2\ell)!(\frac{\nu}{2}-\ell)!^2} \int_{-\infty}^{\infty} w(\xi) \, \rho^{2\ell}(\xi)d\xi.$$

$$(4.10)$$

If there is added to the input "background noise" a small noise signal of mean-square amplitude S, there will be an incremental increase in the average output. From Eqs. (4.2), this increment (which we call the output signal) is, for $\nu = 1$,

$$\sqrt{\frac{2(N+S)}{\pi}} - \sqrt{\frac{2N}{\pi}} = \sqrt{\frac{2N}{\pi}}[\sqrt{1+S/N} - 1] \cong \sqrt{\frac{2N}{\pi}} \frac{1}{2}(\frac{S}{N}),$$

$$S \ll N,$$

and for $\nu = 2, 4, 6, 8, \ldots$,

$$\left[\frac{\nu!}{2^{\nu/2}(\frac{\nu}{2})!}\right]\left[(N + S)^{\nu/2} - N^{\nu/2}\right] \cong N^{\nu/2}\left[\frac{\nu!}{2^{\nu/2}(\frac{\nu}{2})!}\right]\frac{\nu}{2}(\frac{S}{N}), \quad S \ll N.$$

The output noise can be measured as the difference between the
mean square of the output and the square of the average output.
Then the mean-square output signal-to-noise ratio is, for $\nu = 1$,
and $(S/N)_{in} \ll 1$, (from Eq. (4.8)),

$$(S/N)_{out} = \frac{\frac{1}{4}(\frac{S}{N})^2_{in}}{\sum_{k=0}^{\infty} \frac{(2k)!}{2^{2k}(k!)^2} \frac{1}{(2k+1)(2k+2)} \int_{-\infty}^{\infty} w(\xi)\rho^{2k+2}(\xi)\, d\xi} , \quad (4.11)$$

and for $\nu = 2, 4, 6, 8, \ldots$ (from Eq. (4.10)),

$$(S/N)_{out} = \frac{\nu^2/4\ (S/N)^2_{in}}{(\nu/2)!^2 \sum_{\ell=1}^{\nu/2} \frac{2^{2\ell}}{(2\ell)!(\frac{\nu}{2}-\ell)!^2} \int_{-\infty}^{\infty} w(\xi)\rho^{2\ell}(\xi)\, d\xi} . \quad (4.12)$$

Evaluation for Specific Examples

The output signal-to-noise ratio depends upon the correlation
function $\rho(\xi)$ of the input noise (or its spectrum) and upon the
transformed weighting function of the averaging filter (or its
frequency response). The integrals to be evaluated are in each
case of the same form,

$$J = \int_{-\infty}^{\infty} w(\xi)\ \rho^{2\ell}(\xi)\ d\xi . \quad (4.13)$$

This integral can be readily evaluated for at least two forms
of input spectra, for an RC averaging network, subject to the
assumptions that the averaging time is very long, and that the
input bandwidth is at least moderately narrow. We use the
transformed weighting function for an RC averager, from Eq.
(2.9),

$$w(\xi) = \frac{1}{2RC}\ e^{-|\xi|/RC} .$$

a. **Tuned Circuit Spectrum:** The normalized autocorrelation
function of "white" noise after passage through a moderately

high-Q single-tuned circuit filter, of center frequency $\omega_o/2\pi$ and half-bandwidth $\omega_F/2\pi$ is (see Appendix II)

$$\rho(\tau) = e^{-\omega_F|\tau|} \cos \omega_o \tau .$$

Then, for this case, Eq. (4.13) is

$$J = \frac{1}{2RC} \int_{-\infty}^{\infty} e^{-|\xi|/RC} \cos^{2l}\omega_o\xi \; e^{-2l\omega_F|\xi|} d\xi$$

$$= \frac{1}{RC} \int_{0}^{\infty} e^{-[\frac{1}{RC} + 2l\omega_F]\xi} \cos^{2l}\omega_o\xi \; d\xi .$$

If we assume that $\omega_o \gg \omega_F$, we can replace the cosine term with its average value which we found in Eqs. (4.9):

$$J \cong \frac{(2l)!}{RC \; 2^{2l}(l!)^2} \int_{0}^{\infty} e^{-[\frac{1}{RC} + 2l\omega_F]\xi} d\xi = \frac{(2l)!}{2^{2l}(l!)^2[1 + 2l\omega_F RC]} .$$

If we assume now that $RC \gg \frac{1}{\omega_F}$, which simply corresponds to thorough filtering, we have

$$J \cong \frac{(2l)!}{2^{2l}(l!)^2 \; 2l\omega_F RC} .$$

Substituting this value in Eqs. (4.11) and (4.12) gives the mean-square output signal-to-noise ratio for the tuned-circuit input spectrum; for $\nu = 1$,

$$(S/N)_{out} = \frac{2\omega_F RC \; (S/N)^2_{in}}{\sum\limits_{k=0}^{\infty} \left[\frac{(2k)!}{2^{2k}(k!)^2}\right]^2 \frac{1}{(k+1)^3}}$$

$$= 2\omega_F RC \; (S/N)^2_{in} \cdot 0.965 \; ; \; (S/N)_{in} \ll 1;$$

and for $\nu = 2, 4, 6, 8, \ldots\ldots,$

$$(S/N)_{out} = 2\omega_{P}RC(S/N)_{in}^{2} \frac{(\frac{v}{2})^{2}(\frac{v}{2})!^{2}}{\sum\limits_{l=1}^{v/2} \frac{1}{l(\frac{v}{2}-l)!^{2}(l!)^{2}}} \; ; \; (S/N)_{in} \ll 1.$$

Values of $\dfrac{(S/N)_{out}}{2\omega_{P}RC(S/N)_{in}^{2}}$ computed from the above for various

values of v are tabulated in Table 4.1.

<div>

Table 4.1

Tuned-Circuit Spectrum

Power Law of Full-Wave Detector	Relative Output S/N Ratio	Relative Output S/N Ratio
1	.965	-0.12 db
2	1.000	0.00
4	.889	-0.48
6	.650	-1.84
8	.405	-3.90
10	.212	-6.58

</div>

b. Rectangular Spectrum: The normalized autocorrelation function of noise whose spectrum is constant between $(\omega_{o} - \Delta\omega)$ and $(\omega_{o} + \Delta\omega)$ and zero elsewhere is

$$\rho(\tau) = \cos \omega_{o}\tau \; [\frac{\sin\Delta\omega\tau}{\Delta\omega\tau}].$$

Then J (Eq. (4.13)) is

$$J = \frac{1}{2RC} \int\limits_{-\infty}^{\infty} e^{-|\xi|/RC} \cos^{2l} \omega_{o}\xi [\frac{\sin\Delta\omega\xi}{\Delta\omega\xi}]^{2l} \, d\xi.$$

We again replace the cosine term by its average value as before,

and assume that $RC \gg \dfrac{1}{\Delta\omega}$, so that throughout the range where the integrand is appreciably different from zero,

$$e^{-|\xi|/RC} \approx 1.$$

Then

$$J \approx \frac{1}{2RC} \ \frac{(2\ell)!}{2^{2\ell}(\ell!)^2} \int_{-\infty}^{\infty} \left[\frac{\sin\Delta\omega\xi}{\Delta\omega}\right]^{2\ell} d\xi$$

$$= \frac{1}{2\Delta\omega RC} \ \frac{(2\ell)!}{2^{2\ell}(\ell!)^2} \int_{-\infty}^{\infty} \left[\frac{\sin x}{x}\right]^{2\ell} dx.$$

The integral

$$K_\ell = \int_{-\infty}^{\infty} \left[\frac{\sin x}{x}\right]^{2\ell} dx,$$

which can be evaluated by contour integration, has the values given below:

ℓ	K_ℓ
1	π
2	$.6667\,\pi$
3	$.5500\,\pi$
4	$.4794\,\pi$
5	$.4304\,\pi$

By substituting the values of $J = \dfrac{1}{2\Delta\omega RC} \ \dfrac{(2\ell)!}{2^{2\ell}(\ell!)^2} K_\ell$ in Eqs. (4.11) and (4.12), we find, for $v = 1$,

$$(S/N)_{out} = \frac{\frac{2\Delta\omega RC}{\pi}(S/N)^2_{in}}{\sum\limits_{k=0}^{\infty} \left[\frac{(2k)!}{2^{2k}\ k!\ (k+1)!}\right]^2 \frac{K_{k+1}}{\pi}}$$

$$= 2RC\,(\Delta\omega)\,\frac{1}{\pi}\,(S/N)^2_{in} \cdot 0.952$$

and, for $v = 2, 4, 6, 8, \ldots\ldots,$

$$(S/N)_{out} = \frac{2\Delta\omega RC}{\pi} (S/N)^2_{in} \left[\frac{(v/2)^2/(v/2!)^2}{\sum\limits_{\ell=1}^{v/2} \frac{K_\ell/\pi}{(\frac{v}{2}-\ell)!^2 \ell!^2}} \right]$$

Values of $\dfrac{(S/N)_{out}}{\frac{2\Delta\omega RC}{\pi}(S/N)^2_{in}}$ computed from the above for various

values of v are tabulated in Table 4.2.

Table 4.2

Rectangular Spectrum

Power Law of Full-Wave Detector	Relative Output S/N Ratio	Relative Output S/N Ratio
1	0.952	-0.18 db
2	1.000	0.00
4	.858	-0.64
6	.580	-2.33
8	.325	-4.85
10	.157	-8.02

Conclusions

Curves of relative output signal-to-noise ratio are plotted in Fig. 4.1 for these two input spectra. For both input spectra there is a slightly better output signal-to-noise ratio for the square-law detector, although the linear detector is not appreciably worse. The slight superiority of the square-law detector is also predicted by Mayer[3] although his results for the half-wave detector are apparently in error. He predicts that the half-wave detector should be considerably inferior to the full-wave detector; we, and others, feel that, for long averaging times, there should be no difference. Burgess[4] finds that the square-law detector has a similar slight superiority with
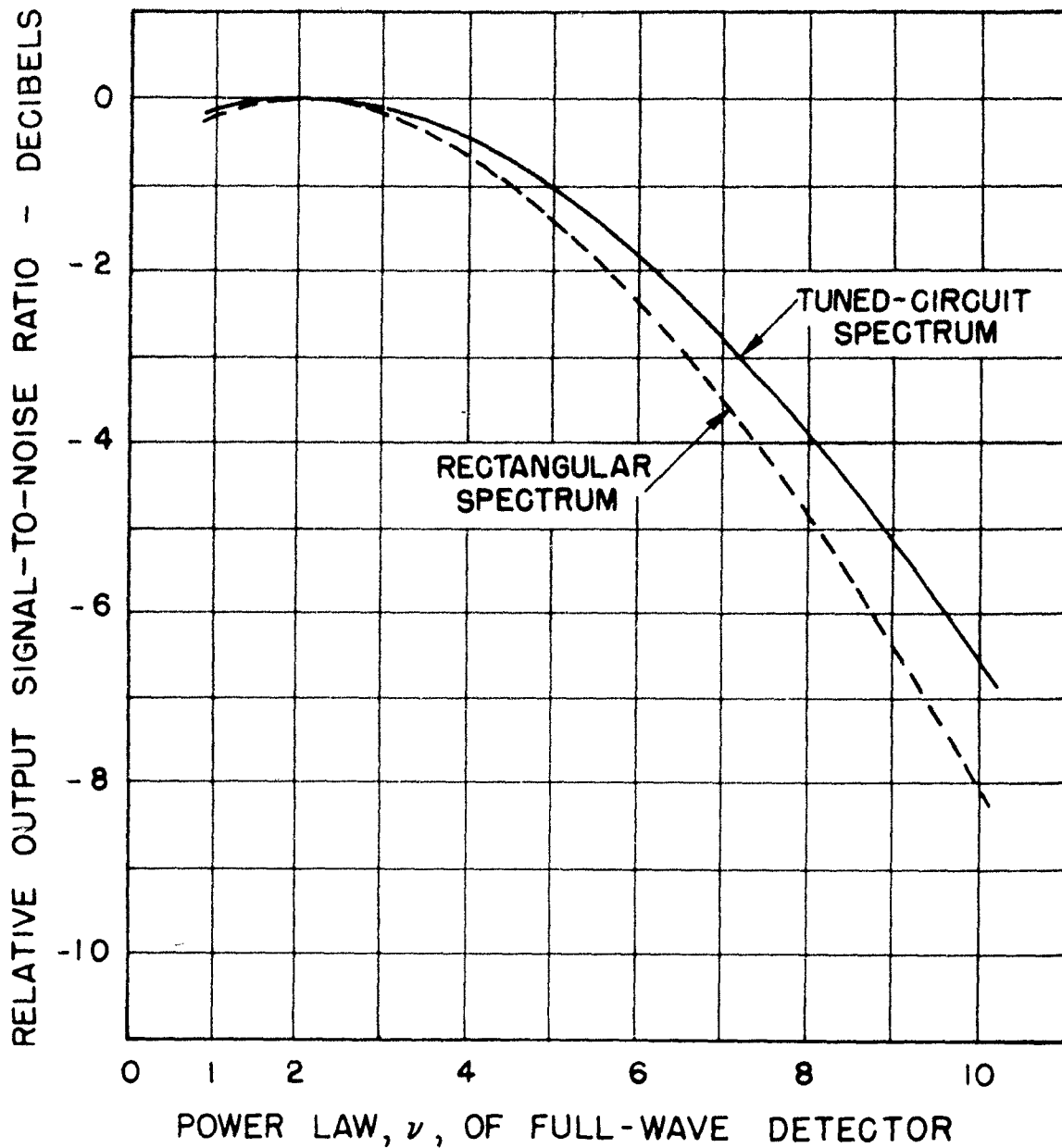
Fig. 4.1. Relative output signal-to-noise ratio for two different input spectra as functions of the power law of the detector.

respect to output signal-to-noise ratio in the detection of a sinusoid in noise, although his work is based on different assumptions concerning the averaging time.

References

1. Bennett, W. R., "The Response of a Linear Rectifier to Signal and Noise," J. Acoust. Soc. Am. 15, 164-172 (January 1944); Rice, S. 0., "Mathematical Analysis of Random Noise," Bell Syst. Tech. J. 23, 282-332 (July 1944); 24, 46-158 (January 1945); Middleton, D., "The Response of Biased, Saturated Linear and Quadratic Rectifiers to Random Noise," J. Appl. Phys. 17, 778-801 (October 1946); Kac, M., and A. J. F. Siegert, "On the Theory of Noise in Radio Receivers with Square Law Detectors," J. Appl. Phys. 18, 383-397 (April 1947); Middleton, D., "Some General Results in the Theory of Noise through Non-Linear Devices," Quart. Appl. Math. 5, 445-498 (January 1948); Middleton, D., "Rectification of a Sinusoidally Modulated Carrier in the Presence of Noise," Proc. I.R.E. 36, 1467-1477 (December 1948), Burgess, R. E., "The Rectification and Observation of Signals in the Presence of Noise," Phil. Mag. 42, 475-503 (May 1951).

2. Lawson, J. L., and G. E. Uhlenbeck, Threshold Signals, McGraw-Hill, New York (1950), p. 55.

3. Mayer, H. F., Radio Noise Considerations, Solar Noise Technical Report No. 1, School of Electrical Engineering, Cornell University, Ithaca, New York, August 1949.

4. Burgess, R. E., "The Rectification and Observation of Signals in the Presence of Noise," Phil. Mag. 42, 475 (May 1951).

V.
OTHER CORRELATOR-TYPE CIRCUITS

Two other circuits which behave in much the same way as a multiplier-averager have been analyzed. Although these circuits do not produce quite as high output signal-to-noise ratios as a multiplier-averager, they do have characteristics which may be advantageous in certain uses, and one of them is considerably easier to construct and operate. The first to be discussed is the polarity coincidence correlator, which measures the degree of correlation of two signals by determining the fraction of time that the instantaneous polarities of the two signals are the same; the other, the linear rectifier correlator, is the same as the multiplier-averager shown in Fig. 3.4 with the square-law rectifiers replaced with linear rectifiers. The first of these is thus seen to be at least similar in operation to a conventional phase meter, and the second is simply a form of the coherent detector.

The Polarity Coincidence Correlator

The polarity coincidence correlator is an electronic circuit with two inputs, whose output, before averaging, is +1 v when the instantaneous polarities of the two inputs are the same, and -1 v when the inputs have opposite polarities. This operation can be realized by severely clipping both inputs and applying the resultant rectangular voltage waves to any of a variety of coincidence circuits. If the two inputs are incoherent random noises, the average output will be zero, since the two inputs will be of the opposite polarity as often as they are of the same polarity. If the inputs are identical the output will be +1 regardless of the input signal amplitudes. The average output depends on the degree of coherence of the two input signals rather than on their amplitudes, since all amplitude information is removed in the clipping.

The average output of the polarity coincidence correlator

is simply the probability that the instantaneous signs of the two inputs are the same less the probability that the instantaneous signs are different. We can compute this probability only if we know the joint probability density for the two input functions. We assume here that both inputs are gaussian random functions, and our results here are only valid for that case. The probability that the signs of both inputs are positive is

$$p = \int_0^\infty \int_0^\infty P_2(x,y,\tau)\,dx\,dy,$$

where $x(t)$ is one input function,

$y(t-\tau)$ is the other input function,

and $P_2(x,y,\tau)$ is the joint probability density for the gaussian random functions x and y (Eq. (4.3)). In terms of $\rho(\tau)$, the normalized correlation function of $x(t)$ and $y(t)$,

$$p = \frac{1}{2\pi N}\frac{1}{\sqrt{1-\rho^2(\tau)}}\int_0^\infty \int_0^\infty e^{-\frac{x^2 + y^2 - 2xy\rho(\tau)}{2N[1-\rho^2(\tau)]}}\,dx\,dy,$$

where N is the mean square of $x(t)$ and $y(t)$. Paralleling the procedure of Chapter IV, following Eq. (4.4), we write the above as

$$p = \frac{1}{2\pi N}\frac{1}{\sqrt{1-\rho^2(\tau)}}\int_0^\infty \int_0^\infty e^{-\frac{(x-y)^2}{4N[1-\rho(\tau)]}-\frac{(x+y)^2}{4N[1+\rho(\tau)]}}\,dx\,dy$$

and make the change of variables

$$\frac{x+y}{\sqrt{4N[1+\rho(\tau)]}} = u \qquad \text{and} \qquad \frac{x-y}{\sqrt{4N[1-\rho(\tau)]}} = v.$$

$$p = \frac{1}{\pi} \int_0^\infty \int_{-u\sqrt{\frac{1+\rho(\tau)}{1-\rho(\tau)}}}^{+u\sqrt{\frac{1+\rho(\tau)}{1-\rho(\tau)}}} e^{-(u^2+v^2)} \, dv \, du.$$

We then substitute

$$r^2 = u^2 + v^2; \quad u = r \cos \theta; \quad v = r \sin \theta,$$

$$p = \frac{2}{\pi} \int_0^{\tan^{-1}\sqrt{\frac{1+\rho(\tau)}{1-\rho(\tau)}}} \int_0^\infty e^{-r^2} \, r \, dr \, d\theta$$

$$= \frac{1}{\pi} \tan^{-1}\sqrt{\frac{1+\rho(\tau)}{1-\rho(\tau)}} = \frac{1}{4} + \frac{1}{2\pi} \sin^{-1}\rho(\tau).$$

The probability that the signs of both inputs will be negative will also be p, so the probability that the instantaneous signs of both inputs are the same is

$$2p = \frac{1}{2} + \frac{1}{\pi} \sin^{-1}\rho(\tau).$$

The probability that the signs of the two input functions are different must then be

$$1 - 2p = \frac{1}{2} - \frac{1}{\pi} \sin^{-1}\rho(\tau).$$

The average output of the polarity coincidence correlator is the difference of these two probabilities or

$$\overline{F(t)} = \frac{2}{\pi} \sin^{-1}\rho(\tau). \tag{5.1}$$

The average output thus depends only on the normalized cross-correlation of the two input functions. Equation (5.1) is plotted in Fig. 5.1 for the range $\rho(\tau) > 0$; F(t) is clearly an odd function of $\rho(\tau)$.

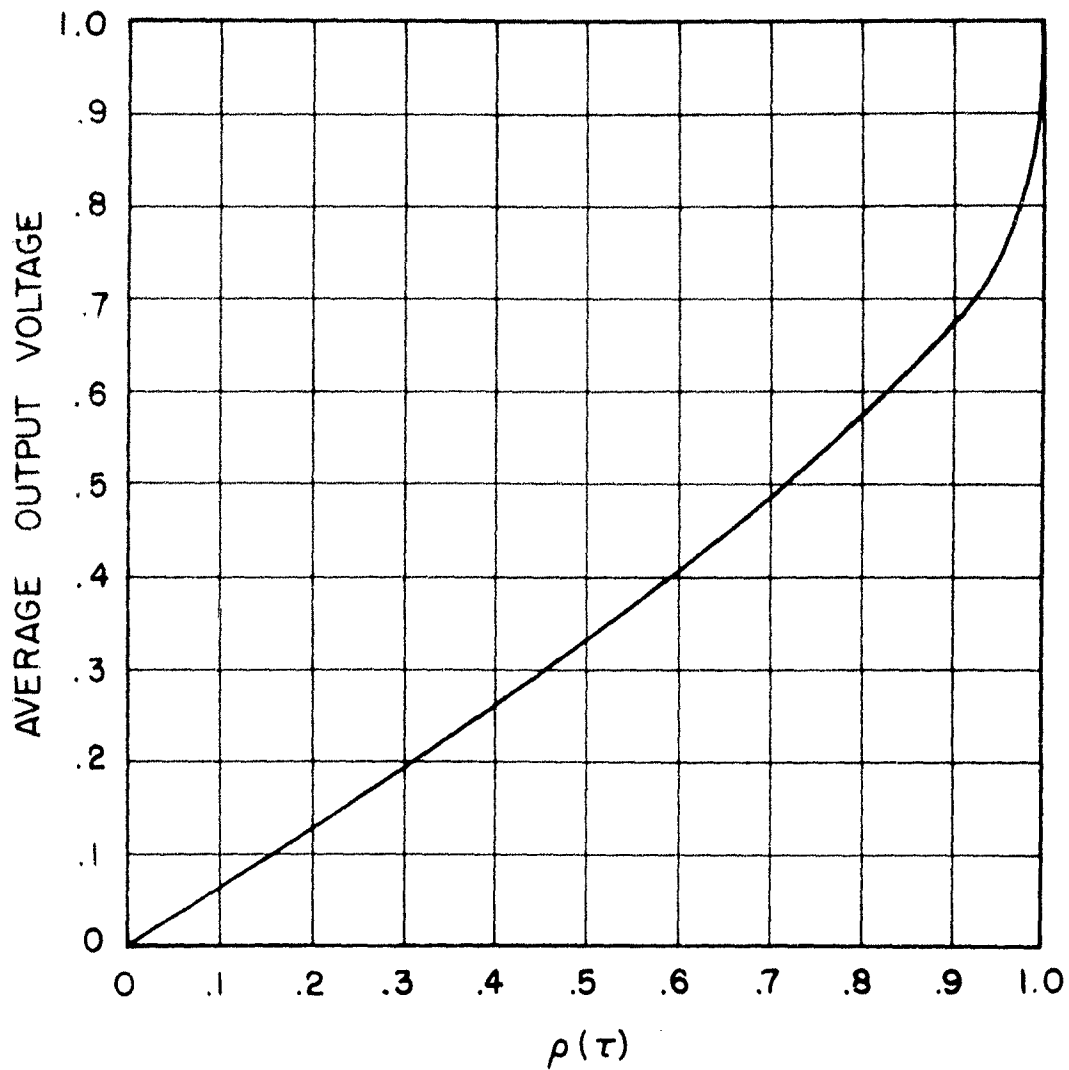If one input function is $[n_1(t) + s(t)]$ and the other is

Fig. 5.1. Average output voltage of the polarity coincidence correlator as a function of the normalized crosscorrelation of the input functions. For negative values of $\rho(\tau)$ the average output is negative; it is an odd function of $\rho(\tau)$.

$[n_2(t) + s(t)]$, where $n_1(t)$, $n_2(t)$ and $s(t)$ are incoherent random functions, and if the mean square of $n_1(t)$ and $n_2(t)$ is N, and the mean square of $s(t)$ is S, the normalized cross-correlation of the inputs is

$$\frac{(S/N)_{in}}{1 + (S/N)_{in}} \ ,$$

where $(S/N)_{in}$ is the mean-square signal-to-noise ratio at either input. In this case, the average output is

$$\overline{F(t)} = \frac{2}{\pi} \sin^{-1} \left[\frac{(S/N)_{in}}{1 + (S/N)_{in}} \right] \ .$$

$$\cong \frac{2}{\pi} (S/N)_{in}, \qquad (S/N)_{in} \ll 1. \qquad (5.2)$$

If one input signal is $[n_1(t)$ and $s(t)]$, as defined above, and the other is simply $s(t)$, the normalized cross-correlation of the input functions is

$$\sqrt{\frac{(S/N)_{in}}{1 + (S/N)_{in}}}$$

and the average output is

$$\overline{F(t)} = \frac{2}{\pi} \sin^{-1} \sqrt{\frac{(S/N)_{in}}{1 + (S/N)_{in}}}$$

$$\cong \frac{2}{\pi} \sqrt{(S/N)_{in}} \ , \qquad (S/N)_{in} \ll 1. \qquad (5.3)$$

The determination of the mean-square output noise (after averaging) has not been attempted for the general case. However, for small input signal-to-noise ratios, it is logical to assume that the output noise is practically the same as that when the signal is completely absent, which can be evaluated when the inputs are incoherent gaussian noises. This is probably the greatest output noise, since, for an infinite input signal-to-noise ratio, the output noise vanishes. We can consider the polarity coincidence correlator as a multiplier-

averager in which the inputs are severely clipped to an amplitude of ± 1 before multiplication. Van Vleck has shown that the autocorrelation function of such strongly clipped gaussian noise is

$$R(\tau) = \frac{2}{\pi} \sin^{-1}\rho(\tau),$$

where $\rho(\tau)$ is the normalized ($\rho(0) = 1$) autocorrelation function of the noise before clipping.[1] When both inputs to the polarity coincidence correlator are uncorrelated but have the same autocorrelation function, $\rho(\tau)$, the mean-square output of the averaging filter will be

$$\overline{F^2(t)} = 2 \int_0^\infty w(\xi)R^2(\xi)\, d\xi,$$

where $w(\xi)$ is the transformed weighting function of the filter. If we assume that the noises have the same spectrum as a narrow-band tuned-circuit filter,

$$\rho(\tau) = e^{-\omega_F|\tau|} \cos\omega_0\tau,$$

where $\omega_F/2\pi$ is the half-bandwidth and $\omega_0/2\pi$ is the center frequency. The mean-square noise output is then

$$\overline{F^2(t)} = 2 \int_0^\infty w(\xi) \frac{4}{\pi^2} \lceil \sin^{-1}(e^{-\omega_F\xi} \cos\omega_0\xi)\rceil\, d\xi.$$

Now, for an RC filter, $w(\xi) = \frac{1}{2RC} e^{-|\xi|/RC}$ and we assume that $\omega_F \gg \frac{1}{RC}$ so, where the rest of the integrand is appreciably different from zero, $w(\xi) \cong w(0) = \frac{1}{2RC}$. We have then

$$\overline{F^2(t)} = \frac{4}{\pi^2 RC} \int_0^\infty [\sin^{-1}(e^{-\omega_F\xi} \cos\omega_0\xi)]^2\, d\xi.$$

Now $\sin^{-1}x = x + x^3/6 + 3x^5/40 + 5x^7/112 + \ldots$

so

$$[\sin^{-1}x]^2 = x^2 + \frac{x^4}{3} + \frac{8}{45}x^6 + \frac{4}{35}x^8 + \ldots \qquad .$$
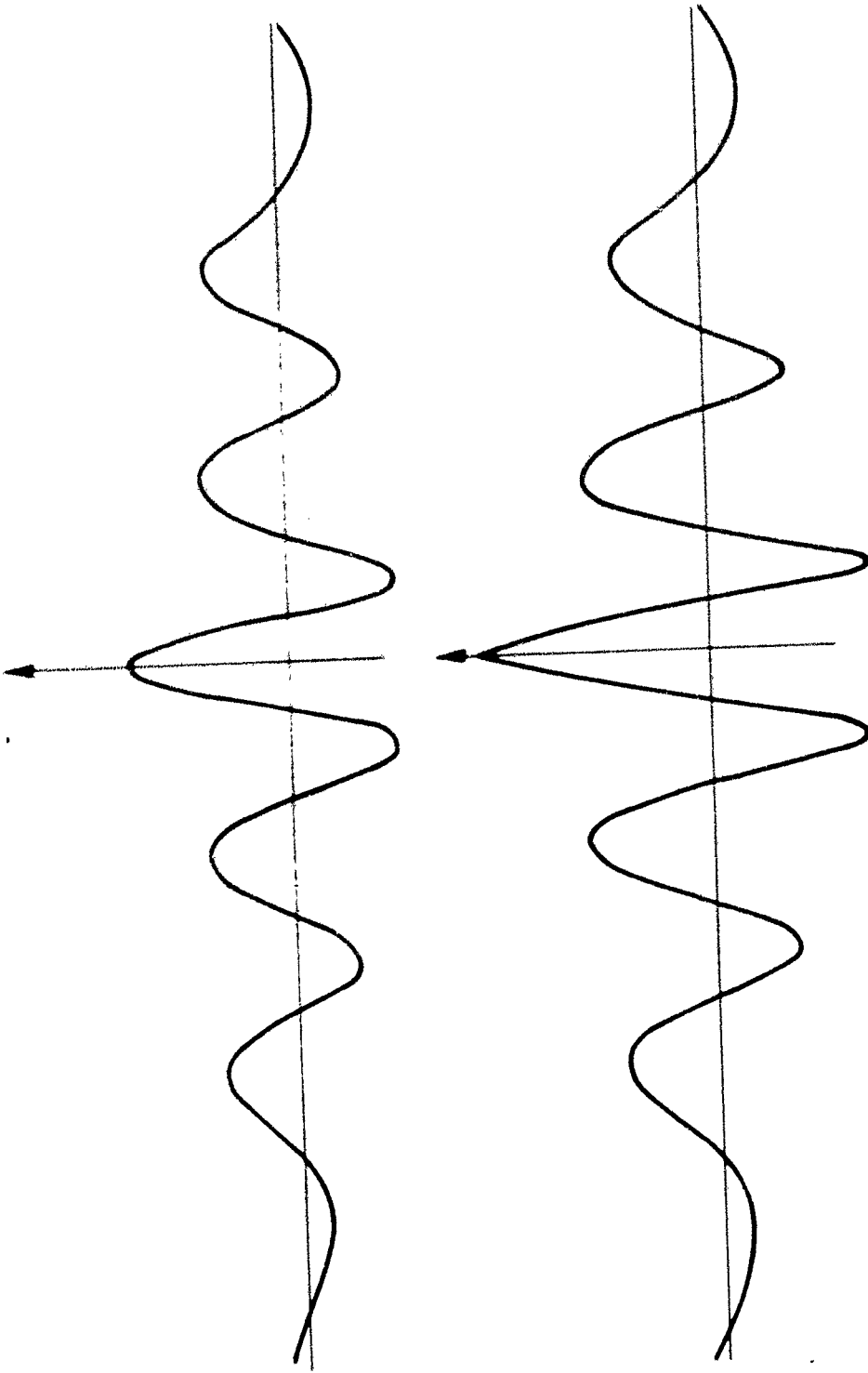
Fig. 5.2. Above: The autocorrelation function of random noise which has a single-tuned-circuit-spectrum. Below: The autocorrelation function (as it would be measured by the polarity coincidence correlator of Gaussian noise having the same spectrum. The delay scale is slightly distorted because the delay was obtained by rotation of an acoustic array.

Then

$$\overline{F^2(t)} = \frac{4}{\pi^2 RC} \int_0^\infty \left[e^{-2\omega_F \xi} \cos^2 \omega_o \xi + 1/3 \; e^{-4\omega_F \xi} \cos^4 \omega_o \xi \right.$$

$$\left. + \frac{8}{45} \; e^{-6\omega_F \xi} \cos^6 \omega_o \xi + \frac{4}{35} \; e^{-8\omega_F \xi} \cos^8 \omega_o \xi + \ldots \right] d\xi.$$

Since we also assume $\omega_F \ll \omega_o$, we can replace the $\cos^n \omega_o \xi$ by their average values

$$\overline{\cos^n \phi} = \frac{n!}{2^n (\frac{n}{2}!)^2} \quad , \qquad n \text{ even},$$

$$= 0, \; n \text{ odd.}$$

Using

$$\int_0^\infty e^{-n\omega_F \xi} \, d\xi = \frac{1}{n\omega_F} \quad ,$$

.we find that the mean-square noise is approximately

$$\overline{F^2(t)} = \frac{4}{\pi^2 RC\omega_F} \left[\frac{1}{4} + \frac{1}{32} + \frac{1}{108} + \frac{1}{1280} + \ldots \right] = \frac{1.164\ldots}{\pi^2 RC \, \omega_F} \quad . \quad (5.4)$$

For small input signal-to-noise ratios, then, the output mean-square signal-to-noise ratio is (from Eq. (5.2))

$$(S/N)_{out} = \frac{1}{1.164} \circ 4RC \, \omega_F (S/N)^2_{in} \; . \qquad (5.5)$$

By reference to Table 2.1, we find that for a multiplier-averager with inputs $[s(t) + n_1(t)]$ and $[s(t) + n_2(t)]$ having the same statistical properties as in the above example, the mean-square output signal-to-noise ratio for small input signals is

$$4RC\omega_F (S/N)^2_{in} \; \circ$$

The polarity coincidence correlator then has a disadvantage for the above spectrum of a factor 1.164 in small-signal-mean-square output signal-to-noise ratio, or 0.7 db. The 0.7 db might be

considered the penalty one pays for not making use of the informa-
tion contained in the clipped portions of the input voltage wave-
forms.

If one input is pure signal, and if the signal-to-noise
ratio at the other input is very small, we can assume that the
output noise is the same as above (Eq. (5.4)). The mean-square
output signal-to-noise ratio for this arrangement is then (from
Eq. (5.3))

$$(S/N)_{out} = \frac{1}{1.164} \cdot 4RC\omega_F(S/N)_{in}. \qquad (5.6)$$

From Table 2.1 it can be seen that the small-signal output signal-
to-noise ratio of a multiplier-averager used in exactly the same
way is

$$4RC\, \omega_F(S/N)_{in},$$

so the polarity coincidence correlator again has a disadvantage
of 0.7 db, for this particular input spectrum and averager.

The polarity coincidence correlator is almost, but not
quite, a normalized correlator; that is, a correlator which
determines the quantity

$$\frac{\overline{x(t)y(t-\tau)}}{\sqrt{\overline{x^2(t)} \cdot \overline{y^2(t-\tau)}}},$$

which is a normalized correlation function. The average output
of such a correlator would be a straight diagonal line on the
graph of Fig. 5.1. The polarity coincidence correlator does
measure the cross-correlation of the clipped input signals.
This means that the autocorrelation function of a sine wave, as
measured by the polarity coincidence correlator, will be saw-
toothed rather than cosinusoidal, and all correlation functions
measured by it (except those of already strongly clipped waves)
will be more or less distorted. As an example, the normalized
correlation function of gaussian noise which has been passed
through a single tuned-circuit filter is plotted at the top
in Fig. 5.2 and the autocorrelation function of the same noise,

as it would be measured by the polarity coincidence correlator
is shown at the bottom. If sufficiently large incoherent
noises were added to each input so that the input normalized
cross-correlation did not ever exceed 0.7, the measured cor-
relation function would be little distorted.

It is possible that a polarity coincidence correlator
could be built more easily than a multiplier-averager; if so,
its performance with respect to output signal-to-noise ratio
is not enough worse than that of a true correlator to rule it
out of consideration. It has the advantage in a practical
application that the input signals would not require automatic
gain control, as is the case with a multiplier-averager, which
may be easily overloaded. The greatest difficulty in its con-
struction will probably be found in the clipping circuits,
where absolute symmetry of clipping must be maintained.

A polarity coincidence correlator consisting of two
clipper-amplifier circuits (Fig. 5.3) and a coincidence-averager
circuit (Fig. 5.4) has been constructed. Note in Fig. 5.3 that
a potentiometer is provided at the output of the clipper cir-
cuits to allow adjustment of the output amplitude. This was
necessitated by the fact that the contact potentials of the
various type-6AL5 twin diodes varied greatly, and it was not
found possible, even by selecting tubes, to make the output
amplitudes from different clipper circuits match exactly with-
out such an adjustment. Measurements made by the methods
described in Chapter III indicate that this correlator's out-
put signal-to-noise ratio for small input signals is inferior
to that of the multiplier-averager by 2 db, when the same in-
put spectra (tuned-circuit, $Q = 4$) and averaging networks
(RC = 0.1 sec) are used. Because of a possible error of ± 1.5 db
in the measurement, we can only conclude from it that the theoret-
ical predictions are roughly confirmed.

Linear Rectifier Correlator

It will be seen that the linear rectifier correlator is of

the same form as a phase-sensitive detector or coherent detector, of which thorough analyses have been already made.[2] We here determine only the average output of the linear rectifier correlator in terms of the properties of the input functions and estimate the small-signal output signal-to-noise ratio.

Figure 5.5 is a block diagram of a linear rectifier correlator. By comparison with Fig. 3.4 it may be seen that the linear rectifier correlator is simply a multiplier-averager of the quarter-difference-squares type, with the square-law rectifiers replaced by linear rectifiers.

We assume that the inputs to a linear rectifier correlator are $[s(t) + n_1(t)]$ and $[s(t-\tau) + n_2(t)]$, where $s(t)$, $n_1(t)$, and $n_2(t)$ are independent, gaussianly distributed, random functions. The sum of these input signals is $s(t) + s(t-\tau) + n_1(t) + n_2(t)$ and the difference is $s(t) - s(t-\tau) + n_1(t) - n_2(t)$. Now the average output of a full-wave linear rectifier, whose input, x, is gaussianly distributed and has the mean square σ^2, is (Eq.(4.2))

$$\sigma\sqrt{\frac{2}{\pi}} \ . \tag{5.7}$$

We cannot simply determine the mean-square amplitudes of the sum and the difference of the input signals by adding the mean squares of the four individual components, because $s(t)$ and $s(t-\tau)$ are not independent functions. We note that

$$\overline{[s(t) + s(t-\tau)]^2} = \overline{s^2(t)} + \overline{2s(t)s(t-\tau)} + \overline{s^2(t-\tau)}$$
$$= 2R(0) + 2R(\tau),$$

where $R(\tau)$ is the autocorrelation function of $s(t)$. The mean square of the sum of the input signals is then

$$\overline{[s(t) + s(t-\tau) + n_1(t) + n_2(t)]^2} = 2[R(0) + R(\tau) + N]$$

and the mean-square of the difference is

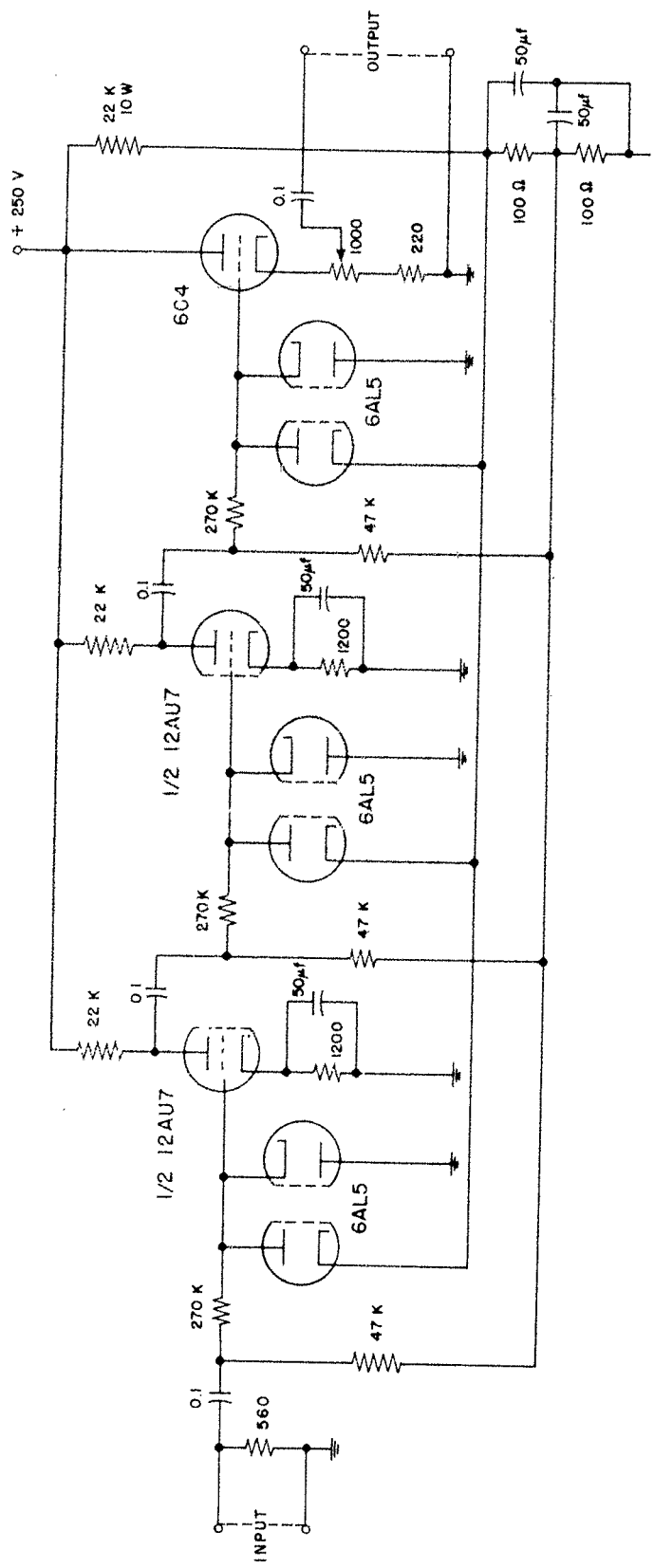$$\overline{[s(t) - s(t-\tau) + n_1(t) - n_2(t)]^2} = 2[R(0) - R(\tau) + N]$$

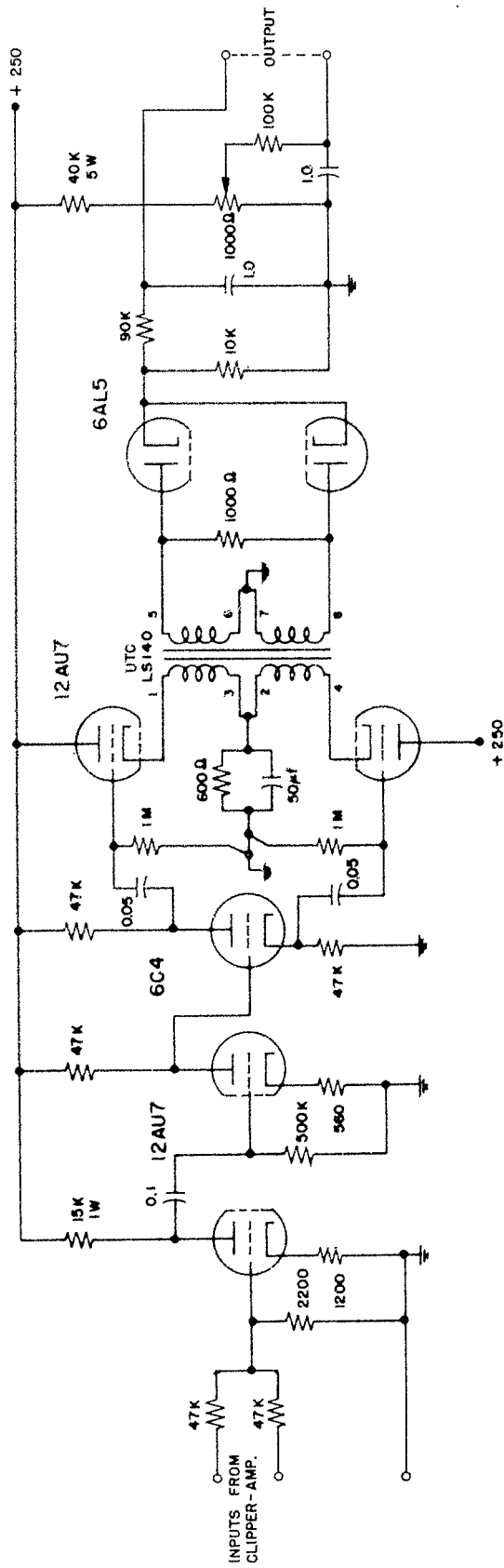Fig. 5.3. Clipper-amplifier unit for polarity coincidence correlator.

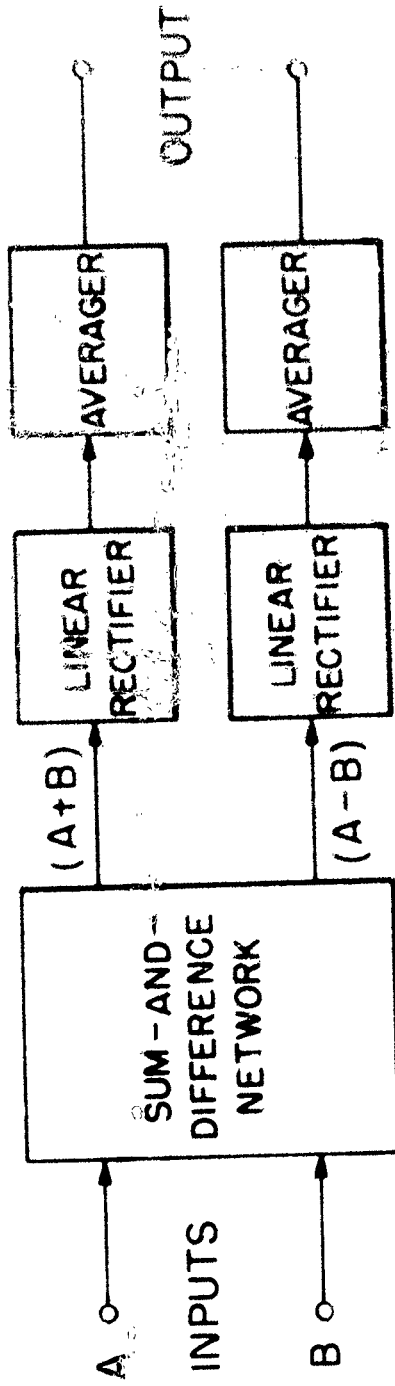Fig. 5.4. Coincidence-averager unit for polarity coincidence correlator.

Fig. 5.5. Block diagram of the linear rectifier correlator.

where $N = \overline{n_1^2(t)} = \overline{n_2^2(t)}$, the mean square of the background noises. The average output of the linear rectifier correlator is the difference of the average outputs of the sum and the difference rectifiers, and is (from Eq. (5.7)),

$$\sqrt{\tfrac{2}{\pi}}\sqrt{2[R(0)+R(\tau)+N} - \sqrt{\tfrac{2}{\pi}}\sqrt{2[R(0)-R(\tau)+N]}$$

$$= \frac{2}{\sqrt{\pi}}\left[\sqrt{R(0)+R(\tau)+N} - \sqrt{R(0)-R(\tau)+N}\right].$$

If we set $R(0) = S$, the mean square of $s(t)$, we can write the average output as

$$\overline{F(t)} = \frac{2}{\sqrt{\pi}}\left[\sqrt{N+S[1+\rho(\tau)]} - \sqrt{N+S[1-\rho(\tau)]}\right] , \qquad (5.8)$$

where $\rho(\tau)$ is the normalized cross-correlation of the inputs. We can expand the above by the binomial theorem, and we have

$$\overline{F(t)} = \frac{2\sqrt{N}}{\sqrt{\pi}}\left[\sqrt{1+(S/N)[1+\rho(\tau)]} - \sqrt{1+(S/N[1-\rho(\tau)]}\right]$$

$$= \frac{2\sqrt{N}}{\sqrt{\pi}}\left[1 + \frac{1}{2}\frac{S}{N}[1+\rho(\tau)] + \ldots -1 - \frac{1}{2}\frac{S}{N}[1-\rho(\tau)] + \ldots\right]$$

$$\cong 2\sqrt{\frac{N}{\pi}}\left(\frac{S}{N}\right)_{in}\rho(\tau), \qquad (S/N)_{in} \ll 1 .$$

Therefore, if there is a large enough incoherent noise background, the average output of the linear rectifier correlator will be directly proportional to the signal autocorrelation function.

If $N = 0$, corresponding to the use of the linear rectifier correlator to measure a correlation function, the average output will be (from Eq. (5.8)),

$$F(t) = 2\sqrt{\frac{S}{\pi}}\,[\sqrt{1+\rho(\tau)} - \sqrt{1-\rho(\tau)}]. \qquad (5.9)$$

A graph of this function, normalized, is shown in Fig. 5.6. Because of the great similarity between Figs. 5.6 and 5.1, it may be seen that the distortion of an autocorrelation function as measured by the linear rectifier correlator will be nearly the same as that if it were measured by a polarity coincidence

correlator; Fig. 5.2 may be considered typical of the distortion
caused by either device.

Consideration of the circuit leads to the conclusion that
the output signal-to-noise ratio of the linear rectifier corre-
lator, for small input signal-to-noise ratio, is as much inferior
to that of the multiplier-averager as the linear detector is
inferior to the square-law detector in this respect. In Chapter
IV the difference was shown to be less than 0.2 db for two dif-
ferent input spectra. Experimental measurements with a linear
rectifier correlator constructed according to the schematic
diagram of Fig. 5.7 are in agreement with this prediction.
There is little difference, when the input signal-to-noise ratio
is small, between a multiplier-averager and a linear rectifier
correlator.

The linear rectifier correlator is simple to construct
however, high-quality sum-and-difference transformers should
be used. Unlike the vacuum-tube multiplier-averagers it is
independent of vacuum-tube characteristics, and does not require
a-c and d-c power supply regulation. In fact, if contact recti-
fiers are used, as in the circuit of Fig. 5.7, the linear
rectifier correlator can be made completely independent of
power supplies and no-signal zero drift can be eliminated. It
has the disadvantage of distorting correlation functions in
much the same way as the polarity coincidence correlator. This
distortion is, however, of little importance to anyone using
the correlator as a signal detection device.

References

1 Lawson, J. L. and G. E. Uhlenbeck, Threshold Signals,
   McGraw-Hill, New York (1950), p. 58.

2 Middleton, D., and R. M. Hatch, Jr., The Coherent Detector,
   Technical Report No. 80, Cruft Laboratory, Harvard University,
   Cambridridge, Massachusetts (July 7, 1948). Also, Smith, R. A
   "The Relative Advantage of Coherent and Incoherent Detectors;
   A Study of Their Output Noise Spectra under Various Con-
   ditions," Proc. Instn. Elect. Engrs. (London) 98 (Part III),
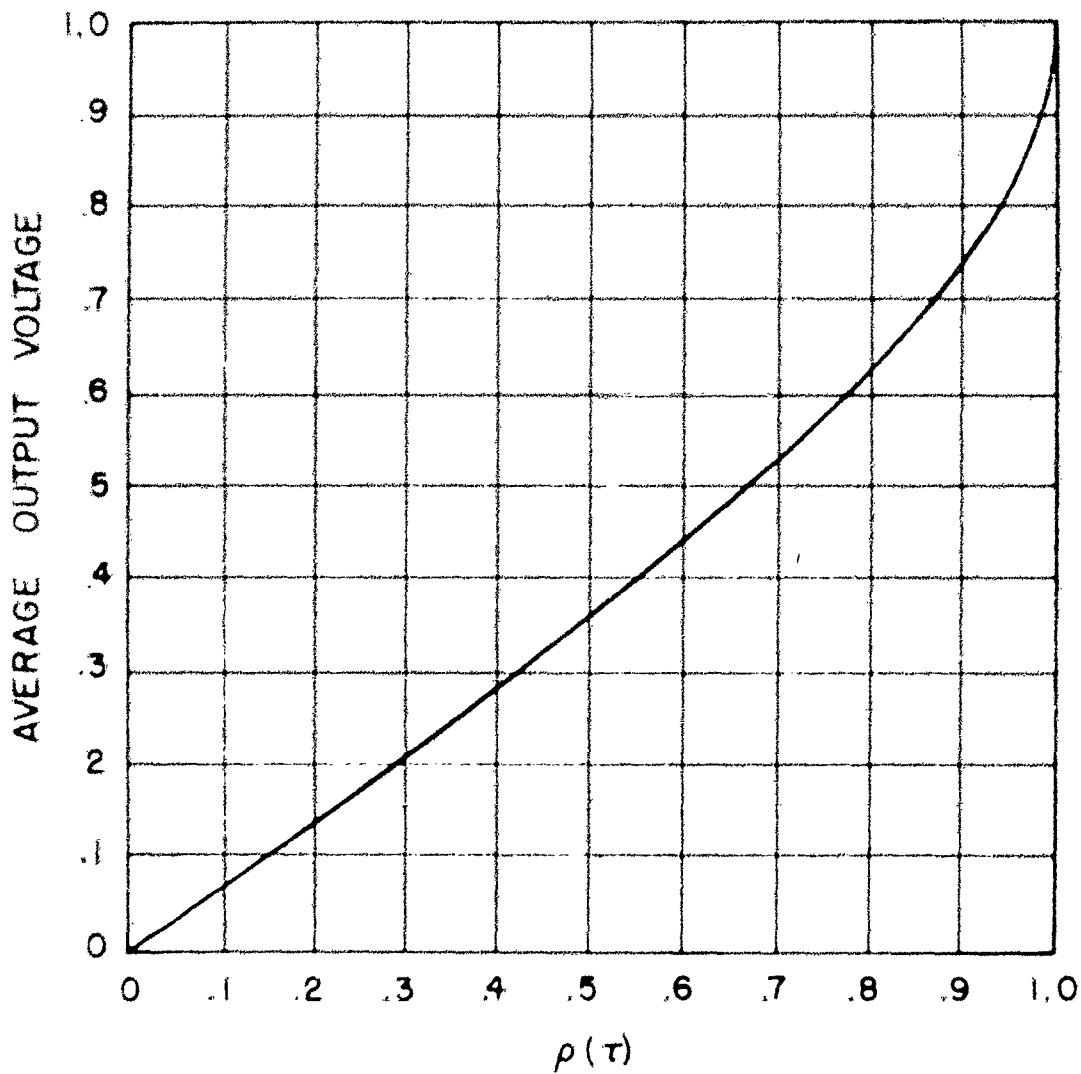   401-406 (September, 1951).

Fig. 5.6. Average output voltage (normalized) of a linear rectifier correlator as a function of the normalized crosscorrelation of the inputs, $\rho(\tau)$. For negative values of $\rho(\tau)$ the average output is negative; it is an odd function of $\rho(\tau)$.
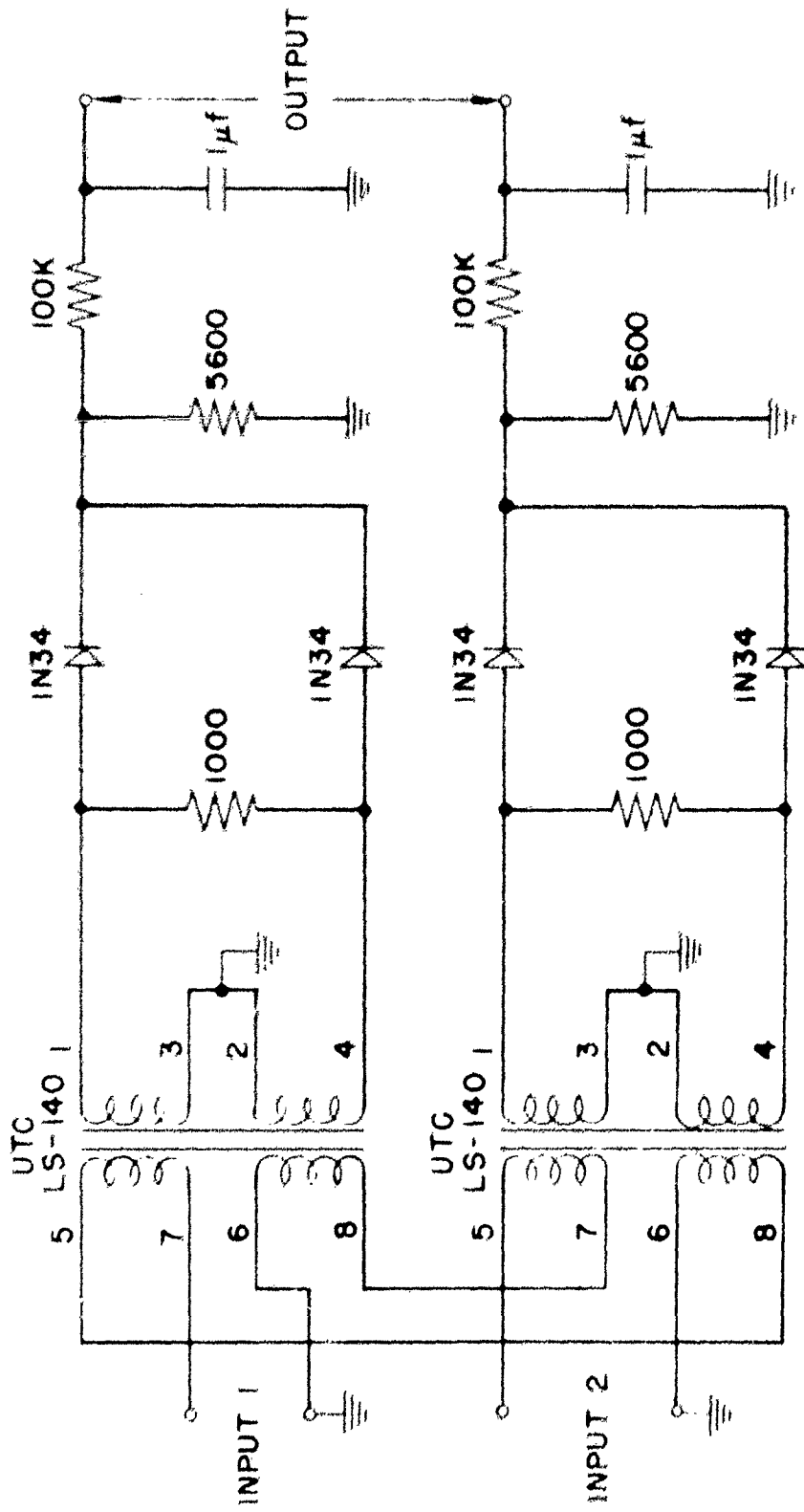
Fig. 5.7. Schematic diagram of a linear rectifier correlator.

Appendix I

EVALUATION OF THIRD-ORDER CORRELATION FUNCTION

We wish to evaluate the third-order autocorrelation function

$$R(\tau_1, \tau_2, \tau_3) = \langle v(t)v(t-\tau_1)v(t-\tau_2)v(t-\tau_3) \rangle$$

in terms of the ordinary autocorrelation function

$$R(\tau) = \langle v(t)v(t-\tau) \rangle .$$

For simplicity of notation, we write

$$R(\tau_1, \tau_2, \tau_3) = \langle v(t_1)v(t_2)v(t_3)v(t_4) \rangle \qquad (A1\ 1)$$

where, of course, $t = t_1$

$$\tau_1 = t_1 - t_2$$

$$\tau_2 = t_1 - t_3$$

and

$$\tau_3 = t_1 - t_4 .$$

A sample of $v(t)$ in an interval of length T is expanded in a Fourier series (cf. Eq. (1-6)) and this expression is substituted in Eq. (A1-1) above

$$R(\tau_1, \tau_2, \tau_3) =$$

$$\left\langle \sum_{n=1}^{\infty} [a_k \cos\omega_k t_1 + b_k \sin\omega_k t_1] \cdot \sum_{n=1}^{\infty} [a_k \cos\omega_k t_2 + b_k \sin\omega_k t_2] \right.$$

$$\left. \sum_{n=1}^{\infty} [a_k \cos\omega_k t_3 + b_k \sin\omega_k t_3] \sum_{n=1}^{\infty} [a_k \cos\omega_k t_4 + b_k \sin\omega_k t_4] \right\rangle .$$

where $\omega_k = 2\pi k/T$. Writing in different summation integers in each sum above allows us to write the above product of sums as

a sum of products

$$R(\tau_1, \tau_2, \tau_3) =$$

$$\left\langle \sum_{n=1}^{\infty} \sum_{n=1}^{\infty} \sum_{n=1}^{\infty} \sum_{n=1}^{\infty} [a_k \cos \omega_k t_1 + b_k \sin \omega_k t_1] \cdot [a_\ell \cos \omega_\ell t_2 + b_\ell \sin \omega_\ell t_2] \right.$$

$$\left. \cdot [a_m \cos \omega_m t_3 + b_m \sin \omega_m t_3] \cdot [a_n \cos \omega_n t_4 + b_n \sin \omega_n t_4] \right\rangle . \qquad (A1.2)$$

This now consists of many terms of the form

$$\langle a_k a_\ell a_m a_n \rangle \; \overline{\cos \omega_k t_1 \; \cos \omega_\ell t_2 \; \cos \omega_m t_3 \; \cos \omega_n t_4} ,$$

where we have interchanged the operations of adding and averaging and have made use of the ergodic theorem.

For gaussian noise, the properties of the coefficients given in Eqs. (1.7) apply here, and we see that $\langle a_k a_\ell a_m a_n \rangle = 0$ unless the indices are at least equal in pairs. Then the only nonvanishing terms are those where at least

$$\text{(a)} \quad k = \ell \quad \text{and} \quad m = n,$$

$$\text{(b)} \quad k = m \quad \text{and} \quad \ell = n,$$

$$\text{or} \quad \text{(c)} \quad k = n \quad \text{and} \quad \ell = m.$$

The terms for the case $k = \ell = m = n$ will be discussed below. Making the substitutions indicated above as (a), (b), and (c), we can write the nonvanishing terms in the quadruple sum as three double sums:

$$\left\langle \sum_{m=1}^{\infty} \sum_{n=1}^{\infty} [a_m \cos \omega_m t_1 + b_m \sin \omega_m t_1] \cdot [a_m \cos \omega_m t_2 + b_m \sin \omega_m t_2] \right.$$

$$\left. \cdot [a_n \cos \omega_n t_3 + b_n \sin \omega_n t_3] \cdot [a_n \cos \omega_n t_4 + b_n \sin \omega_n t_4] \right.$$

$$+ \sum_{m=1}^{\infty} \sum_{n=1}^{\infty} [a_m \cos \omega_m t_1 + b_m \sin \omega_m t_1] \cdot [a_n \cos \omega_n t_2 + b_n \sin \omega_n t_2]$$

$$\cdot [a_m \cos \omega_m t_3 + b_m \sin \omega_m t_3] \cdot [a_n \cos \omega_n t_4 + b_n \sin \omega_n t_4]$$

$$+ \sum_{m=1}^{\infty} \sum_{n=1}^{\infty} [a_m \cos \omega_m t_1 + b_m \sin \omega_m t_1] \cdot [a_n \cos \omega_n t_2 + b_n \sin \omega_n t_2]$$

$$\cdot [a_n \cos \omega_n t_3 + b_n \sin \omega_n t_3] \cdot [a_m \cos \omega_m t_4 + b_m \sin \omega_m t_4] \Big\rangle .$$

Using the further properties of the coefficients that $\langle a_m b_n \rangle = 0$ for all m, n and $\langle a_n^2 \rangle = \langle b_n^2 \rangle$, we can write the above as

$$\sum_{m=1}^{\infty} \sum_{n=1}^{\infty} \langle a_m^2 \rangle \langle a_n^2 \rangle \cos \omega_m(t_1 - t_2) \cos \omega_n(t_3 - t_4)$$

$$+ \sum_{m=1}^{\infty} \sum_{n=1}^{\infty} \langle a_m^2 \rangle \langle a_n^2 \rangle \cos \omega_m(t_1 - t_3) \cos \omega_n(t_2 - t_4)$$

$$+ \sum_{m=1}^{\infty} \sum_{n=1}^{\infty} \langle a_m^2 \rangle \langle a_n^2 \rangle \cos \omega_m(t_1 - t_4) \cos \omega_n(t_2 - t_3) .$$

Now the terms in Eq. (A1.2) for the case $k = \ell = m = n$ have coefficients of the form $\langle a_n^4 \rangle$. In Eq. (1.2) we proved that, for the case of gaussian statistics,

$$\langle a_n^4 \rangle = 3\sigma^4 = 3(\langle a_n^2 \rangle)^2,$$

so these terms are included exactly in the above three double sums as the cases where $m = n$. By comparison with Eq. (1.9) we have immediately

$$\langle v(t_1)v(t_2)v(t_3)v(t_4) \rangle = R(t_1-t_2)R(t_3-t_4)$$

$$+ R(t_1-t_3)R(t_2-t_4) \qquad \Bigg\} \quad (A1.3)$$

$$+ R(t_1-t_4)R(t_2-t_3)$$

or

$$R(\tau_1, \tau_2, \tau_3) = R(\tau_1)R(\tau_3 - \tau_2)$$

$$+ R(\tau_2)R(\tau_3 - \tau_1) \qquad\qquad (A1.3)$$

$$+ R(\tau_3)R(\tau_2 - \tau_1) \; .$$

This formula is proved by Fano in a different way for a slightly less general case.[A1]

The generalization of Eq. (A1.3) to a third-order cross-correlation function will be stated here without proof:

$$v_A(t_1)v_B(t_2)v_C(t_3)v_D(t_4)> = R_{AB}(t_1 - t_2)R_{CD}(t_3 - t_4)$$

$$+ R_{AC}(t_1 - t_3)R_{BD}(t_2 - t_4)$$

$$+ R_{AD}(t_1 - t_4)R_{BC}(t_2 - t_3)$$

or

$$R_{ABCD}(\tau_1, \tau_2, \tau_3) = R_{AB}(\tau_1)R_{CD}(\tau_3 - \tau_2)$$

$$+ R_{AC}(\tau_2)R_{BD}(\tau_3 - \tau_1)$$

$$+ R_{AD}(\tau_3)R_{BC}(\tau_2 - \tau_1) \; .$$

$$(A1.4)$$

Appendix II

DERIVATIONS OF AUTOCORRELATION FUNCTIONS OF NOISE HAVING

RECTANGULAR AND TUNED-CIRCUIT SPECTRA

As indicated in Eq. (1.10), the autocorrelation function of a random noise is the cosine Fourier transform of its intensity spectrum. The integration is here carried out for two examples:

A. Rectangular Spectrum

We assume that the intensity spectrum of a random function has the constant value W between the frequencies $f_0 - \Delta f$ and $f_0 + \Delta f$, and vanishes everywhere else. The center frequency is thus f_0 and the half-bandwidth is Δf. The corresponding autocorrelation function is

$$R(\tau) = W \int_{f_0 - \Delta f}^{f_0 + \Delta f} \cos 2\pi f \tau \, df$$

(A2.1)

$$= 2W\Delta f \left(\frac{\sin 2\pi \Delta f \tau}{2\pi \Delta f \tau} \right) \cos 2\pi f_0 \tau.$$

B. Tuned-Circuit Spectrum

We assume here that the intensity spectrum of the random noise has the same form as the response characteristic of a single-tuned resonant circuit. Noise having this spectrum may be generated by passing wide-band noise through a single-tuned-circuit filter. We shall first examine the analytic expression for the response characteristics of such filters in order to show how our definitions apply to series and parallel resonant circuits.

Series Resonant Circuit: We consider first the series resonant circuit of Fig. A2.1. The ratio of the output voltage to the input voltage is

$$\frac{e_o}{e_i} = \frac{R}{R + j(\omega L - 1/\omega C)} \; .$$

The intensity response spectrum
is given by the absolute value
of the square of the expression:

Fig. A2.1 Series
Resonant Circuit.

$$W_s(\omega) = \left| \frac{e_o}{e_i} \right|^2 = \frac{R^2}{R^2 + (\omega L - 1/\omega C)^2} \; .$$

We introduce the two parameters, ω_o, the resonant frequency, and
ω_p, the damping constant, defined by

$$\omega_o^2 = 1/LC \text{ and } \omega_p = R/2L \; .$$

The response spectrum may then be
written

$$W_s(\omega) = \frac{4\omega_p^2 \omega^2}{(\omega^2 - \omega_o^2)^2 + 4\omega_p^2\omega^2} \; . \tag{A2.2}$$

It is interesting to note that the spectral response of the
parallel circuit of the config-
uration shown in Fig. A2.2 is
of the same form. It is often
valid to assume that a constant
current is applied to the paral-
lel circuit, when it is used as
a filter; the ratio of the output
voltage to the constant input current
is

Fig. A2.2 Parallel Resonant
Circuit of One Type.

$$\frac{e_o}{I} = \frac{1}{1/R' + jC\omega + 1/j\omega L} \; .$$

We again define the parameters ω_o and ω_p, this time defined by

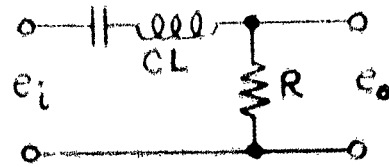$$\omega_o^2 = 1/LC \quad \text{and} \quad \omega_p = 1/2R'C.$$

The intensity response spectrum is then

$$W(\omega) = \left|\frac{e_o}{I}\right|^2 = R'^2 \frac{4\omega_p^2\omega^2}{(\omega^2 - \omega_o^2)^2 + 4\omega^2\omega_p^2},$$

which, except for the factor R'^2, is of the same form as Eq. (A2.2.). (It must be remembered that the response spectrum of a parallel circuit having the resistance in series with the inductance <u>is not of the same form</u>; this case, which we shall call the parallel resonant case in agreement with the literature,[A2] will be discussed briefly at the end of this appendix.)

<u>Spectrum Properties</u>: We shall first examine some of the properties of the series-resonant tuned-circuit spectrum of Eq. (A2.2). The frequency of maximum response is found by solving the equation

$$\frac{dW(\omega)}{d(\omega^2)} = \frac{(\omega^2-\omega_o^2) + 4\omega^2\omega_p^2 - \omega^2[2(\omega^2-\omega_o^2) + 4\omega_p^2]}{[(\omega^2- \omega_o^2)^2 + 4\omega_p^2\omega^2]^2} = 0.$$

The solution is easily seen to be $\omega = \omega_o$; the angular frequency of maximum response is ω_o regardless of the Q of the circuit. The maximum value of $W(\omega)$ is $W(\omega_o) = 1$. Parameters which are a convenient measure of the bandwidth of the spectrum are the two "half-power" points obtained from Eq (A2.2) when

$$W(\omega_h) = \frac{1}{2}W(\omega_o)$$

or

$$\frac{4\omega_p^2\omega_h^2}{(\omega_h^2 - \omega_o^2)^2 + 4\omega_h^2\omega_p^2} = \frac{1}{2}.$$

The solutions of this equation are

$$\omega_h = \sqrt{\omega_o^2 + \omega_p^2} \pm \omega_p$$

The damping constant ω_F is equal to the angular half-bandwidth for all values of Q. However, for low-Q circuits, the frequency of maximum response is not midway between the two half-power points. The Q of a series circuit is defined as the ratio of the series reactance of either reactor at resonance to the series resistance. For the circuit of Fig. A2.1,

$$Q = \omega_o L/R = 1/\omega_o RC = \omega_o/2\omega_F.$$

The total angular frequency bandwidth between the half-power points is

$$2\omega_F = \omega_o/Q.$$

Analytical Properties of $W(\omega)$: Factoring the denominator of Eq (A2.2), we can write $W(\omega)$ as a sum of partial fractions:

$$W(\omega) = \frac{A}{(\omega + \omega' - j\omega_F)} + \frac{B}{(\omega - \omega' - j\omega_F)} + \frac{C}{(\omega + \omega' + j\omega_F)} + \frac{D}{(\omega - \omega' + j\omega_F)} ,$$

$$(A2.3)$$

where $\omega' = \sqrt{\omega_o^2 - \omega_F^2}$ and the quantities A, B, C, and D are given by

$$A = \frac{\omega_F(\omega' - j\omega_F)}{2j\omega'} , \qquad B = \frac{\omega_F(\omega' + j\omega_F)}{2j\omega'}$$

$$C = \frac{\omega_F(-\omega' - j\omega_F)}{2j\omega'} , \qquad D = \frac{\omega_F(-\omega' + j\omega_F)}{2j\omega'} .$$

The function $W(\omega)$ has, in general, four poles in the complex ω-plane. The locations of these poles are indicated by the denominators of the fractions in Eq (A2.3) and are plotted in Fig. A2.3. It will be noted that for $\omega_F < \omega_o$ the four poles are symmetrically located on the circle $|\omega| = \omega_o$. When ω_F is equal to $\omega_o(Q = 1/2)$ the four simple poles merge into two second-order poles at $\omega = \pm j\omega_o$. As ω_F is increased further $(Q < 1/2)$ the two second-order poles split into four simple poles, all lying on the imaginary axis. As ω_F increases from ω_o to ∞, two of these poles move

from the points $\pm$ jω_0 toward the origin, while the other two
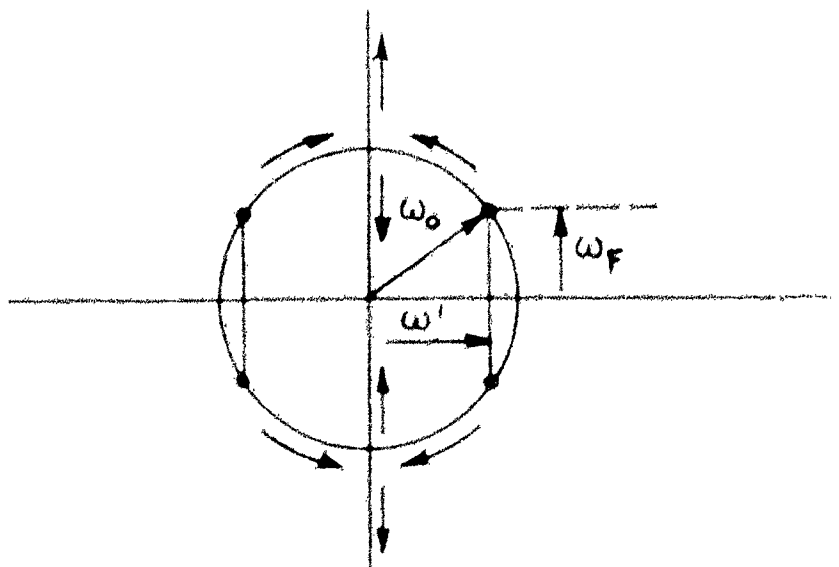move from $\pm$ jω_0 toward $\pm$ j∞.

Fig A2.3 Complex ω-Plane Showing Location of
Poles of Function $W(\omega)$. Arrows Show Motion of
Poles as ω_F Increases, ω_0 Remaining Fixed.

<u>Autocorrelation Function</u>. With the above information we
are now ready to evaluate the autocorrelation function of noise
having the intensity spectrum of Eq (A2.2). In order to ob-
tain the normalized autocorrelation function $\rho(\tau)$ we shall simply
evaluate Eq. (1.10) and normalize the result (so that $\rho(0) = 1$).
Since $W_s(\omega)$ is an even function [Eq (A2.2)], it is possible to
write

$$R(\tau) = \frac{1}{2} \int_{-\infty}^{\infty} W_s(\omega) e^{j\omega\tau} d\omega \qquad (A2.4)$$

We will evaluate the above only for τ positive, since

$$R(-\tau) = R(\tau), \qquad (A2.5)$$

because $R(\tau)$ is an autocorrelation function.

Case I; $0 < \omega_F < \omega_0$. In this case the integral of Eq. (A2.4)
is easily evaluated by means of a contour integral along a path

containing the real axis and a large semicircle around the upper half-plane. Then for $\tau > 0$,

$$R(\tau) = \frac{1}{2} \int_{-\infty}^{\infty} W_s(\omega) e^{j\omega\tau} d\omega$$

$$= 2\pi j \text{ Residue} \left[\frac{1}{2} W(\omega) e^{j\omega\tau} \right]_{\omega = \omega' + j\omega_p}$$
$$\omega = -\omega' + j\omega_p$$

$$= 2\pi j \left[\frac{\omega_p(\omega' - j\omega_p)}{4j\omega'} e^{j(-\omega' + j\omega_p)\tau} + \frac{\omega_p(\omega' + j\omega_p)}{4j\omega'} e^{j(\omega' + j\omega_p)\tau} \right]$$

$$= \frac{\pi\omega_p}{\omega'} e^{-\omega_p\tau} [\omega' \cos\omega'\tau - \omega_p \sin\omega'\tau] .$$

Therefore the normalized autocorrelation function $\rho(\tau)$ is

$$\rho(\tau) = e^{-\omega_p|\tau|} [\cos \omega'\tau - \frac{\omega_p}{\omega'} \sin\omega'|\tau|] ; \qquad (A2.6)$$

absolute value signs are inserted to satisfy Eq. (A2.5).

For very high-Q circuits where $\omega_p \to 0$ and $\omega' \to \omega_0$, the above may be accurately approximated by the usually quoted formula

$$\rho(\tau) = e^{-\omega_p|\tau|} \cos \omega_0\tau \qquad (A2.7)$$

<u>Case II, $\omega_p = \omega_0$.</u> Equation (A2.) gives the correct form of $\rho(\tau)$ for all $Q > 1/2$ However, when $Q = 1/2$, ω_p is equal to ω_0 and ω' is zero, and we must evaluate the integral

$$R(\tau) = 4\omega_p^2 \int_0^{\infty} \frac{\omega^2 \cos\omega\tau}{(\omega^2 + \omega_0^2)^2} d\omega$$

This could also be done by contour integration, but we find[A3] that

$$R(\tau) = \frac{\pi\omega_p^2}{\omega_0} (1 - \omega_0\tau) e^{-\omega_0\tau}$$

Therefore, for $Q = 1/2$,

$$\rho(\tau) = [1 - \omega_o |\tau|] \, e^{-\omega_o |\tau|} . \qquad (A2.8)$$

Case III; $\omega_o < \omega_F$: For very low-Q circuits the contour integral is again useful. In fact, the integral evaluated for Case I above may again be used if we note that ω', as defined by

$$\omega' = \sqrt{\omega_o^2 - \omega_F^2} ,$$

is now an imaginary number. Defining a new parameter,

$$\omega'' = \sqrt{\omega_F^2 - \omega_o^2} ,$$

we find, without further ado,

$$\rho(\tau) = e^{-\omega_F |\tau|} [\cosh \omega'' \tau - \frac{\omega_F}{\omega''} \sinh \omega'' |\tau|] .$$
$$(A2.9)$$

Parallel Resonant Circuit: The correlation functions for the medium and low-Q cases derived above correspond only to response spectra of the circuits of Figs. A2.1 and A2.2. If, for example, the circuit is a parallel resonant circuit of the form shown in Fig. A2.4, the intensity response spectrum is of the form

$$W_p(\omega) = \frac{4\omega_F^2 + \omega^2}{(\omega_o^2 - \omega^2)^2 + 4\omega^2 \omega_F^2} , \qquad (A2.10)$$
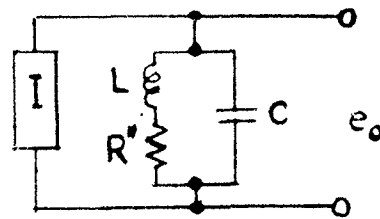
Fig. A2.4 Usual Parallel Resonant Circuit Configuration.

where $\omega_o^2 = 1/LC$ and $\omega_F = R''/2L$. The normalized autocorrelation function of random noise having the spectral intensity given by Eq. (A2.10) has been computed by the same methods as in the previous example. The results are

$$\rho(\tau) = e^{-\omega_F |\tau|} \left[\cos \omega' \tau - \frac{\omega_F}{\omega'} \frac{(\omega_o^2 - 4\omega_F^2)}{(\omega_o^2 + 4\omega_F^2)} \sin \omega' |\tau| \right], \quad Q > 1/2;$$
$$(A2.11)$$

$$\rho(\tau) = e^{-\omega_F |\tau|} \left[1 - \frac{3}{(12\omega_o^2 - 2)} \omega_o |\tau| \right] \quad , \; Q = 1/2;$$

and

$$\rho(\tau) = e^{-\omega_F |\tau|} \left[\cosh \omega''\tau + \frac{\omega_F}{\omega''} \frac{(4\omega_F^2 - \omega_o^2)}{(4\omega_F^2 + \omega_o^2)} \sinh \omega''|\tau| \right] Q < 1/2.$$

When Q is very large, Eq. (2.11) also reduces to Eq. (A2.7).

Response curves for the series and parallel resonant circuits are presented graphically in the literature[A4] Normalized correlation functions for noise having the corresponding spectra are plotted in Fig. A2.5 for various values of Q.
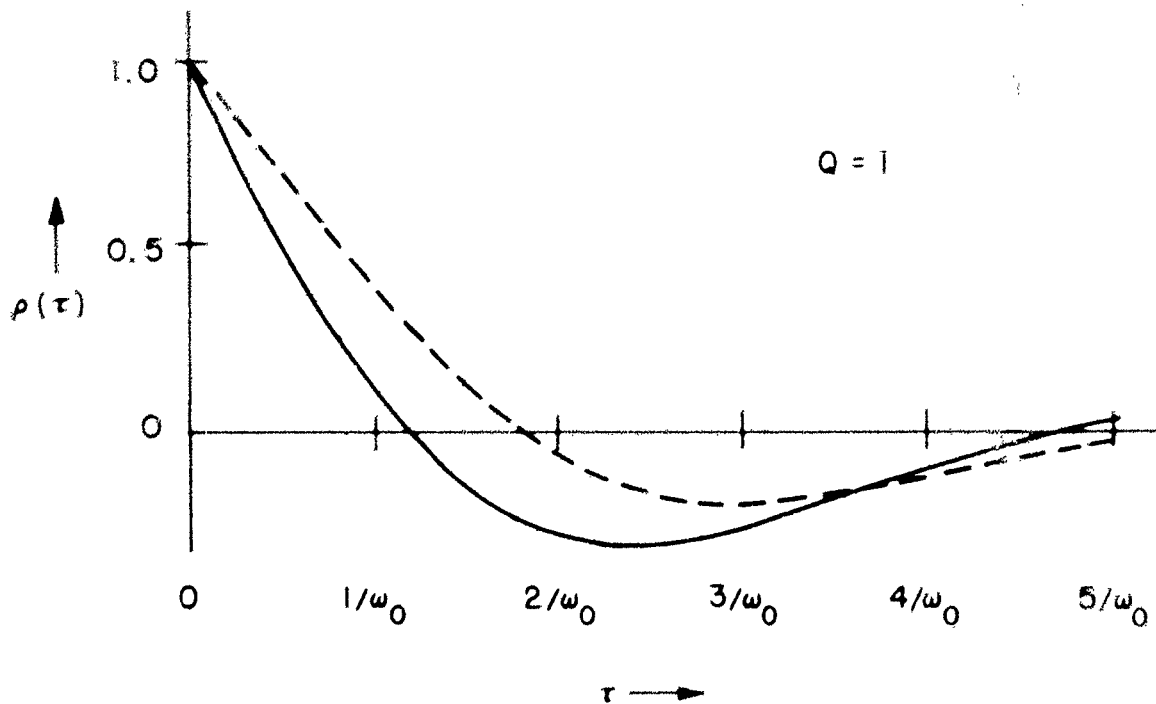
Fig. A2.5. Autocorrelation functions for noise having "tuned-circuit" spectra. Solid curve: Series resonant circuit; Dashed curve: Parallel resonant circuit. Both curves are even functions of τ.

Fig. A2.5. (cont.) Autocorrelation functions for noise having "tuned-circuit" spectra. Solid curve: Series resonant circuit; Dashed curve: Parallel resonant circuit. Both curves are even functions of τ. For $Q \geq 4$, the two curves are practically identical.

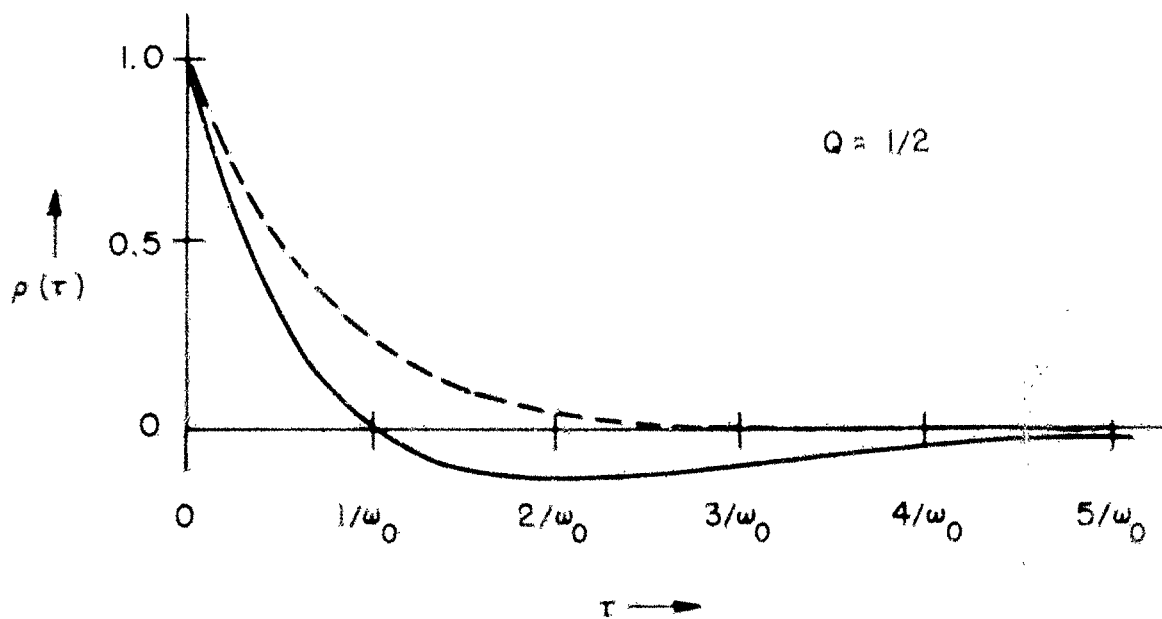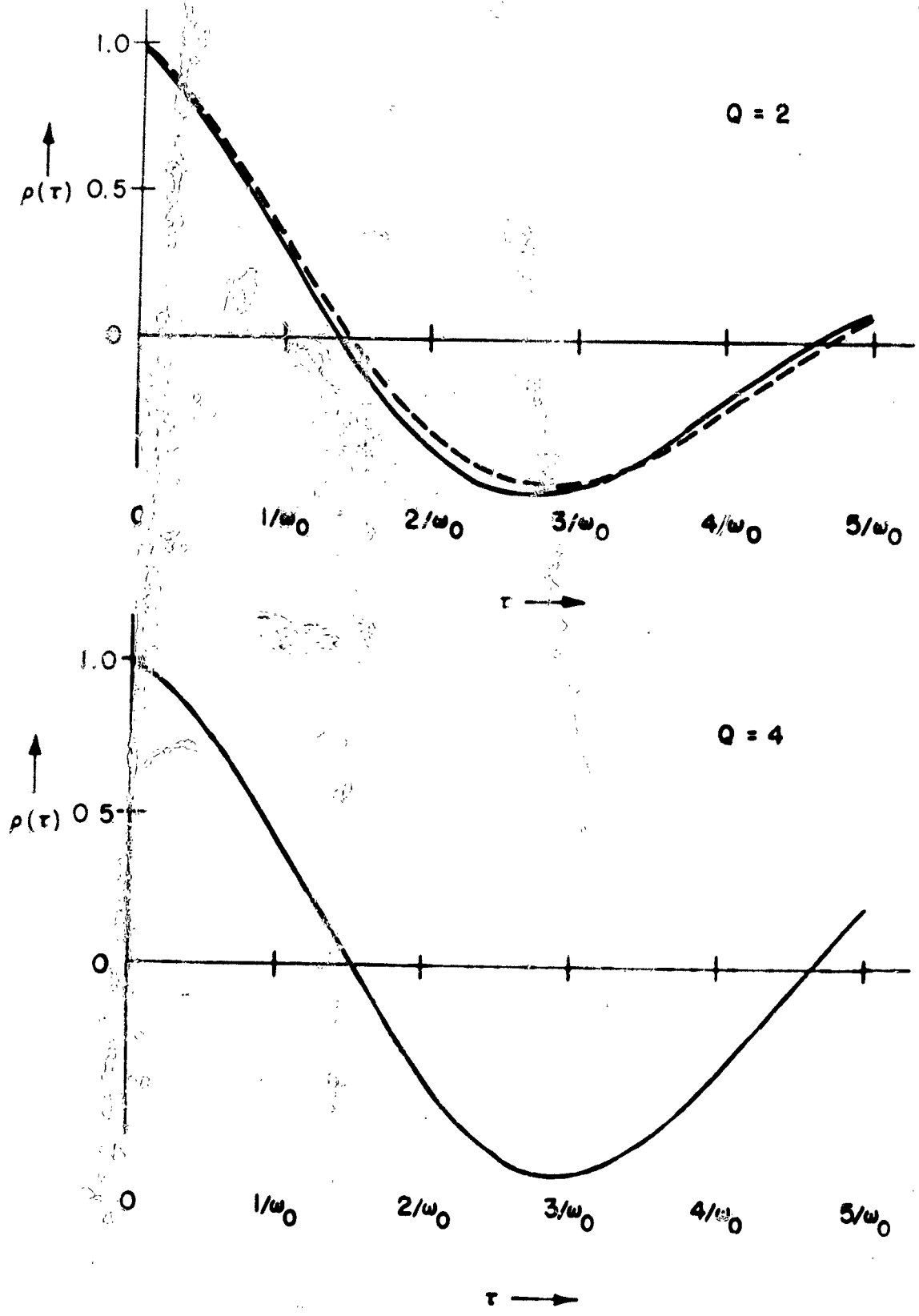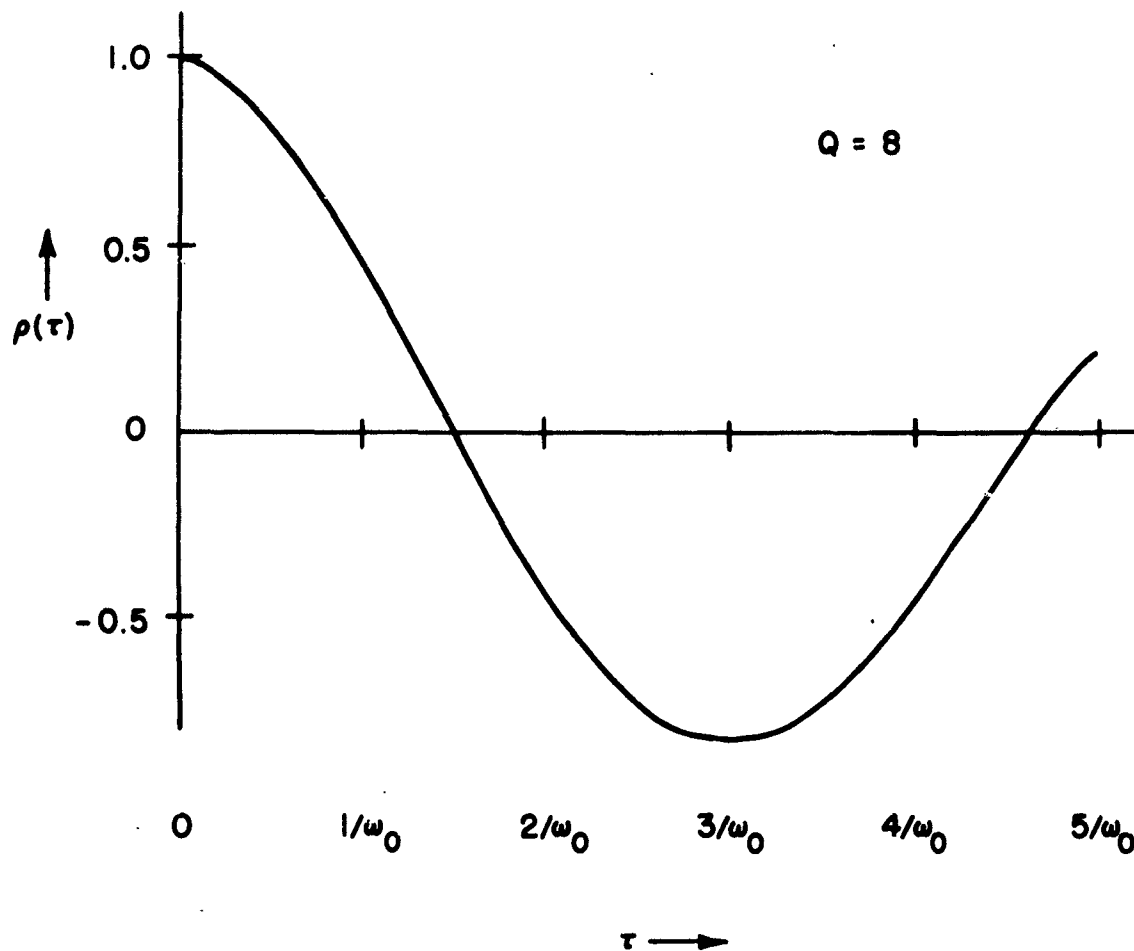Fig. A2.5 (cont.) Autocorrelation functions for noise having "tuned-circuit" spectra. Solid curve: Series resonant circuit; Dashed curve: Parallel resonant circuit. Both curves are even functions of τ. For $Q \geq 4$, the two curves are practically identical.

Appendix III

CORRELATION FUNCTIONS OF THE OUTPUT
OF A FULL-WAVE, v^{TH}-LAW DETECTOR

by

David Middleton and Noel Stone

The dynamic response of a full-wave, v^{th}-law nonlinear device may be represented by

$$I(t) = \beta \left| V(t) \right|^v = g(V(t)) , \qquad (-\infty < t < \infty), (v \geq 0)$$

$$(A3.1)$$

where $I(t)$ is the instantaneous input disturbance, corresponding to the input wave $V(t)$, and β is an appropriate scale factor. As has been shown elsewhere,[45] the full-wave relation (A3.1) may be expressed in terms (more convenient for analytical purposes when $V(t)$ consists of a signal and noise) of a (complex) Fourier transform by

$$I(t) = \frac{1}{2\pi} \int_C f(i\zeta)[e^{i\zeta V(t)} + e^{-i\zeta V(t)}] d\zeta, \qquad (A3.2)$$

where C is a contour extending along the real axis from $-\infty$ to $+\infty$ and indented downward in an infinitesimal semicircle about a possible singularity at $\zeta = 0$. Here $f(i\zeta)$ is the (complex) Fourier transform of the dynamic characteristic $g(v)$, which is calculated in this instance from

$$f(i\zeta) = \int_0^\infty g(V)e^{-iV\zeta} dV , \qquad Im(\zeta) < 0.$$

Specifically, one readily finds here that for (A3.1),

$$f(i\zeta) = \beta \Gamma(v+1)(i\zeta)^{-v-1} . \qquad (A3.4)$$

The autocorrelation function of $I(t)$ is[A6]

$$R_I(t) = \left\langle \overline{I(t_1)I(t_2)} \right\rangle \text{ stat. av.} = \frac{1}{4\pi^2} \int\int_{C \; C} f(i\xi_1)f(i\xi_2) \cdot$$

(A3.5)

$$\cdot \left\langle \overline{\left(e^{i\xi_1 V_1} + e^{-i\xi_1 V_1}\right)\left(e^{i\xi_2 V_2} + e^{-i\xi_2 V_2}\right)} \right\rangle_{\text{stat.av.}} d\xi_1 d\xi_2 \; ,$$

where the statistical average is taken over the random portions of the input $(V(t))$ and the time-average over the phases of the signal, if it is periodic. If it is not, as is frequently the case here, when the signal portion of $V(t)$ is itself a noise wave, this time average is replaced in the usual manner by an additional statistical average, it being assumed here that there is no correlation between signal and noise, in any case. Equation (A3.5) may be somewhat simplified, to

$$R_I(t) = \frac{1}{2\pi^2} \int_C \int_C f(i\xi_1)f(i\xi_2)[F_2(\xi_1, \xi_2; t)_V$$

(A3.6)

$$+ F_2(-\xi_1, \xi_2; t)_V]d\xi_1 d\xi_2 \; ,$$

in which F_2 is the <u>characteristic function</u> (i.e., the Fourier transform of the probability density $W_2(V_1, V_2; t)$ of the input wave $V(t)$. [For the $V(t)$ assumed here, the following symmetry properties of F_2 are easily established:

$$F_2(-\xi_1, \xi_2; t)_V = F_2(\xi_1, -\xi_2; t)_V; \; F_2(-\xi_1, -\xi_2; t)_V$$

(A3.7)

$$= F_2(\xi_1, \xi_2; t)_V \; ;$$

stationary ergodic ensembles are also assumed throughout.]

Let us now determine $R_I(t)$ for a variety of input waves $V(t)$. We summarize below some of the principal results:

I. <u>$V(t)$ = noise alone</u>:

For normal random noise the characteristic function F_2

associated with the second-order probability density $W_2(V_1, V_2; t)$ is[A6]

$$F_2(\xi_1, \xi_2; t)_V = e^{-\frac{\psi}{2}(\xi_1^2 + \xi_2^2 + 2\rho(t)\xi_1\xi_2)}, \qquad (A3.8)$$

where $\psi(t) = \psi\rho(t)$ is the autocorrelation function of the input noise $V(t)$, $\rho(t)$ is the _normalized_ correlation function; and $\psi = \overline{V^2}$. (It is assumed that $\langle V \rangle = 0$.) From (A3.6) we get

$$R_I(t) = \frac{\Gamma(\nu+1)^2\beta^2}{\pi^2} \int_C \int_C (i\xi_1)^{-\nu-1}(i\xi_2)^{-\nu-1} \cdot$$

$$\cdot \cosh[\psi\rho(t)\xi_1\xi_2]e^{-\frac{\psi}{2}(\xi_1^2 + \xi_2^2)} d\xi_1 d\xi_2$$

$$= 4 \sum_{n=0}^{\infty} \frac{\psi^{2n}\rho(t)^{2n}}{(2n)!} h_{o,2n}^2, \qquad (A3.9)$$

where the amplitude functions $h_{o,2n}$ are

$$h_{o,2n} = \frac{i^{-\nu-1}\beta\Gamma(\nu+1)}{2\pi} \int_C e^{-\psi\xi^2/2} \xi^{2n-\nu-1}d\xi, \qquad (A3.10)$$

$$= (-1)^n\beta(-\nu/2)_n 2^{n+\nu/2}\psi^{\frac{\nu}{2}-1-n}\Gamma(\frac{\nu+1}{2})/\sqrt{\pi},$$

in which $(\alpha)_n = \alpha(\alpha+1)\cdots(\alpha+n-1)$; $(\alpha)_0 = 1$. The final result is[A7]

$$R_I(t) = (2\psi)^{\nu} \frac{\beta^2}{\pi} \Gamma(\frac{\nu+1}{2})^2 {}_2F_1(-\nu/2, -\nu/2; 1/2; \rho^2(t))$$

$$= \frac{(2\psi)^{\nu}\beta^2}{\pi} \Gamma(\frac{\nu+1}{2})^2 \sum_{n=0}^{\infty} \frac{(-\nu/2)_n^2 \rho(t)^{2n}}{n!(1/2)_n}$$

and $(1/2)_n = (2n)!/2^{2n}n!$

II. V(t) = sum of two statistically independent noise waves:

For the problem considered in Chapter IV of this report, we wish to determine the autocorrelation function of our ν[th] law, full-wave rectifier when the input $V(t) = V_{N_1} + V_{N_2}$, i.e., is the sum of two, uncorrelated noise voltages.[1] The characteristic

function F_2 in (A3.6) now factors into the product of the two characteristic functions of V_{N_1} and V_{N_2}, viz.,

$$F_2(\xi_1,\xi_2;t)_V = F_2(\xi_1,\xi_2;t)_{N_1} \cdot F_2(\xi_1,\xi_2;t)_{N_2}$$

$$= e^{-\frac{(\psi_1+\psi_2)(\xi_1^2+\xi_2^2)}{2}} \qquad (A3.12)$$

$$\cdot e^{-[\psi_1\rho_1(t)+\psi_2\rho_2(t)]\xi_1\xi_2},$$

this last for normal random noise such that $<V_{N_1}> = <V_{N_2}> = 0$. As before, [cf. (A3.8), $<V_{N_1}^2> = \psi_1$, $<V_{N_2}^2> = \psi_2$, etc. Letting

$$\alpha = \frac{\psi_2}{\psi_1} \equiv p(\geq 0) \qquad (A3.13)$$

be the input "signal"-to-noise ratio (V_{N_2} represents a "noise" signal), and following the procedure of (A3.9), we can write here

$$R_I(t) = 4 \sum_{n=0}^{\infty} \frac{\psi_1^{2n}}{(2n)!}[\rho_1(t)+p\rho_2(t)]^{2n}h_{o,2n}^2, \qquad (A3.14)$$

where now $h_{o,2n}$ is given by (A3.10) if $\psi = \psi_1 + \psi_2 = \psi_1(1+p)$. For identical spectral shapes (but different total intensities) the general expression (A3.14) simplifies somewhat to

$$R_I(t) = 4 \sum_{n=0}^{\infty} \psi_1^{2n} \frac{\rho(t)^{2n}}{(2n)!} h_{o,2n}^2(1+p)^{2n} \qquad (A3.15a)$$

$$= [2\psi_1(1+p)]^\nu \sum_n \frac{1}{n}\Gamma(\frac{\nu+1}{2})^2 \sum_{n=0}^{\infty} \frac{(-\nu/2)_n^2\rho(t)^{2n}}{n!\,(1/2)_n} \qquad (A3.15b)$$

since $\rho_1(t) = \rho_2(t) = \rho(t)$ under this assumption. In the case of weak signals, i.e., $p^2 \ll 1$, this reduces still further to

$$R_I(t)\Big|_{p^2 \ll 1} \doteq [2\psi_1(1+p)]^\nu \cdot \frac{\beta^2}{n}\Gamma(\tfrac{\nu+1}{2})^2 \cdot \sum_{n=0}^{\infty} \frac{(-\nu/2)_n^2\, \rho(t)^{2n}}{n!(1/2)_n} \tag{A3.16a}$$

$$= \frac{\beta^2}{n}[2\psi_1(1+p)]^\nu \Gamma(\tfrac{\nu+1}{2})^2 \; {}_2F_1(-\nu/2,-\nu/2;\,1/2;\rho(t)^2) \tag{A3.16b}$$

Similar techniques may be used for other types of signals; for details see Refs. A5 and A6. Note here that we have obtained a correct and general result, good for all values of $\nu \geq 0$. These results may now be inserted directly into Eq. (4.4) and the output signal-to-noise ratios computed, as indicated [Eqs. (4.11) et seq.] for the various types of smoothing filters and correlation functions $\rho(t)$ considered in this report.

Appendix References

A1. Fano, R. M., Signal-to-Noise Ratio in Correlation Detectors, T. R. No. 186, Research Laboratory of Electronics, Massachusetts Institute of Technology, Cambridge, Massachusetts (February 19, 1951).

A2. Cruft Laboratory Staff, Harvard University, Electronic Circuits and Tubes, McGraw-Hill, New York (1947).

A3. DeHaan, D. Bierens, Nouvelles Tables D'Intégrales Défines, G. E. Stechert, New York (1939), Table 176, No. 8.

A4. Cruft Laboratory Staff, supra, Figs. 10.2, 14.1, 15.1, 15.2, and 16.1.

A5. Technical Report from Cruft Laboratory, Harvard University, by Noel Stone and D. Middleton (in preparation) 1952.

A6. D. Middleton, "Some General Results in the Theory of Noise through Non-Linear Devices," Quart. Appl. Math. 5, 445 (1948). For a general account of the "characteristic function" method used above, see in particular sections 2-4 of this paper. See also, "Noise and Non-Linear Communication Problems," p. 24, Symposium on Application of Autocorrelation Analysis to Physical Problems, Woods Hole, Massachusetts (June 13-14, 1949). Published by ONR, Washington, D. C. (May, 1950).

A7. Reference A6, Eq. (7.5) without the odd-order terms in $\rho(t)$. For further details, see Ref. A5.

BIBLIOGRAPHY

Bennett, W. R., "The Response of a Linear Rectifier to Signal and Noise," J. Acoust. Soc. Am. 15, 164-172 (January 1944).

Bode, H. W., and C. E. Shannon, "A Simplified Derivation of Linear Least-Square Smoothing and Prediction Theory," Proc. I.R.E. 38, 417-425 (April 1950).

Burgess, R. E., "The Rectification and Observation of Signals in the Presence of Noise," Phil. Mag. 42, 475-503 (May, 1951).

Chance, B., V. Hughes, E. F. McNichol, D. Sayre, and F. C. Williams, Waveforms, McGraw-Hill, New York, 1949.

Cheatham, T. P., Jr., An Electronic Correlator, Technical Report No. 122, Research Laboratory of Electronics, Massachusetts Institute of Technology, Cambridge, Massachusetts, March 28, 1951.

Davenport, W. B., Jr., Correlator Errors Due to Finite Observation Intervals, Technical Report No. 191, Research Laboratory of Electronics, Massachusetts Institute of Technology, Cambridge, Massachusetts, March 8, 1951.

Davenport, W. B., Jr., R. A. Johnson, and D. Middleton, "Statistical Errors in Measurements on Random Time Functions," J. Appl. Phys. 23, 377-388 (April 1952).

Eckart, Carl, The Measurement and Detection of Steady A-C and D-C Signals in Noise, University of California Marine Physical Laboratory of the Scripps Institution of Oceanography, October 4, 1951.

Eckart, Carl, The Theory of Noise Suppression of Linear Filters, University of California Marine Physical Laboratory of the Scripps Institute of Oceanography, October 8, 1951.

Fano, R. M., Signal-to-Noise Ratio in Correlation Detectors, Technical Report No. 186, Research Laboratory of Electronics, Massachusetts Institute of Technology, Cambridge, Massachusetts, February 19, 1951.

James, H. M., N. B. Nichols, and R. S. Phillips, Theory of Servomechanisms, McGraw-Hill, New York, 1947.

Johnson, R. A., and D. Middleton, The Theory of Measurements on Random Time Functions, Technical Report No. 125, Cruft Laboratory Harvard University, Cambridge, Massachusetts, May 1951.

Kac, M., and A. J. F. Siegert, "On the Theory of Noise in Radio Receivers with Square Law Detectors," J. Appl. Phys. 18, 383-397 (April 1947).

Khintchine, A., "Korrelationstheorie stationärer stochastischen Prozesse," Math. Ann. 109, 604-615(1934).

Lawson, J. L., and G. E. Uhlenbeck, Threshold Signals, McGraw-Hill, New York (1950).

Lee, Y. W., Application of Statistical Methods to Communication Problems, Technical Report No. 181, Research Laboratory of Electronics, Massachusetts Institute of Technology, Cambridge, Massachusetts, September 1, 1950.

Marshall, B. O., Jr., "An Analogue Multiplier," Nature (London) 167, 29-30 (January 6, 1951).

Mayer, H. F., Radio Noise Considerations, Solar Noise Technical Report No. 1, School of Electrical Engineering, Cornell University, Ithaca, New York, August 1949.

Middleton, D., "On the Theory of Random Noise:Phenomenological Models, I," J. Appl. Phys. 22, 1143-1152 (September 1951); II, J. Appl. Phys. 22, 1153-1163 (September 1951). See also Errata J. Appl. Phys. 22, 1326 (November 1951).

Middleton, D., "Rectification of a Sinusoidally Modulated Carrier in the Presence of Noise," Proc. I.R.E. 36, 1467-1477 (December 1948).

Middleton, D., "Some General Results in the Theory of Noise through Non-Linear Devices," Quart. Appl. Math. 5, 445-498 (January 1948).

Middleton, D., "The Effect of a Video Filter on the Detection of Pulsed Signals in Noise," J. Appl. Phys. 21, 734-740 (August 1950).

Middleton, D., "The Response of Biased, Saturated Linear and Quadratic Rectifiers to Random Noise," J. Appl. Phys. 17, 778-801 (October 1946).

Middleton, D., and R. M. Hatch, Jr., The Coherent Detector, Technical Report No. 80, Cruft Laboratory, Harvard University, Cambridge, Massachusetts, July 7, 1949.

Office of Naval Research, Symposium on Applications of Autocorrelation Analysis to Physical Problems, Department of the Navy, Washington, D. C., May 1950.

Price, Robert, _An FM-AM Multiplier of High Accuracy and Wide Range_, Technical Report No. 213, Research Laboratory of Electronics, Massachusetts Institute of Technology, Cambridge, Maasachusetts, October 4, 1951.

Ragazzini, J. R., "The Effect of Fluctuation Voltages on the Linear Detector," _Proc. I.R.E._ 30, 277-288 (June 1942).

Rice, S. O., "Mathematical Analysis of Random Noise," _Bell Syst. Tech. J._ 23, 282-332 (July 1944); 24, 46-158 (January 1945).

Singleton, H. E., _A Digital Electronic Correlator_, Technical Report No. 152, Research Laboratory of Electronics, Massachusetts Institute of Technology, Cambridge, Massachusetts, February 21, 1950.

Smith, R. A., "The Relative Advantage of Coherent and Incoherent Detectors: A Study of Their Output Noise Spectra under Various Conditions," _Proc. Inst. Elect. Engrs._ 98 (Part III) 401-406 (September 1951).

Somerville, M. J., "An Electronic Multiplier," _Electronic Eng._ 24, 78-80 (February 1952).

Van Vleck, J. H., and D. Middleton, "A Theoretical Comparison of the Visual, Aural, and Meter Reception of Pulsed Signals in the Presence of Noise," _J. Appl. Phys._ 17, 940-971 (November 1946).

Weinberg, L., and L. G. Kraft, _Experimental Study of Nonlinear Devices by Correlation Methods_, Technical Report No. 178 Research Laboratory of Electronics, Massachusetts Institute of Technology, Cambridge, Massachusetts, January 20, 1951.

Wiener, N., _Extrapolation, Interpolation, and Smoothing of Stationary Time Series_, John Wiley, New York, 1950.

Wiener, N., "Generalized Harmonic Analysis," _Acta Math._ 55, 117-258 (1930).

Wiener, N., _The Fourier Integral and Certain of Its Applications_, Dover, New York.

Woodward, P. M., "Information Theory and the Design of Radar Receivers," _Proc. I.R.E._ 39, 1521-1524 (December 1951).

Woodward, P. M., and I. L. Davies, "Information Theory and Inverse Probability in Telecommunication," _Proc. Inst. Elect. Engrs._ (London) 99, (Part III), 37-44 (March 1952).

1	Research and Development Board Pentagon Building Washington 25, D. C.
2	Chief of Naval Research Attn: Acoustics Branch, Code 411 Office of Naval Research Washington 25, D. C.
1	Director Naval Research Laboratory Washington 25, D. C. Attn: Technical Information Officer

Commanding Officer
U. S. Navy Office of Naval Research
Branch Offices:

1	Boston
1	New York
1	Chicago
1	Pasadena

3	Officer in Charge Office of Naval Research Navy No. 100, Fleet Post Office New York, New York
1	Director U. S. Navy Underwater Sound Reference Laboratory Office of Naval Research Orlando, Florida
1	Director Naval Research Laboratory Sound Division Washington 20, D. C.
1	Director U. S. Naval Electronics Laboratory San Diego 52, California
1	U. S. Naval Academy Naval Postgraduate School Physics Department Monterey, California Attn: Prof. L. E. Kinsler

1   Director
     Naval Ordnance Laboratory
     White Oaks, Maryland
     Attn: Sound Division

1   Director
     Marine Physical Laboratory
     University of California
     U. S. Navy Electronics Laboratory
     San Diego 52, California

1   Director
     U. S. Navy Underwater Sound Laboratory
     Fort Trumbull
     New London, Connecticut

1   Director
     David Taylor Model Basin
     Carderock, Maryland
     Attn: Sound Section

1   Director
     Ordnance Research Laboratory
     Pennsylvania State College
     State College, Pennsylvania

     Navy Department
     Bureau of Ships
     Washington 25, D. C.
1   Attn: Code 847
1   845
1   665E

1   Naval Medical Research Institute
     Naval Medical Center
     Bethesda, Maryland
     Attn: LCDR D. Goldman, NMC

1   U. S. Undersea Warfare Committee
     Navy Department
     Washington 25, D. C.

1   Massachusetts Institute of Technology
     Acoustics Laboratory
     Cambridge 39, Massachusetts
     Attn: Prof. R. H. Bolt

1	Catholic University of America Washington 17, D. C. Attn: Prof. K. F. Herzfeld
1	Brown University Department of Applied Physics Providence 12, Rhode Island Attn: Prof. R. B. Lindsay
1	University of California Department of Physics Los Angeles, California
1	Princeton University Department of Electrical Engineering Princeton, New Jersey
1	Utah University Salt Lake City 1, Utah Attn: Dr. P. J. Elsey
1	Western Reserve University Department of Chemistry Cleveland, Ohio Attn: Dr. Ernest Yeager
1	Commanding Officer Naval Air Development Center Johnsville, Pennsylvania
1	Woods Hole Oceanographic Institute Woods Hole, Massachusetts Attn: Mr. Vine
1	National Bureau of Standards Sound Section Washington 25, D. C.
1	California Institute of Technology Pasadena, California Attn: Dr. Epstein
1	Commanding Officer Air Force Cambridge Research Laboratory 230 Albany Street Cambridge 39, Massachusetts
1	Los Alamos Scientific Laboratory P. O. Box 1663 Los Alamos, New Mexico Attn: Dr. G. L. Campbell

1   Bell Telephone Laboratories
Murray Hill, New Jersey
Attn: Dr. W. E. Kock

1   U. S. Atomic Energy Commission
Library Section, Technical Information
Branch, ORE
P. O. Box E
Oak Ridge, Tennessee
Attn: Dr. I. A. Warheit

1   University of California
Radiation Laboratory
Information Division
Room 128, Bldg. 50
Berkeley, California

1   Lamont Geological Observatory
Torre Cliffs
Palisades, New York

1   Document Room
Research Laboratory of Electronics
Massachusetts Institute of Technology
Cambridge 39, Massachusetts
Attn: Mr. Hewitt

1   Federal Telecommunications Laboratory
500 Washington Avenue
Nutley, New Jersey

1   Hudson Laboratory
Columbia University
145 Palisades, Dobbs Ferry
New York

1   Director
Defense Research Laboratory
University of Texas
Austin, Texas

1   Director
David Taylor Model Basin
Carderock, Maryland
Attn: Technical Library

1   Walter G. Cady
Norman Bridge Laboratory
California Institute of Technology
Pasadena, California

1	Case Institute of Technology Department of Physics University Circle Cleveland 6, Ohio Attn: R. S. Shankland
1	California Institute of Technology Department of Chemical Engineering Pasadena, California Attn: Dr. M. S. Plesset
1	Department of Electrical Engineering U. S. Naval Academy Annapolis, Maryland
1	Lois A. Noble, Librarian The Brush Development Company 3405 Perkins Avenue Cleveland 14, Ohio
1	Kellex Corporation Silver Spring Laboratory Silver Spring, Maryland
1	Technical Library Bell Telephone Laboratories Murray Hill, New Jersey
1	National Academy of Sciences Committee on Undersea Warfare 2101 Constitution Avenue Washington 25, D. C. Attn: Dr. John S. Coleman
1	Commanding Officer U. S. Naval Ordnance Test Station Inyokern, California Attn: Reports Unit